

BRL CR 272

# B R L

CONTRACT REPORT NO. 272

NUMERICAL ANALYSIS OF LAMINATED,  
ORTHOTROPIC COMPOSITE STRUCTURES

Prepared by

University of Illinois  
Aeronautical and Astronautical  
Engineering Department  
Urbana, Illinois

November 1975

Approved for public release; distribution unlimited.

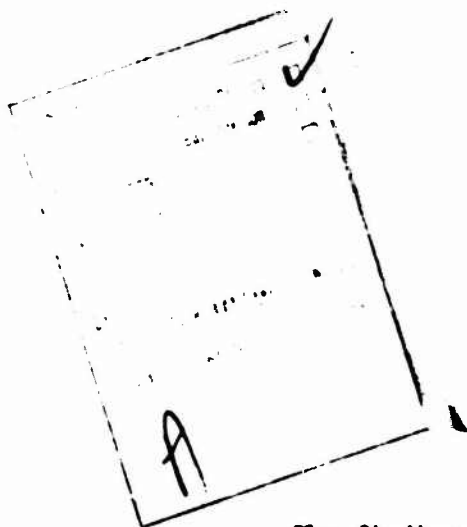
USA BALLISTIC RESEARCH LABORATORIES  
ABERDEEN PROVING GROUND, MARYLAND

ADA018875

Destroy this report when it is no longer needed.  
Do not return it to the originator.

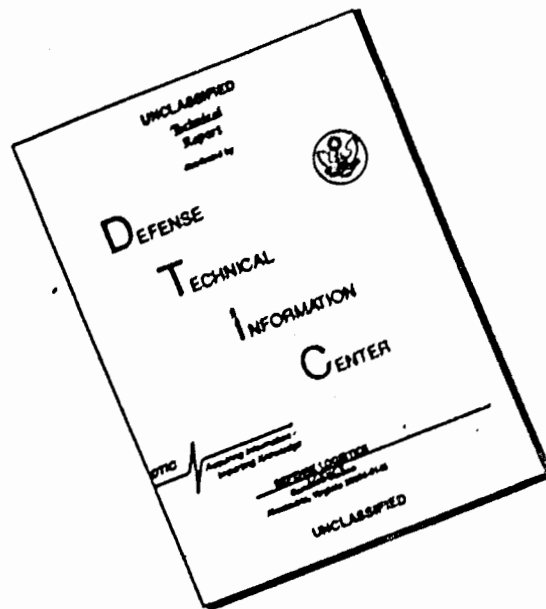
Secondary distribution of this report by originating  
or sponsoring activity is prohibited.

Additional copies of this report may be obtained  
from the National Technical Information Service,  
U.S. Department of Commerce, Springfield, Virginia  
22151.



The findings in this report are not to be construed as  
an official Department of the Army position, unless  
so designated by other authorized documents.

# DISCLAIMER NOTICE



THIS DOCUMENT IS BEST QUALITY AVAILABLE. THE COPY FURNISHED TO DTIC CONTAINED A SIGNIFICANT NUMBER OF PAGES WHICH DO NOT REPRODUCE LEGIBLY.

UNCLASSIFIED

SECURITY CLASSIFICATION OF THIS PAGE (When Data Entered)

REPORT DOCUMENTATION PAGE		READ INSTRUCTIONS BEFORE COMPLETING FORM	
1. REPORT NUMBER	2. GOVT ACCESSION NO.	3. RECIPIENT CATALOG NUMBER	
Contract Report Number 272		⑨	
⑥ Numerical Analysis of Laminated, Orthotropic Composite Structures.		5. TYPE OF REPORT & PERIOD COVERED	
		BRL Contractor Report 1 Jan 74 to 31 Dec 74	
		6. PERFORMING ORG. REPORT NUMBER	
		NONE	
		8. CONTRACT OR GRANT NUMBER(s)	
⑩ A.R./Zak		⑮ DAAD05-73-C-0197	
9. PERFORMING ORGANIZATION NAME AND ADDRESS		10. PROGRAM ELEMENT, PROJECT, TASK AREA & WORK UNIT NUMBERS	
Aeronautical and Astronautical Engr. Dept. University of Illinois Urbana, Illinois		62603A, 1M562603A286, 002AJ	
11. CONTROLLING OFFICE NAME AND ADDRESS		12. REPORT DATE	
USA Ballistic Research Laboratories Aberdeen Proving Ground, Maryland 21005		⑪ NOV 1975 ⑫	
		13. NUMBER OF PAGES	
		116 ⑬ 116p	
14. MONITORING AGENCY NAME & ADDRESS (if different from Controlling Office)		15. SECURITY CLASS. (of this report)	
US Army Materiel Command 5001 Eisenhower Avenue Alexandria, VA 22333		Unclassified	
		15a. DECLASSIFICATION/DOWNGRADING SCHEDULE	
16. DISTRIBUTION STATEMENT (of this Report)			
Approved for public release; distribution unlimited. ⑰ BRL			
⑭ DA-1-M-562603-H-286		⑱ CH-272	
17. DISTRIBUTION STATEMENT (of the abstract entered in Block 20, if different from Report)			
⑰ 1-M-562603-H-28600			
18. SUPPLEMENTARY NOTES			
19. KEY WORDS (Continue on reverse side if necessary and identify by block number)			
Anisotropic, Orthotropic, Analysis, Finite Element, Three Dimensional Deformations			
20. ABSTRACT (Continue on reverse side if necessary and identify by block number)			
This report presents the two main lines of investigation which were carried out during the past contract year. One investigation was intended to check-out previously developed finite-element computer programs on a large degree-of-freedom composite material model. This was done by applying the analysis to a restraints for this problem are presented and discussed. The second line of investigation was concerned with developing fracture models for composite materials. Two different models were developed. One model deals with interla-			

176005

2/5

UNCLASSIFIED

SECURITY CLASSIFICATION OF THIS PAGE(When Data Entered)

minar failure and the other predicts the matrix failure within an individual composite ply. No suitable experimental results are presently available to check out the first model but the second model is found suitable for explaining experimental results dealing with a nonlinear response of certain cylindrical models loaded to failure by internal pressure. These results, obtained from experiments performed at the Ballistic Research Laboratories, show that pronounced nonlinear structural response occurs at a fraction of failure load which suggests that an appreciable degradation of material occurs at relatively low stress levels. It is shown that this phenomenon can be explained by a model that assumes that the shear modulus in the plane of the fibers is reduced by matrix material failure parallel to the fibers.

UNCLASSIFIED

SECURITY CLASSIFICATION OF THIS PAGE(When Data Entered)

TABLE OF CONTENTS

	Page
I. INTRODUCTION . . . . .	7
II. LINEAR STRESS ANALYSIS OF RECOILLESS RIFLE . . . . .	8
Finite-element model . . . . .	8
Numerical results . . . . .	10
III. NONLINEAR MATERIAL RESPONSE . . . . .	11
Experimental results . . . . .	11
Linear Stress Analysis . . . . .	12
Methods of Analysis . . . . .	14
A. Interlaminar Slip . . . . .	14
B. Matrix Material Failure . . . . .	18
IV. CONCLUSIONS . . . . .	21
FIGURES . . . . .	22
APPENDIX A INPUT CARD DESCRIPTION . . . . .	51
APPENDIX B PROGRAM LISTING FOR INTERLAMINAR FAILURE ANALYSIS	61
DISTRIBUTION LIST . . . . .	113

### LIST OF ILLUSTRATIONS

Figure		Page
1.	Nozzle section of the recoilless rifle.	22
2.	Center section of the recoilless rifle.	23
3.	Forward section of the recoilless rifle.	24
4.	Finite-element grid in the I,J coordinates for the aft section.	25
5.	Finite-element grid in the I,J coordinates for the center section.	26
6.	Finite-element grid in the I,J coordinates for the forward section.	27
7.	Finite-element grid for recoilless rifle.	28
8.	Internal pressure distribution.	29
9.	Radial distribution of fiber and hoop stress at axial location z = 139.7 mm.	30
10.	Radial distribution of fiber and hoop stresses at axial location z = 223.5 mm.	31
11.	Radial distribution of fiber and hoop stresses at axial location z = 322.5 mm.	32
12.	Radial distribution of the magnitude of the shear stress $\sigma_{ns}$ at axial location z = 139.7 mm.	33
13.	Radial distribution of the magnitude of the shear stress $\sigma_{ns}$ at axial location z = 223.5 mm.	34
14.	Radial distribution of the magnitude of the shear stress $\sigma_{ns}$ at axial location z = 322.5 mm.	35
15.	Axial distribution of axial stress, hoop stress, and maximum shear stress in the adhesive layer.	36
16.	Axial distribution of the maximum fiber stress $\sigma_n$ and shear stress $\sigma_{ns}$ .	37
17.	Longitudinal strain measured as a function at internal pressure.	38
18.	Circumferential strain measured as a function of internal pressure.	39
19.	Arrangement of orthotropic plies in the test cylinder.	40
20.	Experimental Test Arrangement.	41
21.	Nondimensional slope variation with pressure.	42

Figure		Page
22.	Axial distribution of the shear stress $\sigma_{rz}$ .	43
23.	Radial distribution of the fiber stress $\sigma_n$ calculated by using 4 elements to represent each ply in the thickness direction.	44
24a.	Nodal point on interlaminar plane.	45
24b.	Relative slip at the nodal point following failure.	45
25.	Simplified computer flow chart showing the arrangement of the iterative schemes.	46
26a.	Cylindrical configuration used in the numerical example.	47
26b.	Finite-element grid used in the numerical calculations.	47
27.	Macroscopic model of composite material subject to shear stress.	48
28.	Dependence of shear modulus factor on the shear strain.	49



## I INTRODUCTION

During the first part of this investigation two finite-element models were developed<sup>1,2</sup> for the purpose of analysis of laminar, orthotropic structures in the form of bodies of revolution. The models allow for orthotropic axes to be arbitrarily oriented with respect to the cylindrical coordinates. Because of this, the models allow for three components of displacements including the two components in the meridian plane and the circumferential component. As a result, the models can be used to analyze unbalanced laminar configurations and interlaminar stresses can be predicted. The two models which have been developed differ in the basic finite-element shape which was used. The shape is defined by the cross-section of the elements in the meridian plane.

In the first model<sup>1</sup>, a nine degree-of-freedom, straight sided, triangular element was used. In this element, the three components of displacement are defined at each corner of the triangle and a linear displacement variation is assumed inside the element. In the second model<sup>2</sup>, a higher order, isoparametric element was used with quadratic displacement variations for two of the meridian displacements and a linear variation for the circumferential component. These elements are triangular with curved sides and mid-side nodes in addition to the corner nodes. Each of these elements possesses fifteen degrees-of-freedom.

A number of numerical examples were analyzed with both of these models to check-out the methods and the associated computer programs. One of these examples was analyzed by both models and was intended to compare the relative accuracy of each method. It was found that, for an equivalent number of total degrees-of-freedom, the results given by both methods were very close<sup>2</sup>. Although the total number of degrees-of-freedom in both models was the same, fewer of the isoparametric elements had to be used. The conclusion from this study was that each of these models was equally accurate and either one could be used for any given problem.

The various examples which were analyzed<sup>1,2</sup> during check-out contained relatively few degrees of freedom. However, both computer programs were designed to handle much larger problems and consequently it was desired to check-out this capability. Since both of these programs are similar in their solution of the global matrix equations, it was decided to apply only one of these programs to a large problem. For this, the model with the straight sided elements<sup>1</sup> was chosen since it permitted a large number of elements to be used for a given total number of degrees-of-freedom. This fact was advantageous in the problem to be analyzed since it permitted more flexibility in modelling the orthotropic plies of the structure. The problem analyzed corresponds to a recoilless rifle configuration made up from a large number of orthotropic, fiberglass plies. The analysis of

---

<sup>1</sup>A. R. Zak, "Second Quarterly Report," U.S. Army Contract No. DAAD05-73-C-0197.

<sup>2</sup>A. R. Zak, "Final Report," U. S. Army Contract No. DAAD05-73-C-0197, January, 1974.

this structure and the numerical results will be discussed in the first part of this report.

The second line of investigation was concerned with the failure analysis of laminated structures. Two possible modes of failure were postulated and numerical methods necessary to examine them were developed. These methods are related to the linear finite-element method discussed previously.<sup>1</sup> The first mode of failure to be examined consists of interlaminar cracking. In this model an ultimate shear stress is assigned to the region between the composite plies and the plies are allowed to slip relative to each other when this stress is exceeded. In the second model the failure is assumed to occur inside the matrix of an individual ply. This failure is gradual since the matrix stresses are not uniform and, consequently, higher stressed regions would fail first. The consequence of such failure is a reduction in the effective transverse material properties of the total composite ply.

Each of these failure modes was considered a possible explanation of certain experimental results, which were obtained at the Ballistic Research Laboratories<sup>3</sup>. In these experiments a strong nonlinear response was observed when certain laminated cylindrical specimens were loaded up to the failure level. The cylinders were loaded by time dependent internal pressure and produced a nonlinear strain-pressure history. Both the longitudinal and the circumferential strains were measured and the response was found to be nonlinear even at loads only a fraction of the ultimate value. This suggests that a measurable degradation of the material properties occurs, and the objective was to determine if either one of the failure models could explain this behavior. This study is described in the second part of the report.

## II LINEAR STRESS ANALYSIS OF RECOILLESS RIFLE

### Finite-Element Model

The cross-section of the recoilless rifle is shown in three parts in Figures 1 to 3. It can be seen that the rifle is composed of two sections of fiber-reinforced composite material joined together by an adhesive layer. The composite material is arranged in helical and hoop plies. The helical plies are arranged in pairs with equal and opposite wrap angle. There are two distance scales used in the radial direction in Figures 1 to 3. One scale is used for the internal surface and another scale, 3.58 times larger, is used for distances inside the cross-section. Consequently, the model looks 3.58 times as thick as the real structure. However, in the finite-element stress analysis, the correct dimensions are used.

<sup>3</sup>J. N. Majerus, W. F. Donovan and R. W. Greene, "Hot Gas Test Fixture with Minimized End Restraints for Rapidly Pressuring Anisotropic Tube Type Structures," Ballistic Research Laboratories, Memorandum Report No. 2459, March 1975. (AD #B003671L)

In the finite-element model, the structure is divided into 1368 elements and the element boundaries are chosen so as to correspond to the boundaries of the composite material plies. A set of elements was also chosen to correspond to the adhesive layer. The finite-element grid can first be illustrated in the I-J coordinates which is shown in Figures 4 to 6. In this coordinate system, each element is represented by a square. This representation of the finite-element grid is useful in establishing the information for the generation of the actual finite-element model as well as other necessary input data. In Figures 4 to 6, the solid lines illustrate the material block cards and the dotted lines are the elements inside each block. Altogether there were 123 material blocks used. One of these blocks was used to define the adhesive layer and the remaining blocks contained composite, orthotropic material. The computer program<sup>1</sup> allows for the orthotropic axes to differ from block to block. In each block the axes of orthotropy in the meridian plane is constant and the helical orientation of the axes can either be constant or vary by a factor of plus or minus<sup>1</sup>. In Figures 4 to 6, the I-J coordinates are shown for selected nodes in order to illustrate the size of the grid. The actual finite-element grid generated in the program and used in the stress analysis is shown in Figure 7. This grid was generated in the computer and as in the case of Figures 1 to 3, two different plotting scales were used in the radial direction in order to illustrate cross-sectional detail.

The elastic orthotropic properties for the composite material which were used in the analysis are given in Table I below:

Table I

Elastic Orthotropic Material Properties for the Composite Material

$E_n$	=	58.6 GPa
$E_s$	=	13.79 GPa
$E_t$	=	13.79 GPa
$\nu_{ns}$	=	.25, $G_{ns}$ = 4.82 GPa
$\nu_{nt}$	=	.25, $G_{nt}$ = 4.82 GPa
$\nu_{st}$	=	.45, $G_{st}$ = 1.379 GPa

The nomenclature in Table I corresponds to the definitions given in Reference 1. The direction n is chosen along the fibers, s is perpendicular to the fibers and in the plane of the lamina, and t is the remaining orthotropic axis in the transverse direction. The mechanical properties for the adhesive layer were assumed to be isotropic and the Young's modulus and Poisson's ratio used was  $E = 3.44$  GPa and  $\nu = 0.35$ .

The load applied to the structure was assumed to be composed of an internal pressure acting on the inside surface of the structure. In the chamber section the pressure was assumed to be uniform and equal to  $6.895 \times 10^7$  Pa. In the barrel section, where the radius is constant, the pressure was continued at the same constant value. In the nozzle throat the pressure was assumed to make a step jump and a uniform pressure of  $1.385 \times 10^7$  Pa was used on the diverging section of the nozzle. This value was chosen as to balance the total load acting on the structure. The pressure load just described is illustrated in Figure 8. It may be noted that although the pressure distribution at the nozzle and barrel sections is somewhat arbitrary, this will not be a critical factor since the largest stresses are produced in the chamber section and these are mainly a function of the chamber pressure. If the chamber pressure should not be equal to  $6.895 \times 10^7$  Pa as used in this analysis, the corresponding stresses can be obtained from this analysis by linear scaling.

### Numerical Results

Because of the large number of degrees-of-freedom involved in this analysis, a great deal of stress and strain data was generated by the solution. At each nodal point the solution generates three components of displacement and for each element two sets of stresses and strains are calculated. One set is in the cylindrical coordinates and the other is along the axes of orthotropy. Consequently, it is practical to present here only a small amount of this data. In choosing the data for presentation, it was observed that the largest stresses occur in the hoop direction and that they are in the chamber region of the structure. Figures 9 to 11 show the radial hoop stress distribution at three different axial stations defined approximately by  $z = 139.7$  mm,  $223.5$  mm and  $322.5$  mm respectively. Also shown in these diagrams are the stresses in the direction of the glass fibers. The hoop stresses are given by the dotted curves and the stresses in the fiber direction are given by the solid curves. In the case of the hoop plies, the two curves obviously coincide and only the solid curve is seen. Figures 12 to 14 show similar results for the shear stresses in the plane of the orthotropic plies at the same values of  $z$ . It can be observed from these figures that there are large variations of the stresses through the thickness and this variation is most pronounced when going from a helical to a hoop ply. As expected, the largest fiber stresses occur in the hoop plies as can be seen from Figures 9 and 10. In Figure 9 two hoop plies exist through the thickness and these produce the two peaks shown. In Figure 10 we also encounter two hoop layers leading to two peaks, and furthermore, there is a pronounced dip in the curves as the adhesive layer is crossed. The results in Figure 11 show stresses through helical plies only, but there is still a large variation due to change in helical angle through the thickness. The largest transverse shear stresses occur in the helical plies and these stresses are also discontinuous from one ply to another.

Other interesting results are the stresses in the adhesive layer. In Figure 15 a plot is given showing the variation of the maximum shear stress, the hoop stress, and the longitudinal stress as a function of

the coordinate  $z$ . The failure of the adhesive layer would be governed by the maximum shear stress which can be seen from Figure 15 to be about  $6.2 \times 10^7$  Pa. Further results are shown in Figure 16 where an axial distribution is shown of the maximum fiber stress and the maximum transverse shear stress through the thickness of the cross-section. It can be seen that a large variation of these stresses exists in both the nozzle and the chamber sections.

In conclusion, it is interesting to note the maximum fiber stress and its location. The maximum fiber stress occurred in element number 927 and its magnitude was  $168.7 \times 10^7$  Pa. This element is in the hoop ply region and its approximate position is identified in Figure 3. The average coordinates for this element are  $r = 58.6$  mm and  $z = 202.8$  mm.

### III NONLINEAR MATERIAL RESPONSE

#### Experimental Results

Figures 17 and 18 show one set of typical results of an experimental investigation conducted at the Ballistic Research Laboratories<sup>3</sup>. In this study a set of cylindrical fiber reinforced models was subjected to time dependent internal pressure loads which eventually led to total structural failure. The specimens were made from S glass fibers with six plies as shown in Figure 19. The four internal plies were constructed with a 54 degree helix angle and the two outside plies with an 83 degree angle. These angles were alternated in each successive ply in order to produce a balanced structure. The length of each cylinder was 388.62 mm, the inside diameter was 67.56 mm and the ply thicknesses are given in Figure 19.

The cylinders were loaded by burning about 0.09 kg of propellant which produced a time dependent pressure-time curve. The ends of each cylinder were sealed by plugs as shown in Figure 20. These plugs did not apply an appreciable axial load to the cylinder, and as the cylinder expanded some amount of gas was released between the cylinder and the plugs. A detailed description of the experimental apparatus can be found in Reference 3.

The results shown in Figures 17 and 18 contain the strain measurements obtainable from strain gages situated on the external surface of the cylinder. The strains are given as a function of the internal pressure. The strain gages were mounted to measure both the circumferential and longitudinal strains as a function of time, and then these strains were correlated with the recorded pressures. These strains were measured at three different points in the cylinder, two of these being at 12.7 mm from the cylinder ends and the third at the center. All three readings are shown in Figures 17 and 18, and it can be seen that there is a measurable experimental difference between the readings. Some of this difference may be attributed to end effects.

However, only a small amount could be explained by this, since as the subsequent numerical calculations showed, the end effects die down quite rapidly.

The results for both the longitudinal, Figure 17, and the circumferential strains, Figure 18, show a pronounced nonlinear response. Furthermore, the nonlinear effects are more pronounced in the longitudinal strains. This can be illustrated by considering the slope of the response curves for both directions. Because of the variation between the different parts of the cylinder, it is necessary to speak of some average response. This is indicated by the solid lines drawn in Figures 17 and 18, which are approximately the average values of the three strain gage readings. In order to illustrate the relative nonlinearity in the two directions, the slopes of these curves were normalized relative to their initial slope at low pressure loadings, and the results of this are illustrated in Figure 21. The relative amount of nonlinearity can be measured by the deviation of this normalized slope from the value of 1.0, and it can be seen that this effect is most pronounced in the longitudinal direction.

### Linear Stress Analysis

As the first step in the nonlinear investigation, a linear stress analysis was performed on the model corresponding to the experimental configuration shown in Figure 19. This was done by using the previously described finite-element program. Because of a symmetry about the center line only one half of the cross-section had to be modelled by the finite-elements. This was done by using 20 nodes over half of the cylinder and 25 nodes in the thickness direction. Each ply was represented by four elements through the thickness. The size of the elements in the longitudinal direction was varied by using smaller elements near the ends of the cylinder. This was done by using two elements 3.17 mm in length followed by two elements 6.34 mm in length. The remaining sixteen elements were divided equally. This grid permitted a good resolution of the end stresses and Figure 22 shows the axial variation of the maximum shear stress  $\sigma_{rz}$ . It can be seen that these stresses are limited to only a very small distance of the ends of the cylinder. The results of this analyses show that the stress conditions are essentially constant over the length of the cylinder. This is expected since the thickness of the cylinder relative to the radius is very small as seen in Figure 19.

Initially there was no guarantee that the orthotropic material properties used in the finite-element analysis would correspond exactly to the experimental model. Consequently, initially a reasonable set of values was chosen and the calculated response was compared to the measured response at low pressure levels. The results of this initial calculation showed insignificant variation of stresses and strains through the thickness of each ply as illustrated in Figure 23 where the fiber  $\sigma_{11}$  is plotted over the thickness of the cylinder. Therefore, in

the subsequent calculations each ply was represented by one element in the thickness direction. This permitted a small grid size and, consequently, much faster execution time. After the initial linear calculation the material properties were adjusted as to agree with the experimental data, and these values are given in Table II below:

Table II

Elastic Orthotropic Material Properties for the Test Cylinder

$E_n$	=	38.2 GPa
$E_s$	=	9.37 GPa
$E_t$	=	9.37 GPa
$\nu_{ns}$	=	0.25, $G_{ns}$ = 3.3 GPa
$\nu_{nt}$	=	0.25, $G_{nt}$ = 3.3 GPa
$\nu_{st}$	=	0.45, $G_{st}$ = .896 GPa

The properties in Table II have the same meaning as in Table I.

In the linear calculation, the actual value of the pressure is not important since the load and the stresses are linearly scaled. Table III below contains some of the results obtained by using a pressure of  $6.895 \times 10^6$  Pa uniformly distributed over the length of the cylinder. The results given are the stresses in the local orthotropic coordinates for each material ply. The plies are numbered starting on the inside of the cylindrical surface. Only four stresses are shown since the remaining two stresses were found to be negligible.

Table III

Calculated Linear Stresses in the Test Cylinder ( $\pm 10^6$  Pa)

<u>Ply Number</u>	<u><math>\sigma_n</math></u>	<u><math>\sigma_s</math></u>	<u><math>\sigma_t</math></u>	<u><math>\sigma_{ns}</math></u>
1	100.8	4.9	-6.6	-25.47
2	99.7	5.0	-6.0	25.3
3	99.0	4.9	-5.5	-25.2
4	97.9	5.0	-4.9	25.2
5	191.7	-13.5	-3.5	-6.3
6	189.6	-12.7	-1.0	6.3

It can be seen from Table III that, as expected, the largest stresses are the normal stresses  $\sigma_n$  along the fibers. The highest fiber stresses occur in the two outside plies which have the helical angle of 83 degrees. The next largest stresses are the shear stresses  $\sigma_{ns}$  and they are more predominant in the four inside plies. The remaining two stresses,  $\sigma_s$  and  $\sigma_t$ , are appreciably smaller. These results suggest that the maximum stress existing in the matrix material are shear stresses resulting from  $\sigma_{ns}$ .

## Methods of Analysis

### A. Interlaminar Slip

One possible failure mode in a laminated, composite structure is the separation of individual plies when interlaminar shear stress exceeds a critical value. If this phenomena would occur in any given structure, it would lead to a nonlinear response. In order to analyze this response it would be necessary to use an iterative, numerical approach. The objective was to develop such a method of analysis by using previously developed<sup>1</sup> finite-element computer program as the basis. The results of this study are presented in this section.

The approach which has been developed can be illustrated by considering the four adjacent elements to a node which lies on the interface between material layers as shown in Figure 24a. The first step in the analysis is to check if a prescribed interlaminar shear stress is exceeded at this point in the material. Since the stresses are calculated in the elements, rather than the nodes, the failure at the node shown in Figure 24a is defined in terms of the resultant shear stresses in the four adjacent elements. The resultant shear stresses are calculated in each lamina parallel to the interlaminar plane. The average of this resultant stress over the adjacent elements is then compared against a prescribed failure criterion.

Referring to Figure 24a the elements above the interlaminar plane are called the upper elements and below they are the lower elements. If the shear stress exceeds the failure criterion at a particular node then there will be a relative motion of the upper and lower elements as illustrated in Figure 24b. This motion will be characterized by the physical condition that the net forces on the upper and lower elements at the given node which has failed will be zero parallel to the interlaminar plane. The slip displacements are characterized by two components for the upper and two for the lower elements. These components can be transformed into the cylindrical coordinates by the relations

$$\begin{aligned} \{\delta^U\} &= [T] \{\Delta^U\} \\ \{\delta^L\} &= [T] \{\Delta^L\} \end{aligned} \quad (1)$$



where  $\{\delta\}$  is the displacement vector in cylindrical coordinates due to nodal slip,  $[T]$  is the transformation matrix, and  $\{\Delta\}$  the two slip components. The superscripts U and L refer to the upper and lower elements. Before the slip has occurred the nodal displacements for each element are known and therefore these known displacements are added to the displacements due to the slip as given by Equations (1). Consequently, the net force components on the upper and lower elements can be expressed in the following form

$$\begin{aligned} \{F^U\} &= \{f^U\} + [Y]\{\Delta^U\} \\ \{F^L\} &= \{f^L\} + [Z]\{\Delta^L\} \end{aligned} \quad (2)$$

where F represents total force and f is the force due to known displacements. The matrices [Y] and [Z] are known and are related to the stiffness matrices. The forces in Equations (2) are originally in cylindrical coordinates and by suitable transformation it is possible to obtain the two force components in the interlaminar plane. These components can be expressed in the form

$$\begin{aligned} \{P^U\} &= \{A^U\} + [B^U]\{\Delta^U\} \\ \{P^L\} &= \{A^L\} + [B^L]\{\Delta^L\} \end{aligned} \quad (3)$$

The condition for failure at a given node is now specified by the requirement of zero inplane forces

$$\begin{aligned} \{P^U\} &= 0 \\ \{P^L\} &= 0 \end{aligned} \quad (4)$$

Equations (3) and (4) represent a set of four algebraic equations in the unknown slip components  $\{\Delta^U\}$  and  $\{\Delta^L\}$ .

In the present method the above analysis is systematically applied to each node. First, each node at which interlaminar failure can occur is identified and checked for failure. If failure criterion is exceeded then slip components are calculated as indicated above.

One calculation at each node is, however, not sufficient. It can be easily seen that if failure occurs at two or more adjacent nodes the calculation of zero forces is not independent at each node. For example, if the condition of zero forces is satisfied at the first node, then when the similar conditions are specified at the adjacent node, the forces at the original node will be changed since they share some of the adjacent elements. Consequently, this calculation for each node is performed more

than once in an iterative fashion. In order to perform these calculations, the finite-element computer program from Reference 1 was used and modified by adding subroutines SET and ITERAT. A partial flow chart showing the relative positions of these two subroutines is given in Figure 25. For convenience this flow chart shows only some of the main subroutines which are pertinent to our discussion. The subroutine SET sets some of the data necessary to define the direction and the areas of possible interlaminar cracking. The iteration for satisfying zero interlaminar forces are performed in the subroutine ITERAT and this calculation is repeated a number of times in the loop DO 900 IS = 1, NSLIP. The parameter NSLIP is an input variable. As will be illustrated in a numerical example, this iteration does converge rather quickly. At each iteration additional slip components are calculated and added to the original displacements. In order to achieve a smooth convergence it was found desirable to modify the calculation slightly by only adding half of the slip displacements to the original displacements in each calculation cycle. The reason for this modification is that adjacent nodes share some of the elements and therefore these elements have their nodal displacements modified twice during each calculation cycle. Once the zero forces are obtained at each node, the overall equilibrium of the structure is disturbed and the total equilibrium has to be recomputed. This is done in the loop DO 900 INP = 1, NEQL, where again NEQL is an input variable. It can be seen that for each calculation of equilibrium the node check for failure and calculation of slip components is performed NSLIP times.

In the modified computer program the input cards are similar to those used in the original linear version<sup>1</sup> except three additional input cards were added. All the input parameters are described in Appendix A. The three additional cards are "Crack Iteration Card", "Crack Direction Card" and "Failure Block Definition Card." The listing of the modified computer program is given in Appendix B.

In order to check out the convergence of this method a simple numerical example was chosen. The example consists of a hollow circular cylinder as shown in Figure 26a. One end of the cylinder is clamped and the other is subject to a shear load of  $6.895 \times 10^7$  Pa over part of the boundary. The cylinder is composed of four orthotropic layers oriented in the axial direction. The finite-element grid used in the analysis is shown in Figure 26b. In the radial direction the elements are chosen to correspond to the orthotropic layers. In the computer program it is possible to specify shear failure at any arbitrary interlaminar region and in this example the failure was specified to be possible in the center interlaminar plane. More specifically, failure was allowed at nodal points 8, 13, and 18 shown in Figure 26b.

The actual failure, and resultant nodal slip will depend on the magnitude of the failure stress. At first the failure stress was chosen at a low value of  $5.5 \times 10^6$  Pa. This caused failure at the nodal points 13 and 18 where the original resultant interlaminar shear stresses were  $6.2 \times 10^6$  Pa and  $2.1 \times 10^7$  Pa respectively. This means

that at the nodal point 18 the ratio of the resultant stress to the failure stress was nearly 4. First the convergence of the nodal equilibrium iteration was examined. This iteration is governed by parameter IS. The measure of how fast this iteration converges are the nodal forces in the plane of failure. In this example it is possible to examine the axial force at node 18 on the upper elements of Figure 23a as a function of IS. This force is given in Table IV as a function of IS together with the initial value.

Table IV

Convergence of the Nodal Equilibrium Iteration

<u>Iteration Number IS</u>	<u>Nodal Force (Newton's)</u>
0	$3.86 \times 10^3$
1	$0.128 \times 10^3$
2	$0.0004 \times 10^3$

It can be seen from Table IV that this iteration step is rapidly convergent.

Consider now the convergence of the iteration on the total equilibrium of the structure. This iteration is governed by the parameter INP. Again it is possible to measure this convergence by the nodal axial force at the node 18. In order to obtain a better feeling for this convergence, the example was also repeated for failure stress of  $17.2 \times 10^6$  Pa. Consequently, at the node 18 the resultant stress exceeds the failure stress by a factor of approximately 1.25. Table V shows the value of nodal force for both values of the failure stress as a function of the iteration parameter INP.

Table V

Nodal Force (Newton's)

<u>Iteration Number INP</u>	<u>Failure Stress <math>5.5 \times 10^6</math> Pa</u>	<u>Failure Stress <math>17.52 \times 10^6</math> Pa</u>
1	$3.87 \times 10^3$	$3.87 \times 10^3$
2	$1.61 \times 10^3$	$1.06 \times 10^3$
3	$.38 \times 10^3$	$0.30 \times 10^3$
4	$.347 \times 10^3$	$0.0084 \times 10^3$

It can be seen from Table V that when the failure stress is closer to the actual stress, then the convergence is faster as expected. However, even when the failure stress has been exceeded by a factor of 4, as in the case of  $5.5 \times 10^6$  Pa failure level, the convergence to 10 percent of the original force is achieved in four cycles.

B. Matrix Material Failure

The results presented in Figure 22 show that the interlaminar stresses in the cylindrical model used in the experimental investigation are very small compared to the other stresses and are confined to a small region near the ends of the cylinder. Consequently, it is not possible that the experimentally observed nonlinear effects could be explained in this case by the interlaminar failure model described in the previous sections. This suggests that another failure mode is occurring inside the orthotropic plies. Since the nonlinear effects were observed at fiber stresses equal to a fraction of the ultimate values, this suggests that fiber failure can be ruled out as the cause and matrix material failure must be considered.

In order to develop a failure model for the matrix, it is recognized that the transverse shear stress is transferred between the fibers and the matrix, and this stress will depend on the position inside the composite material. This can be illustrated by considering a schematic representation of a composite material as shown in Figure 27. In this diagram, a rectangular cube of the material is shown subjected to shear stress  $\sigma_{ns}$  and the fibers are assumed to be randomly packed. In certain region of the material, labelled A, the fibers may be close together and in other region, labelled B, the fibers will be relatively far apart. If the fiber material is assumed to be much more rigid than the matrix, as is the case for the glass reinforced materials, it can be shown that the shear stress in region A will be appreciably larger than in the region B. For idealized materials with regular fiber arrangement, this variation has been calculated analytically<sup>4,5</sup> and numerically<sup>6,7</sup> by other investigators, but in the case of real materials with random packing this is not possible. Therefore, we proceed with an empirical relationship which states that the local matrix shear stress  $(\sigma_{ns})_m$  is proportional to the overall shear strain in the composite material  $\gamma_{ns}$  and it can be expressed in the form

$$(\sigma_{ns})_m = K \gamma_{ns} \quad (5)$$

<sup>4</sup>J. A. Kies, "Maximum Strains in the Resin of Fiberglass Composites," NRL Report 5752, March 1962.

<sup>5</sup>J. C. Schultz, "Maximum Stresses and Strains in the Resin of a Filament-Wound Structure," Presented at the 18th Annual Meeting of the Reinforced Plastics Conference, SPI, February 1963.

<sup>6</sup>D. F. Adams and D. R. Doner, "Transverse Normal Loading of a Unidirectional Composite," J. Composite Materials, Vol. 1, No. 2, 1967, p. 152.

<sup>7</sup>D. R. Adams and S. W. Tsai, "The Influence of Random Filament Packing on the Transverse Stiffness of Unidirectional Composites," J. Composite Materials, Vol. 3, July 1969, p. 368.

where  $K$  is a proportionality parameter and varies throughout the composite material. Some idea of how  $K$  can vary can be obtained from the previous studies on idealized materials, and it has been found to be dependent on the fibers and the matrix.<sup>4,5,6,7</sup>

Consider now the problem of matrix failure. Since the various regions of the matrix are subjected to different levels of shear stress, the failure of the material will proceed gradually through the material with the regions most highly stressed failing first. Consequently, for a given shear strain  $\gamma_{ns}$  a certain amount of matrix will fail which in turn will lead to the reduction of the shear modulus  $G_{ns}$ . We can express this by the relation

$$G_{ns} = G_{ns0} P(\gamma_{ns}) \quad (6)$$

where  $G_{ns0}$  is the original value of the modulus, and the function  $P(\gamma_{ns})$  contains the modulus reduction factor which depends on the applied shear strain  $\gamma_{ns}$ , the elastic properties of the components, and the fiber geometry. Once the geometry of the composite material and the ultimate stress are determined we can regard Equation (6) as a function of  $\gamma_{ns}$  only. In view of the fact that the random fiber configuration in real materials prevents deterministic solution, we must regard Equation (6) as an empirical relation to be established experimentally. The objective here is to do this using the experimental results described in the previous section.

As the first step in determining the relation expressed by Equation (6), it is assumed that the shear failure will only occur in the four inner plies where the maximum shear stress occurs as seen in Table III. In the next step a specific value of the function  $P(\gamma_{ns})$  in Equation (6) is chosen. The first choice can be denoted by  $P_1$  and therefore the shear modulus is given by

$$G_{ns} = G_{ns0} P_1 \quad (7)$$

At this point it is not known what internal pressure level  $p$  will produce the particular amount of failure corresponding to  $P_1$ . Consequently, the pressure is chosen in the form

$$p = cp_0 \quad (8)$$

where  $p_0$  is a convenient known level of pressure, which in our case we used  $6.895 \times 10^6$  Pa and  $c$  is an unknown factor. Stress analysis is now performed using the pressure  $p_0$ . From this analysis we can use either the results for the circumferential or the longitudinal strains to compare to the results obtained by initial calculation for the undamaged material using  $G_{ns0}$  modulus. In this analysis the longitudinal strains were compared. For this comparison a ratio  $\epsilon_z/\epsilon_{z0}$  is calculated where

$\epsilon_z$  and  $\epsilon_{z0}$  are the strains corresponding to the moduli  $G_{ns}$  and  $G_{ns0}$  respectively. Using the solid line in Figure 17 it is possible to calculate the experimental value for the ratio  $\epsilon_z/\epsilon_{z0}$  as a function of the pressure. At this stage the calculated and the experimental values are compared and this determines the actual pressure which corresponds to the chosen value of  $P_1$  and also, from Equation (8), the constant  $c$  is determined. Knowing this constant, the shear strain corresponding to  $P_1$  is known. By repeating this process for different values of the function  $P(\gamma_{ns})$  given by  $P_2, P_3$  etc., a continuous relation can be established defining this function. In the present calculations four values of  $P(\gamma_{ns})$  were used which varied from  $1/2$  up to  $1/32$ . This last value was found to correspond to the experimental data near the failure region, and it was reasonable not to reduce the modulus any further. Figure 27 shows variation of the function  $P(\gamma_{ns})$  with the shear strain. Using function  $P(\gamma_{ns})$  the circumferential strain was calculated and compared to the experimental results in Figure 18. It can be seen that a good agreement is obtained with the experimental data. The calculated longitudinal response will agree with the solid curve in Figure 17 since this data was used to define  $P(\gamma_{ns})$ .

In the calculations which lead to the results shown in Figure 28, the shear failure was allowed only in the four inner plies. The failure could also occur, to a much smaller extent, in the two outer plies with the helix angle of 83 degrees. Consequently, the results in Figure 28 can be considered as a first approximation. In order to establish the effect of the failure in the outer plies, the function  $P(\gamma_{ns})$  from Figure 28 was used for both plies and stress analysis calculations were repeated allowing both inner and outer plies to fail. The results were only slightly different from those in which only the inner plies failed.

Once the model, which predicts the nonlinear response of this particular cylindrical configuration, has been established, it is possible to use it to examine the effect on the stress levels. One interesting result is the difference in the normal stresses in the fiber direction in the linear and the nonlinear analyses. For example, it is interesting to compare these stresses in the outer plies which carry the highest stresses. Using a pressure value of  $27.58 \times 10^6$  Pa, which is close to the failure load, the ratio of the fiber stresses from the nonlinear to the linear analysis was found to be approximately 1.1. This means that the actual fiber stresses are about 10 percent higher than those predicted by the linear analysis. By the same token it may be mentioned that the fiber stresses in the inner plies are reduced by the nonlinear effects. These results are illustrated in Table VI where the fiber stresses are shown for the undamaged and the damaged situation for the six plies. Two different sets of damaged data are presented and these correspond to allowing matrix damage in the inner plies only, and then allowing both inner and outer plies to fail.

Table IV

Comparison of Fiber Stress  $\sigma_n$  ( $\pm 10^6$  Pa) for  
 Undamaged and Damaged Matrix Situations

<u>Ply Number</u>	<u>Undamaged Stress</u>	<u>Inner Plies Damaged Only</u>	<u>Inner &amp; Outer Plies Damaged</u>
1	100.6	97.3	97.2
2	99.7	95.8	95.6
3	99.0	94.9	94.9
4	97.9	93.4	93.3
5	191.7	216.3	216.9
6	189.6	214.0	214.7

It can be seen from Table IV that the damage in the outer plies produces little additional changes in the stresses.

IV CONCLUSIONS

From the analysis of the recoilless rifle configuration we can conclude that the finite-element computer programs<sup>1,2</sup> which have been developed, are capable of detailed stress analysis of rather complex structures. Since the analysis allows for the modelling of each ply as a separate material, the interlaminar stresses, as well as individual ply stresses, are generated by these programs. These programs should be a valuable tool in future engineering analyses of composite material structures.

Two different models for describing failure of composite materials have been developed. One of these models analyzes interlaminar failure and a computer program has been developed for this model. The computer program uses a finite-element method and an iteration scheme for determining where and when failure occurs. Every time failure occurs at any point in the structure, the total equilibrium of the structure is reevaluated. The second failure model is based on matrix failure inside individual plies by transverse shear stresses. In this model the effect of failure is to reduce the transverse shear modulus of the ply. Using this model, the stress calculation can be performed by linear finite-element model by varying the material properties. The results of this model are compared with nonlinear experimental data for cylindrical six ply models. It is found that this model does predict the correct longitudinal and circumferential response.

ACKNOWLEDGEMENT

This work was sponsored by the U.S. Army Ballistic Research Laboratories, Aberdeen Proving Ground, MD, under Contract No. DAAD05-73-C-0197, as part of the Short-Range Man-Portable Antitank Weapons Technology (SMANT) Program.

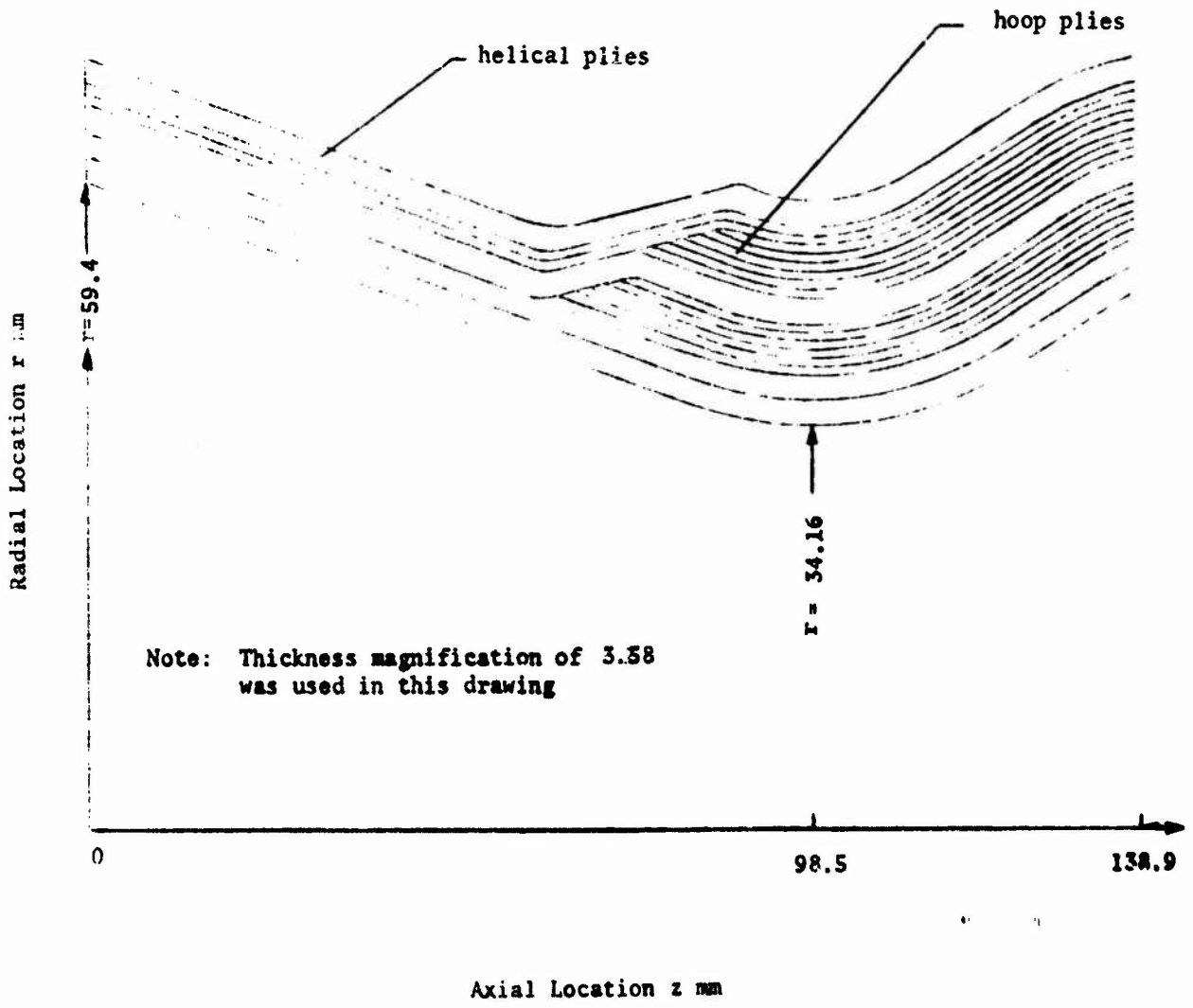


Figure 1. Nozzle section of the recoilless rifle.



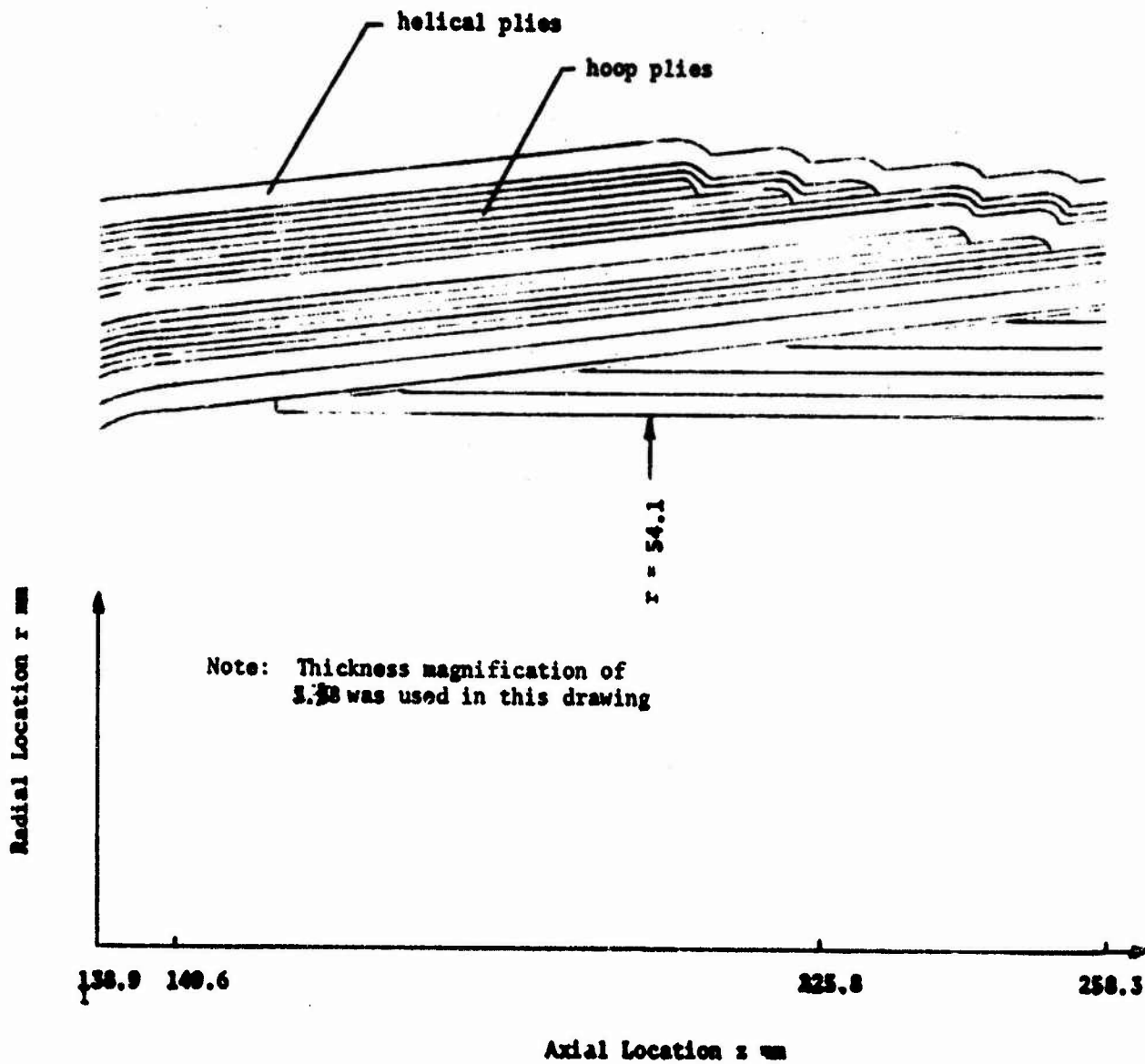


Figure 2. Center section of the recoilless rifle.

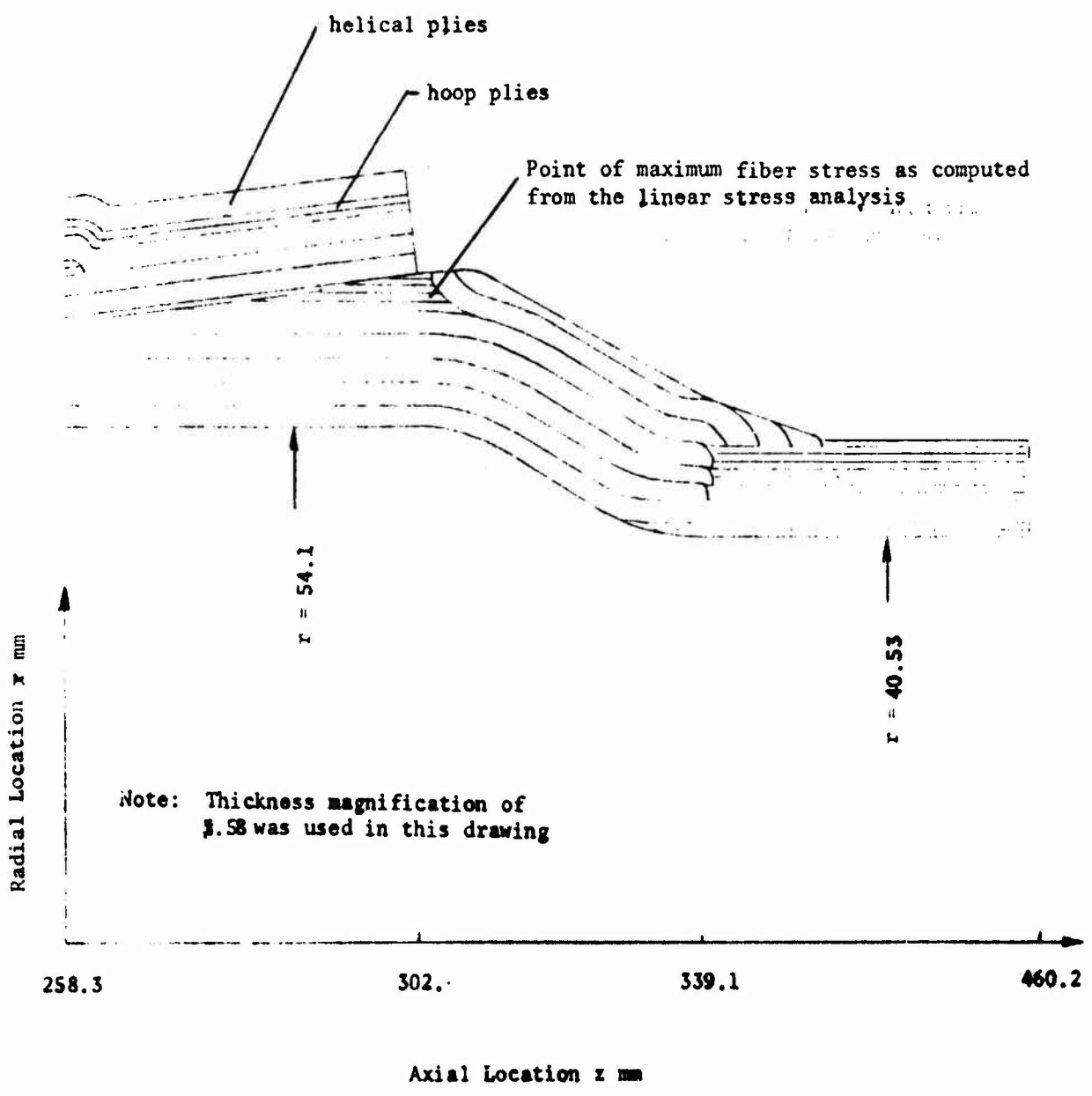


Figure 3. Forward section of the recoilless rifle.

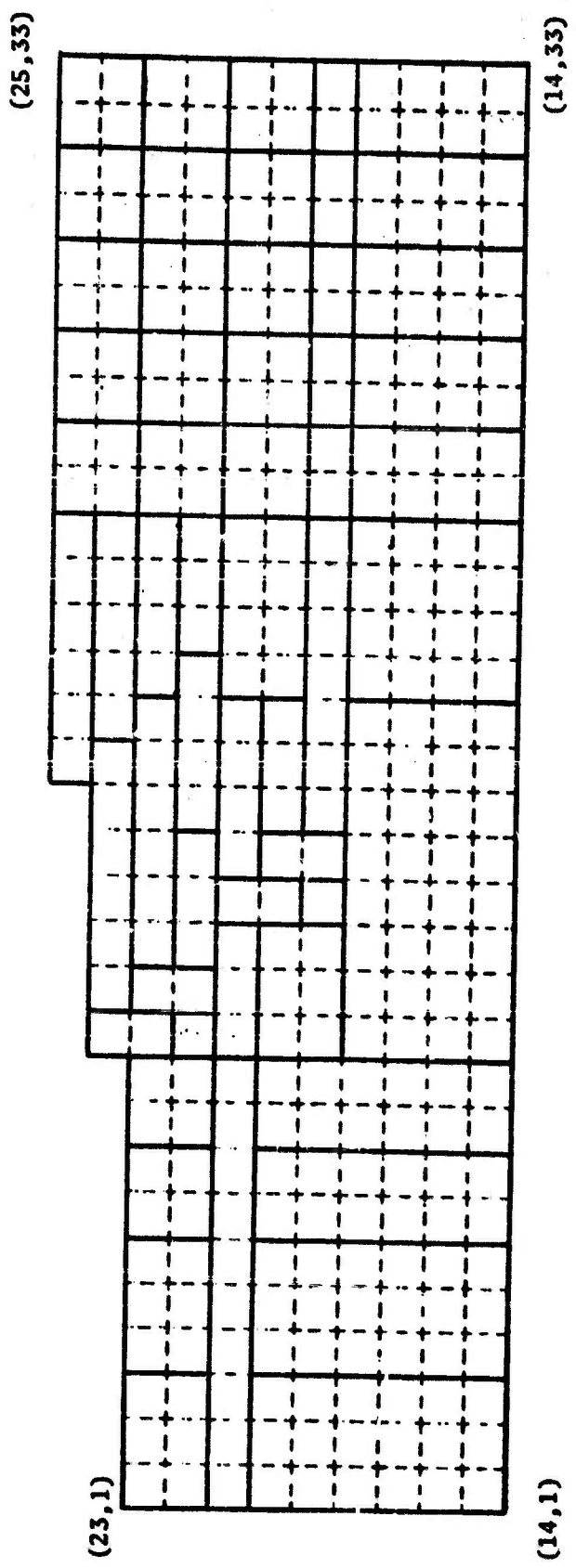
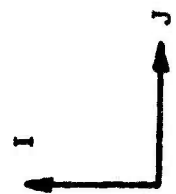


Figure 4. Finite-element grid in the I,J coordinates for the aft section.



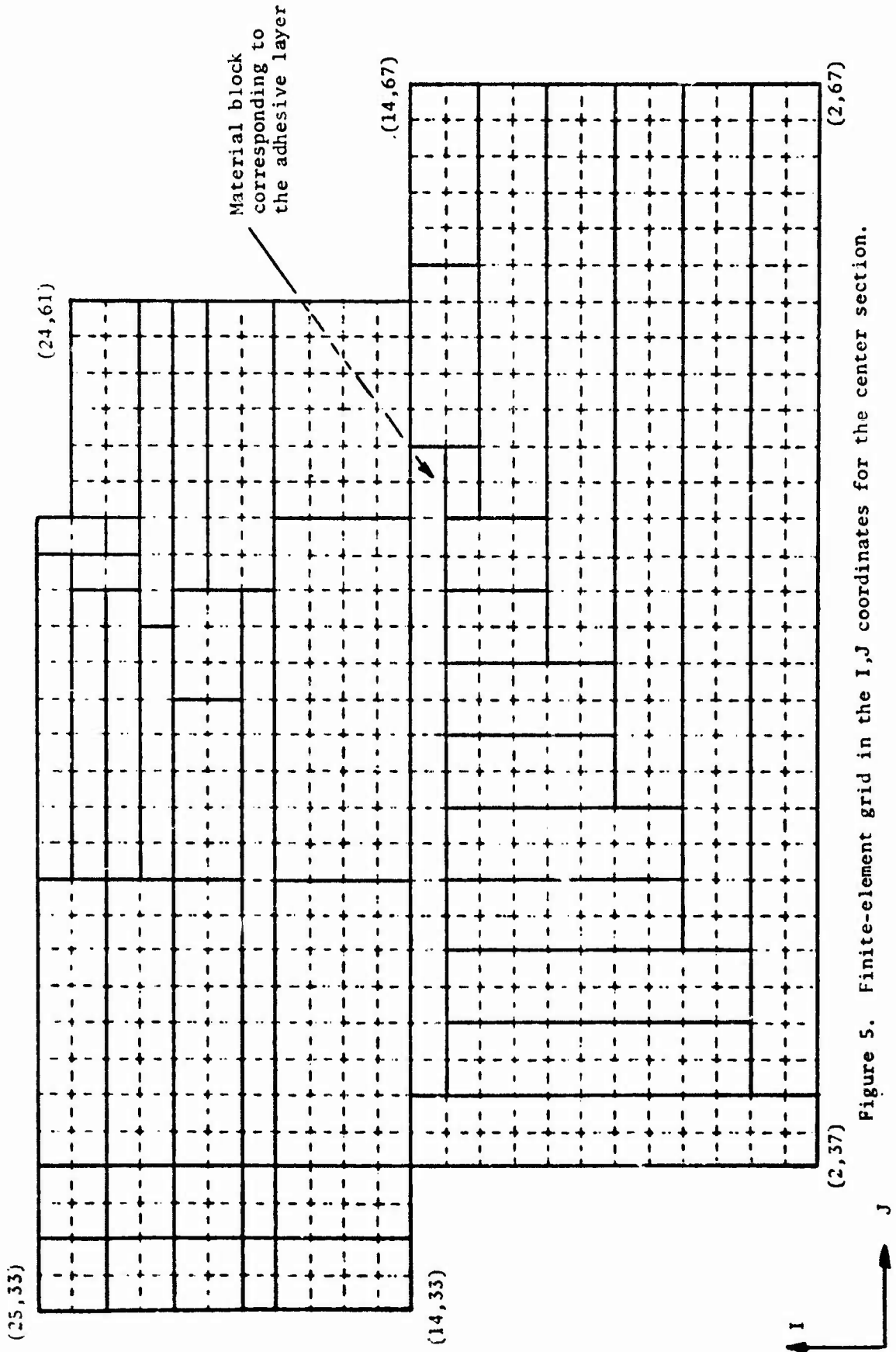


Figure 5. Finite-element grid in the I,J coordinates for the center section.

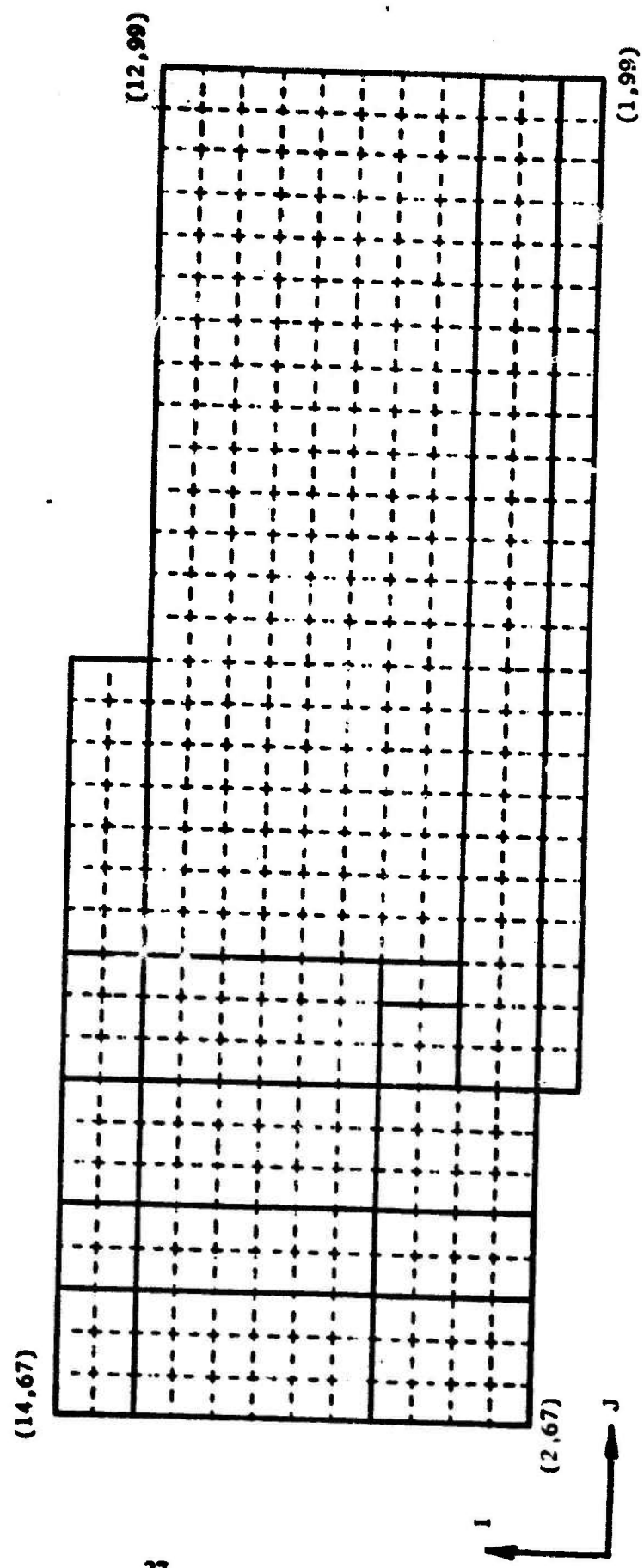


Figure 6. Finite-element grid in the I,J coordinates for the forward section.

Note: Thickness magnification of 20 was used in this diagram.

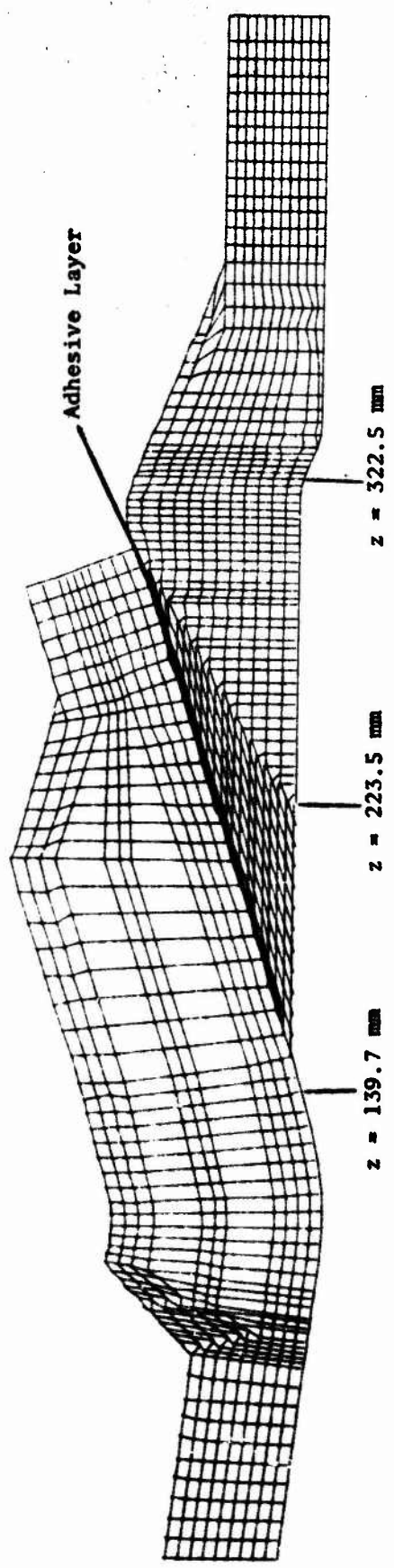


Figure 7. Finite-element grid for recoiless rifle.

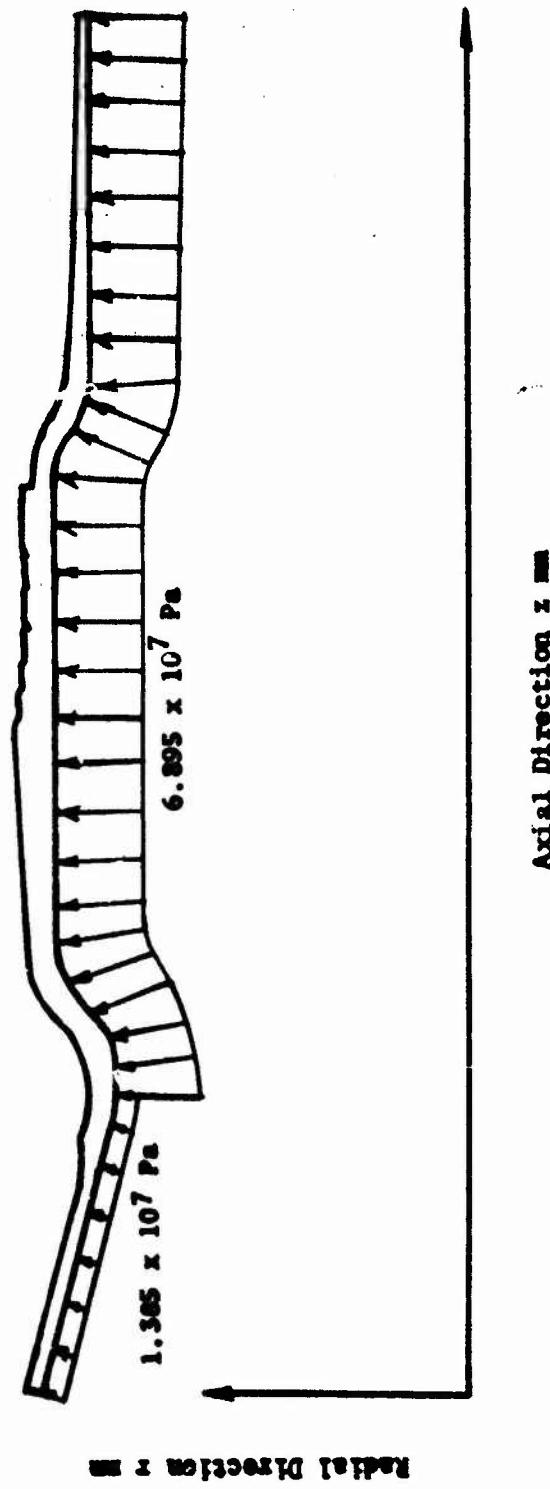


Figure 8. Internal pressure distribution

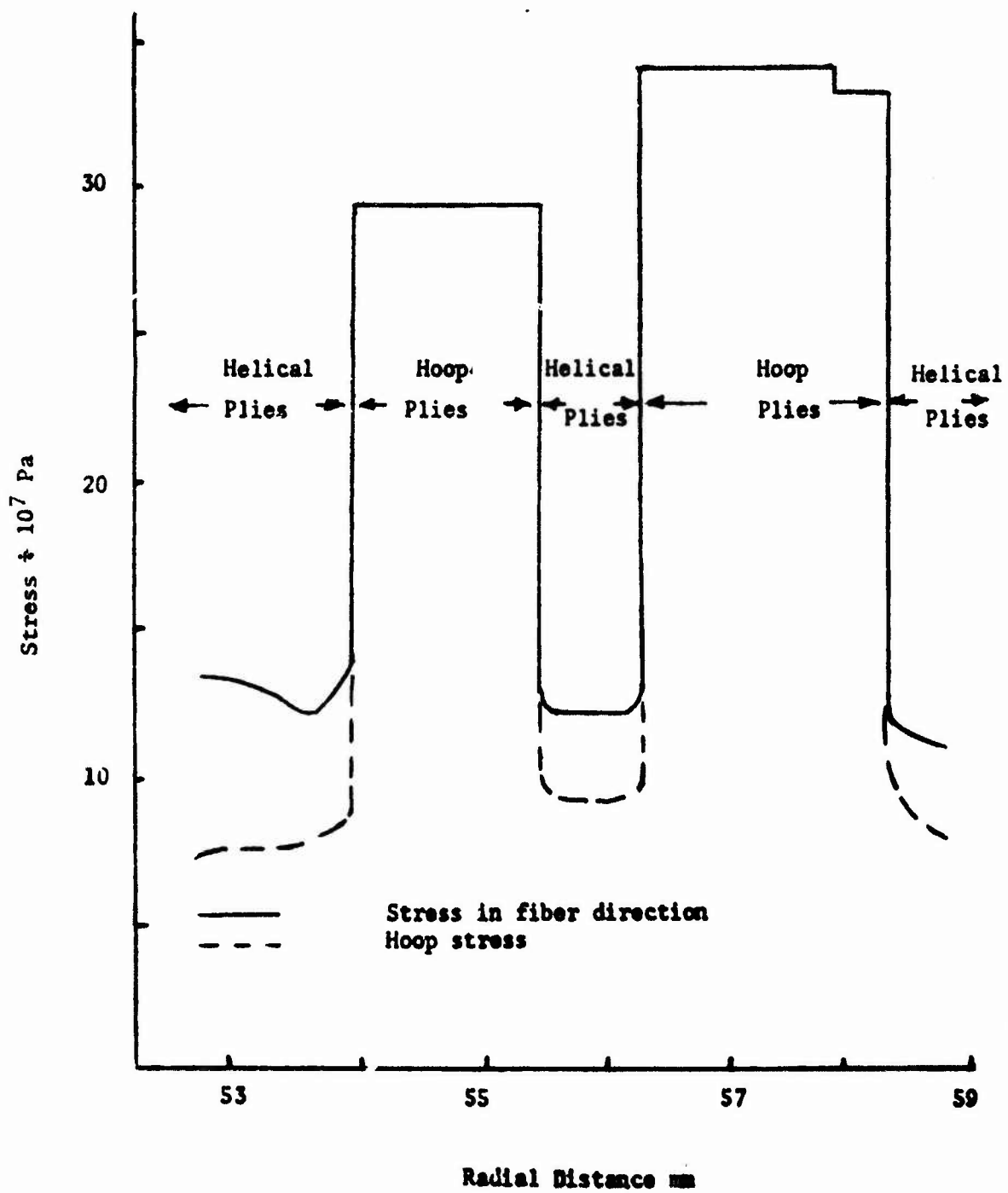


Figure 9. Radial distribution of fiber and hoop stress at axial location  $z = 139.7$  mm.



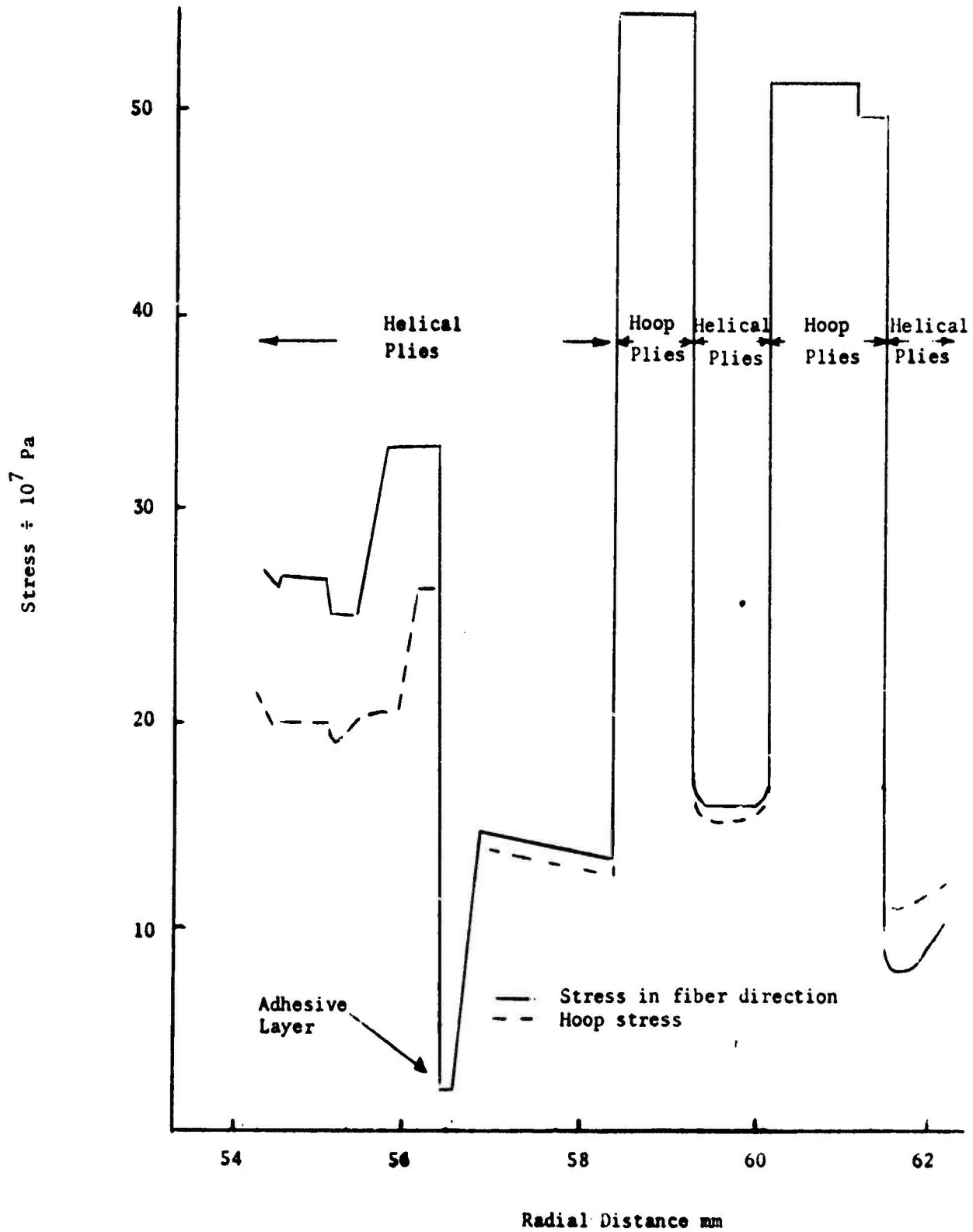


Figure 10. Radial distribution of fiber and hoop stresses at axial location  $z = 223.5$  mm.

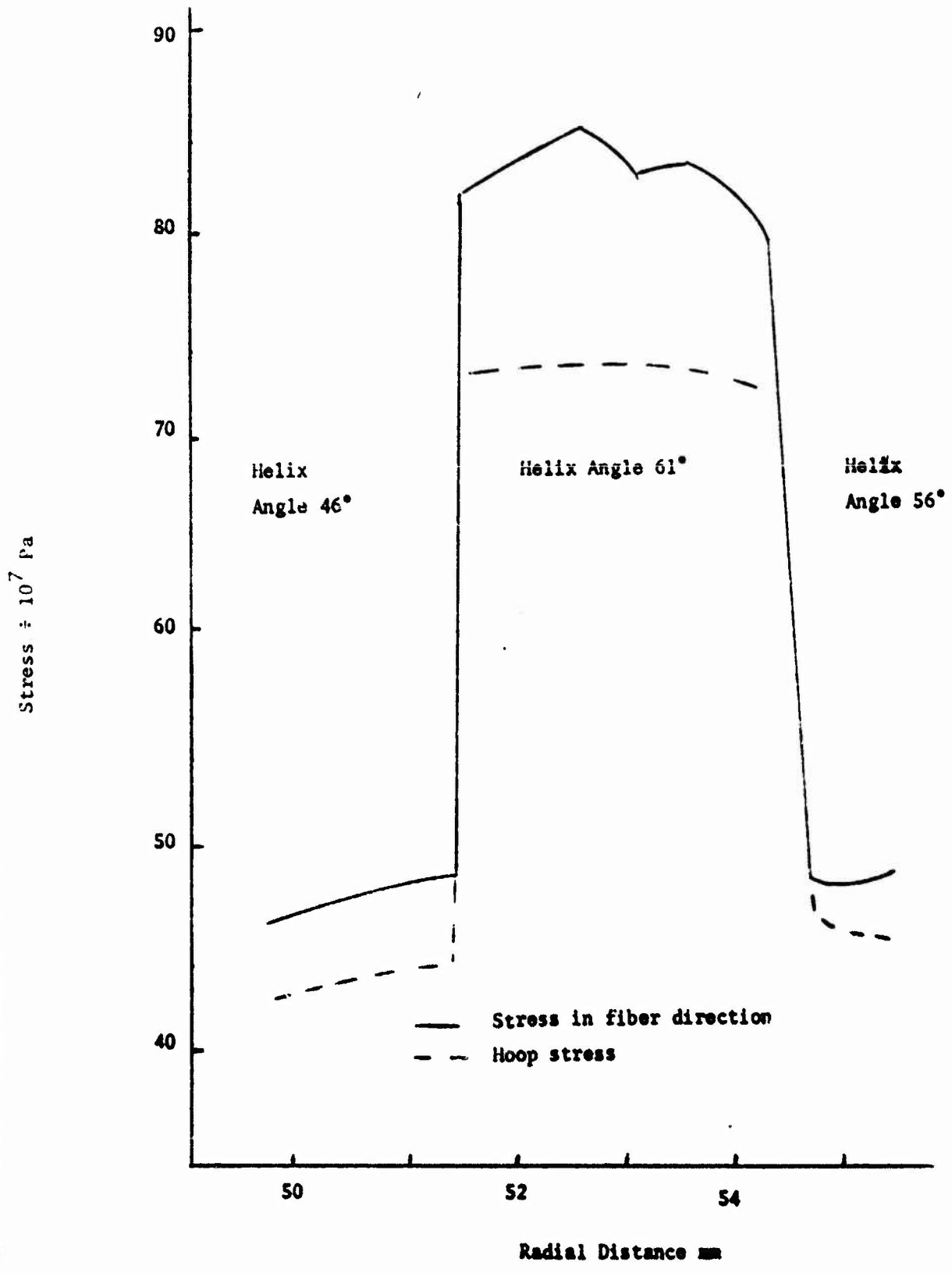


Figure 11. Radial distribution of fiber and hoop stresses at axial location  $z = 322.5$  mm

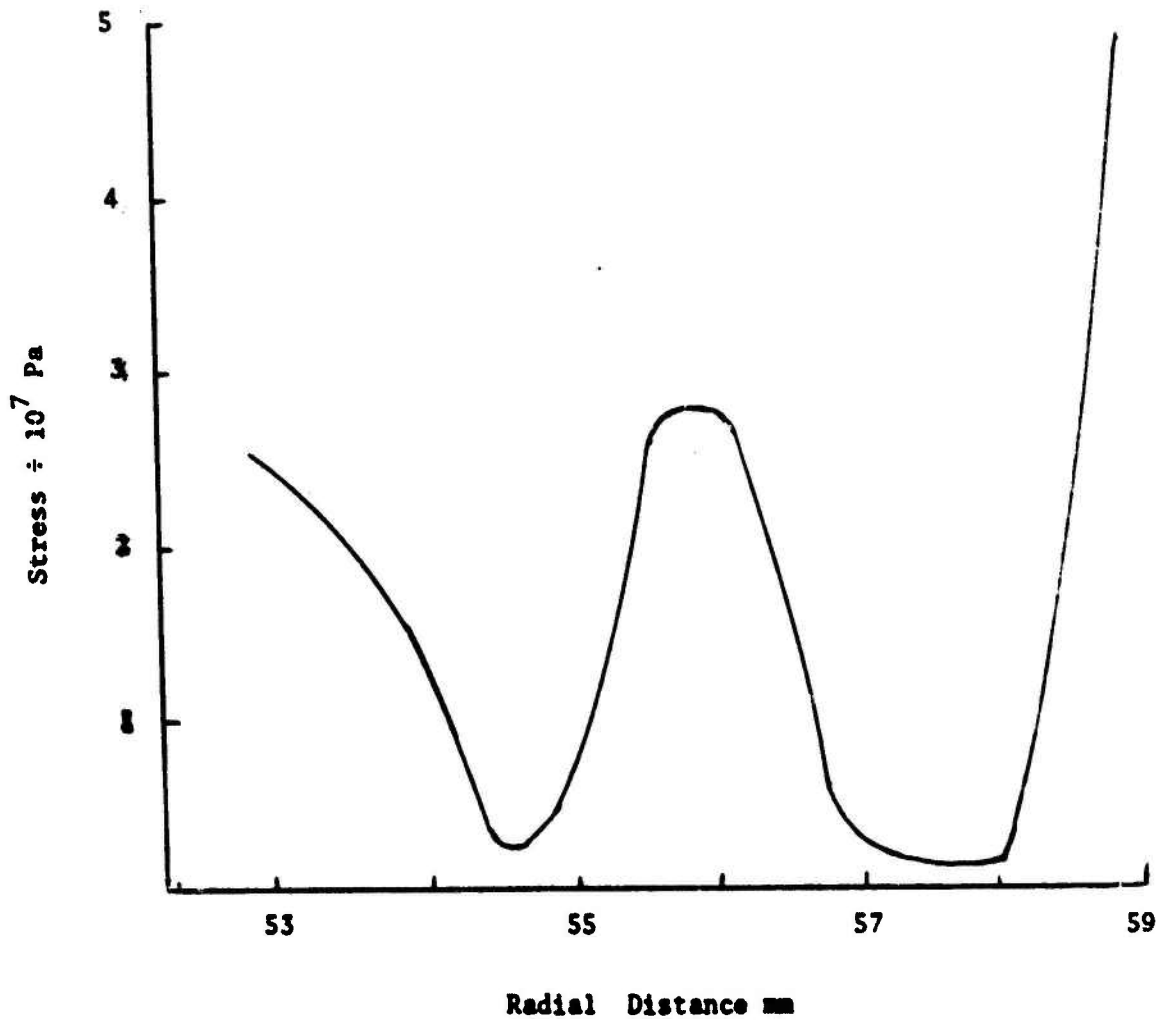


Figure 12. Radial distribution of the magnitude of the shear stress  $\sigma_{ns}$  at axial location  $z = 139.7$  mm.

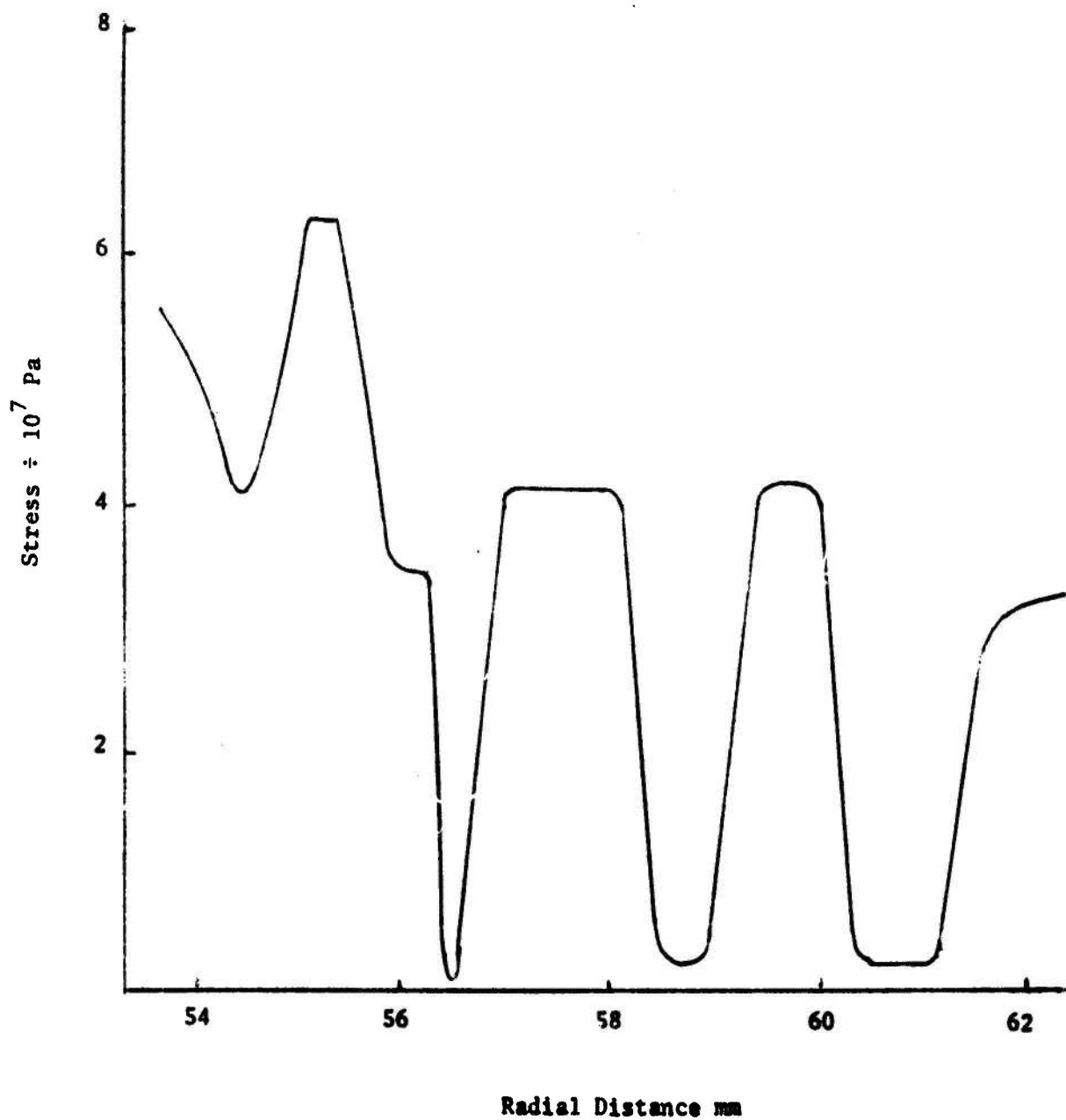


Figure 13. Radial distribution of the magnitude of the shear stress  $\sigma_{ns}$  at axial location  $z = 223.5$  mm.

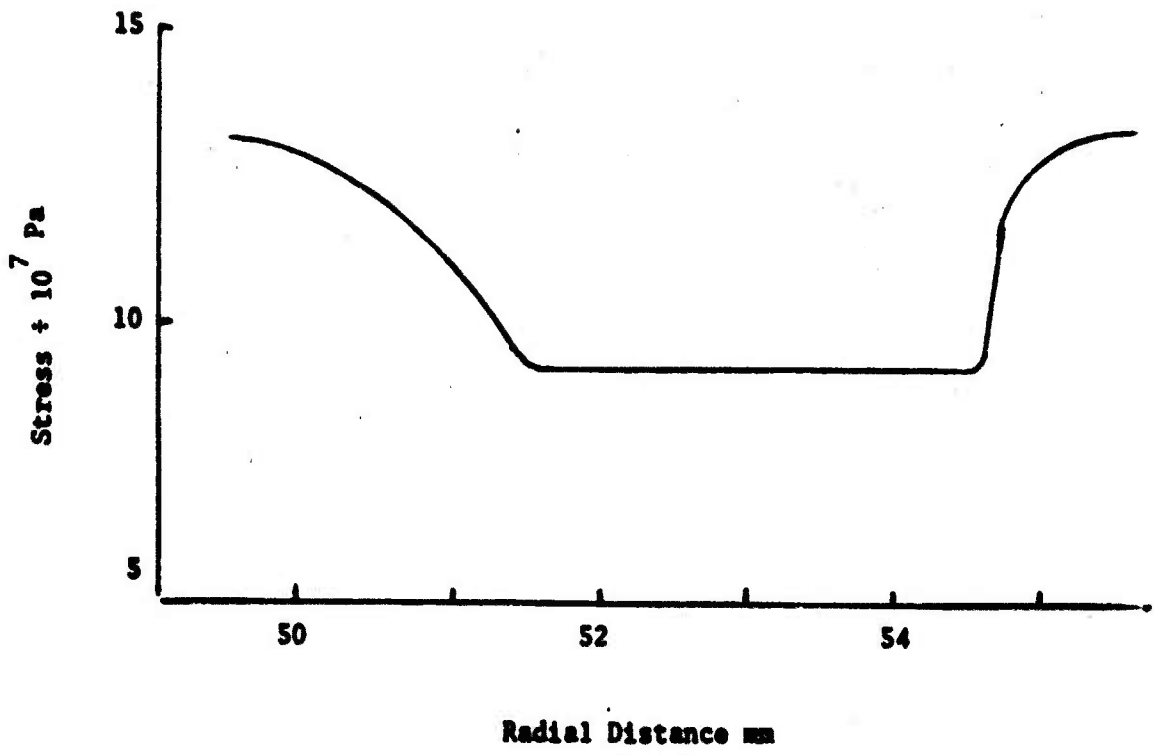


Figure 14. Radial distribution of the magnitude of the shear stress  $\sigma_{ns}$  at axial location  $z = 322.5$  mm.

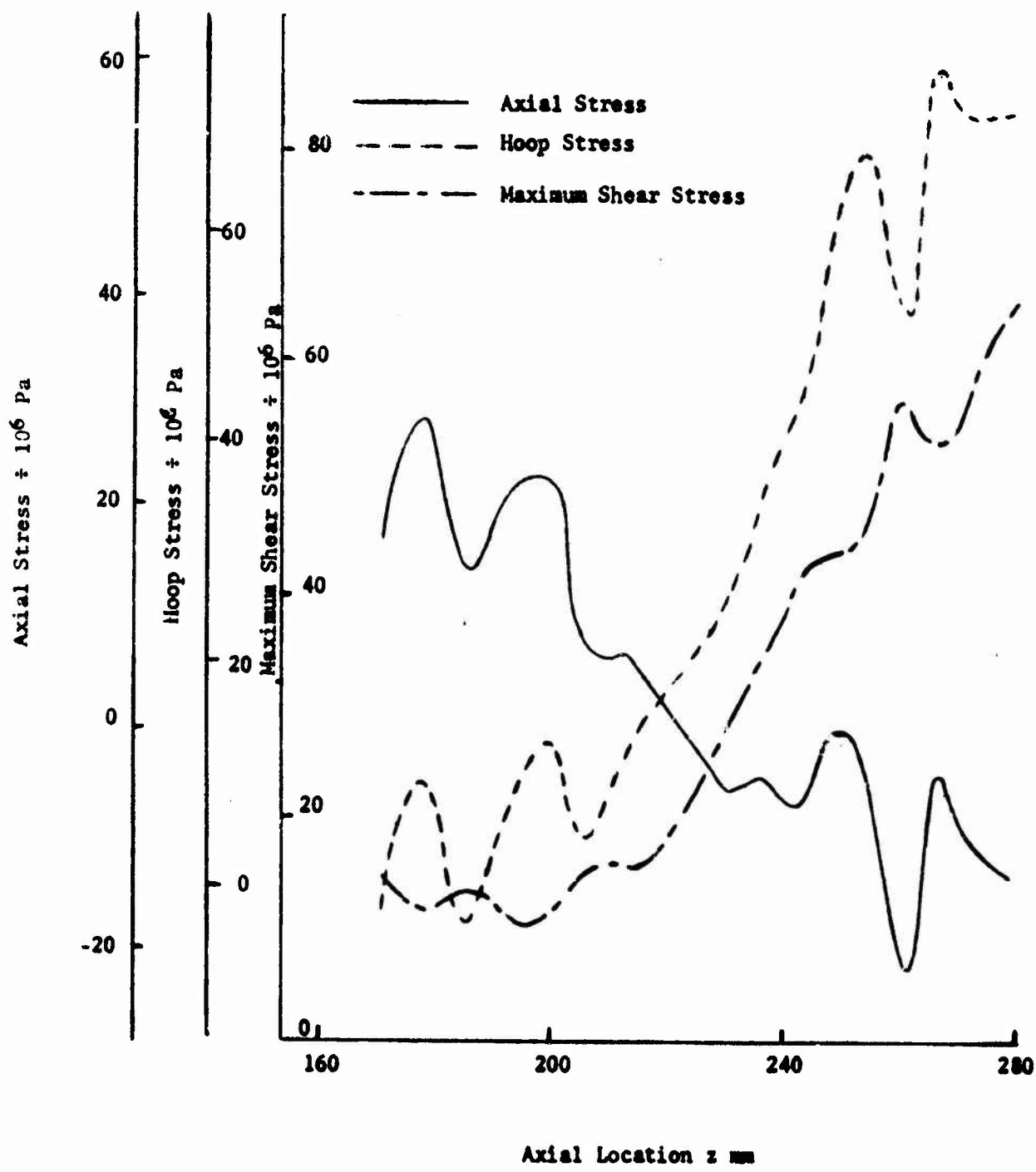


Figure 15. Axial distribution of axial stress, hoop stress, and maximum shear stress in the adhesive layer.

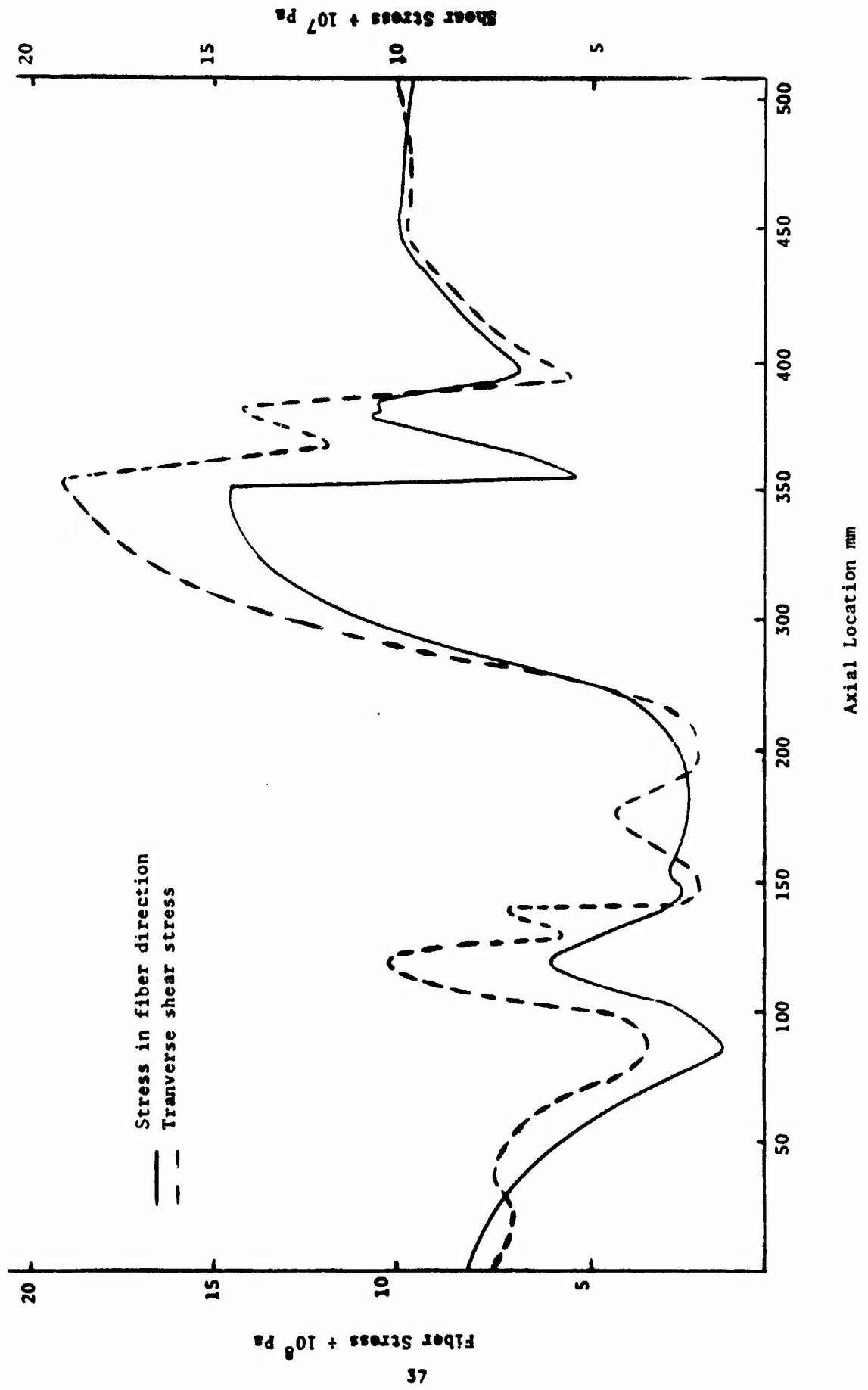


Figure 16. Axial distribution of the maximum fiber stress  $\sigma_n$  and shear stress  $\sigma_{ns}$ .

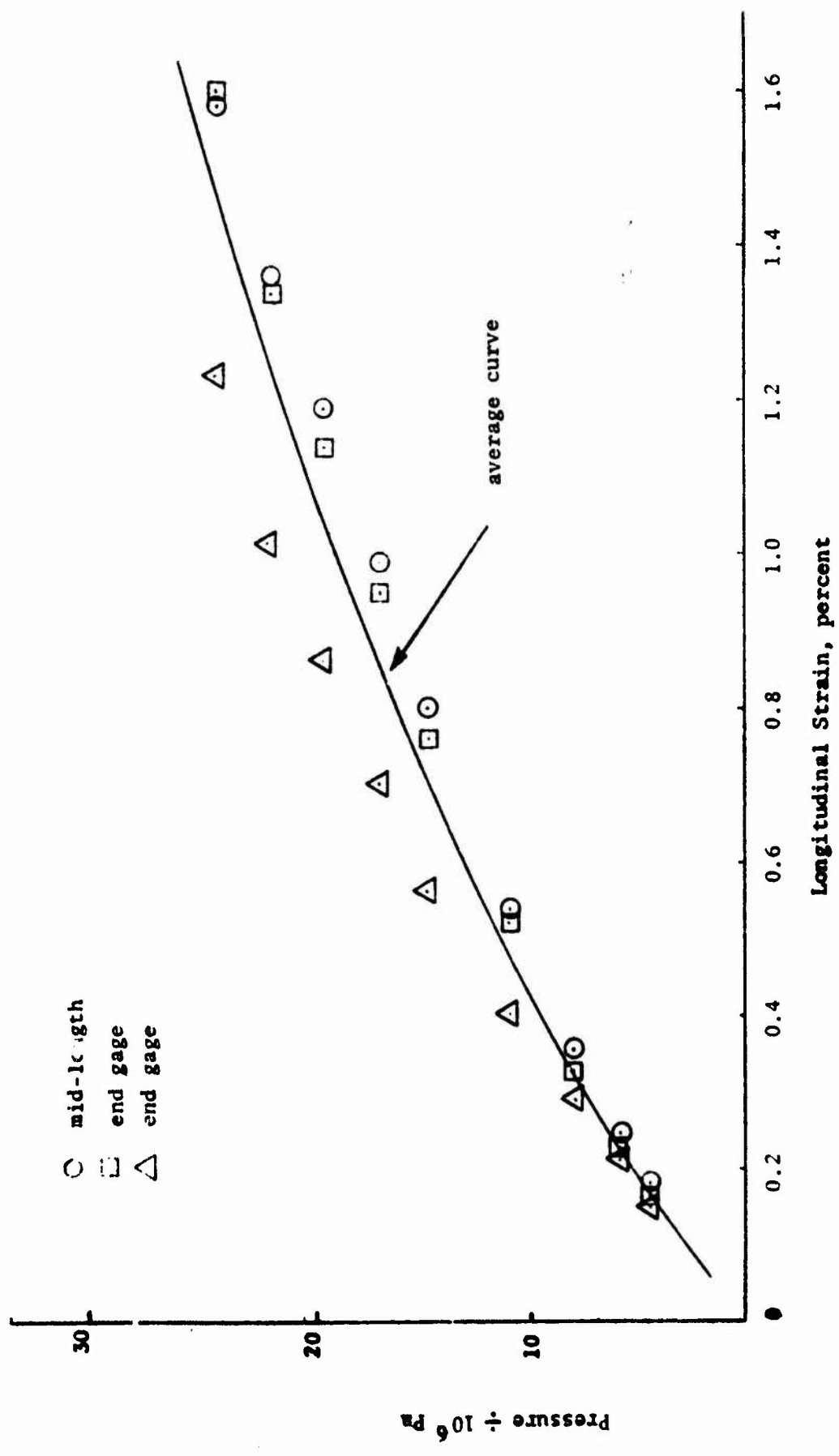


Figure 17. Longitudinal strain measured as a function of internal pressure.



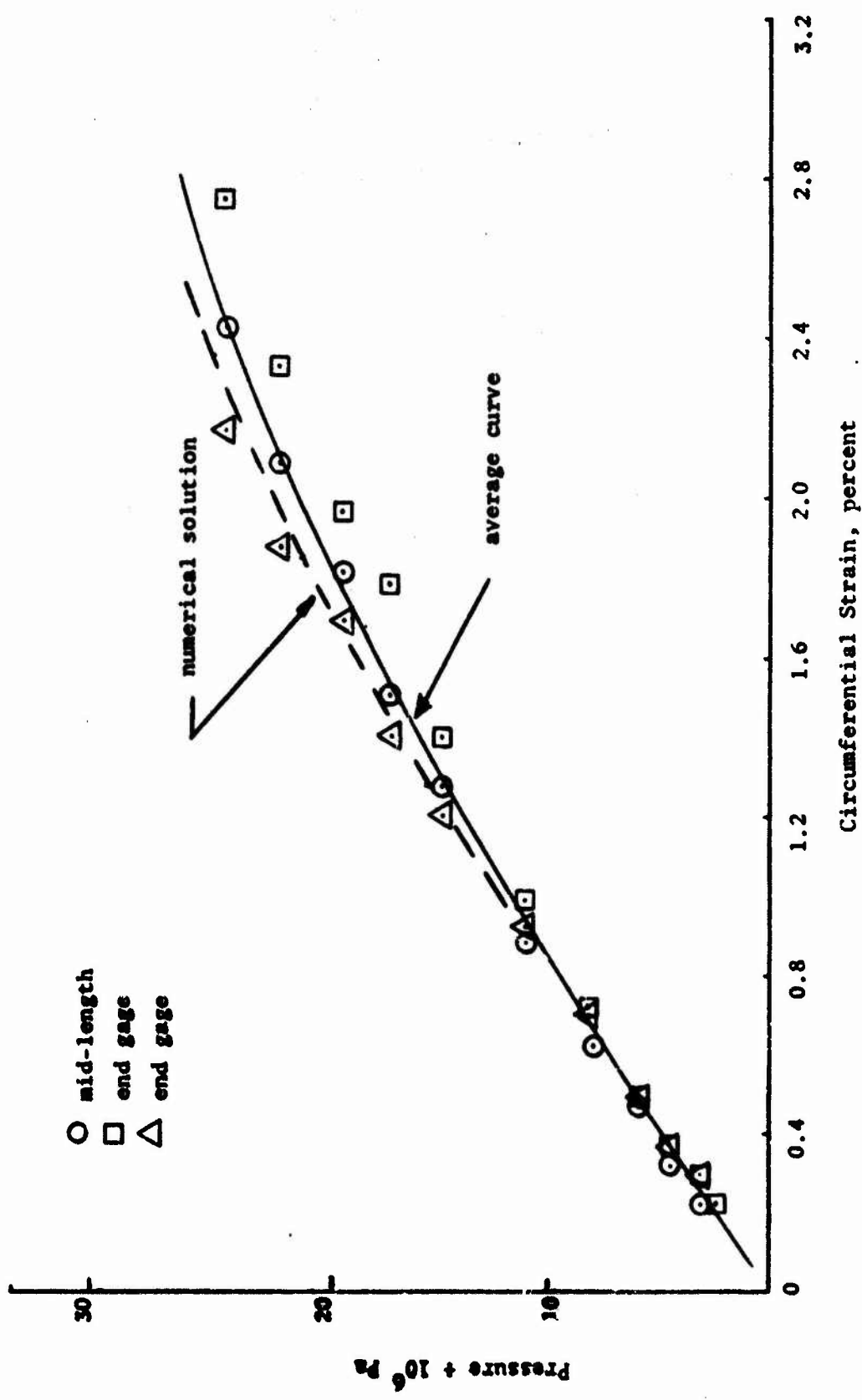


Figure 18. Circumferential strain measured as a function of internal pressure.

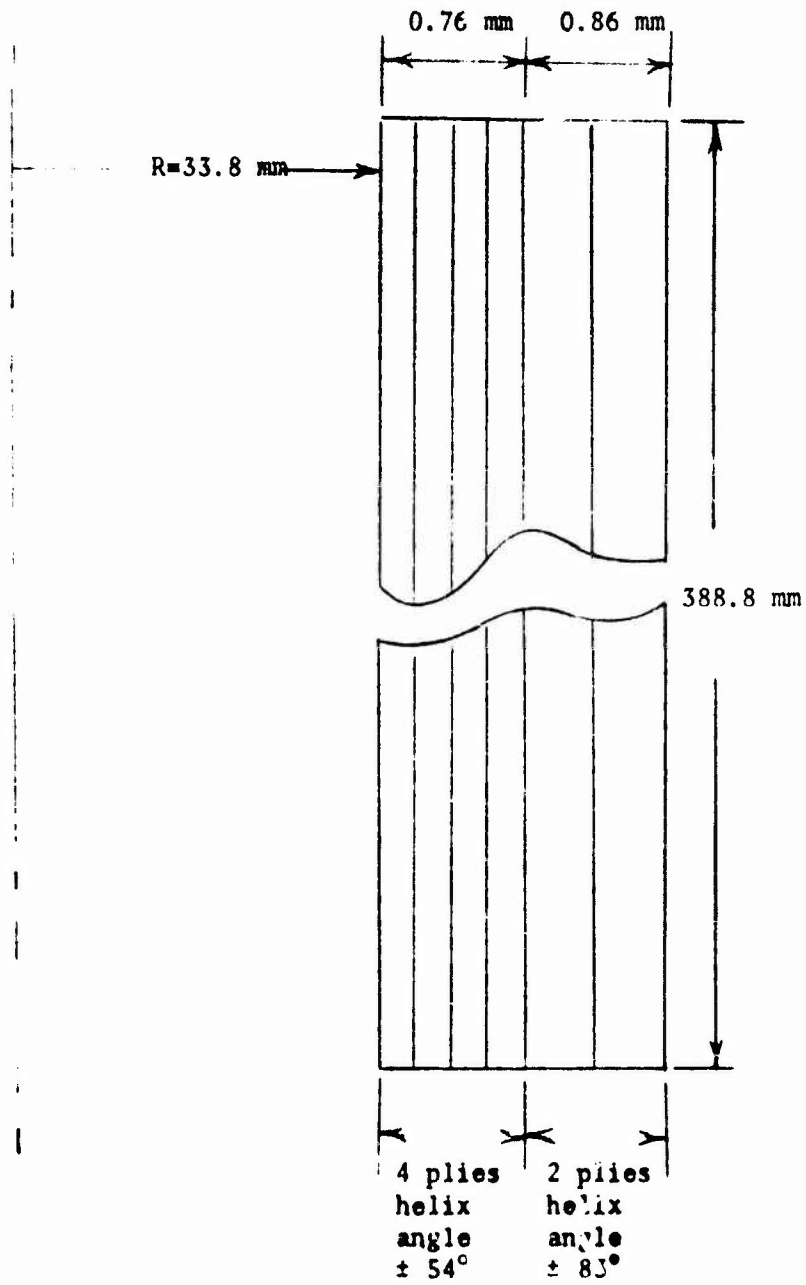


Figure 19. Arrangement of orthotropic plies in the test cylinder.

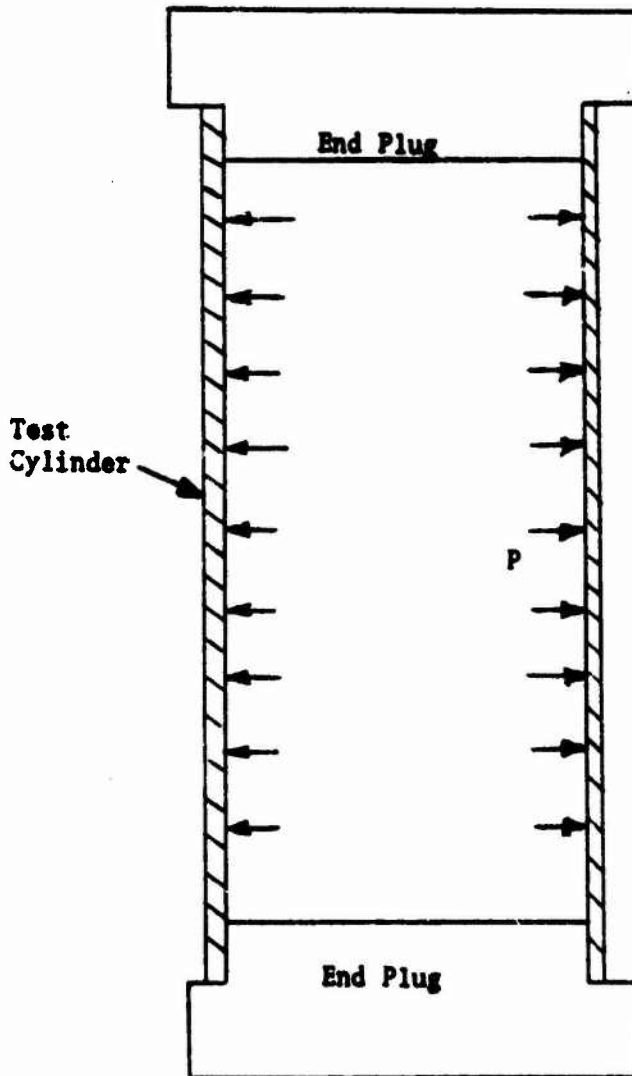


Figure 20. Experimental Test Arrangement.

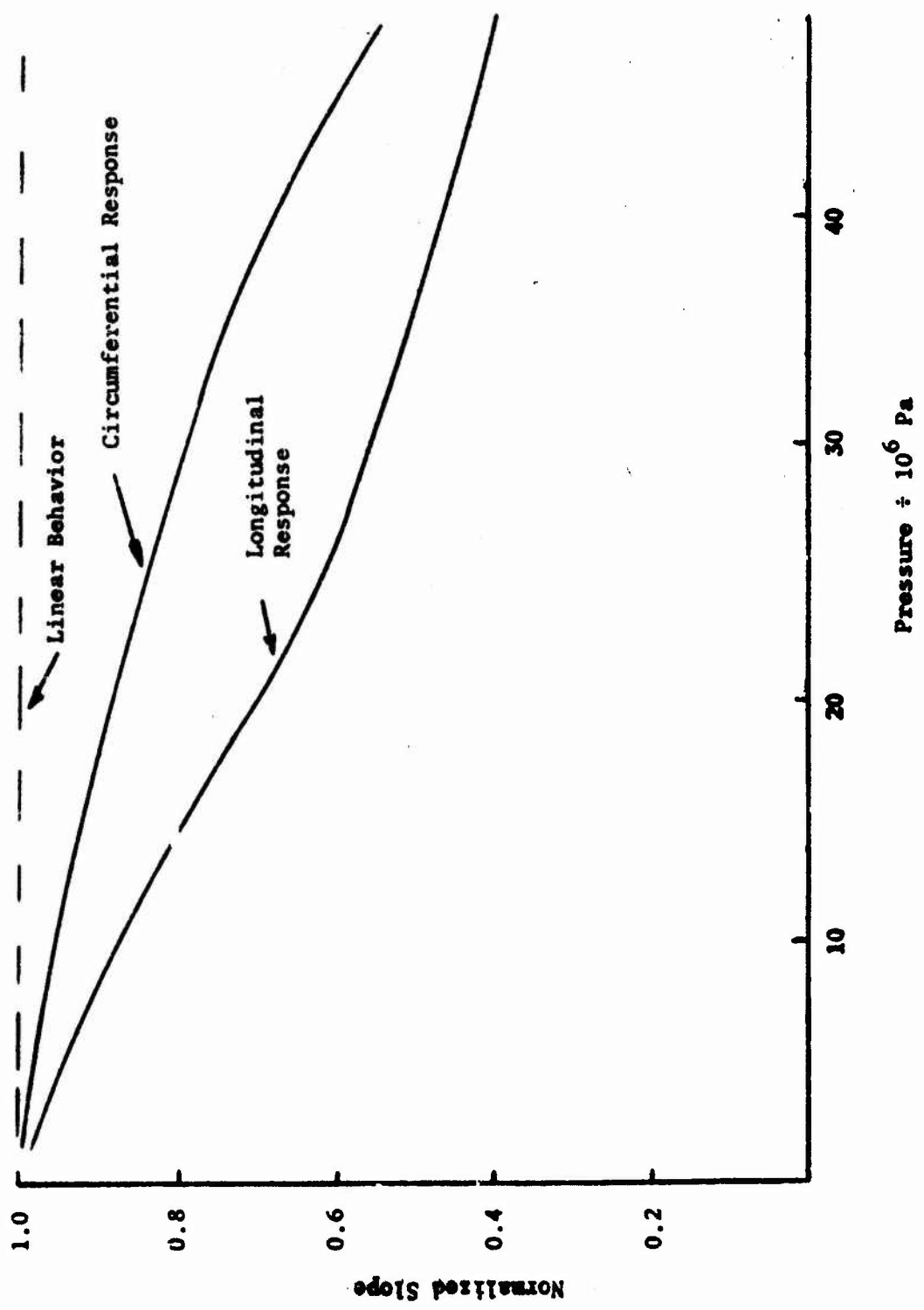


Figure 21. Nondimensional slope variation with pressure

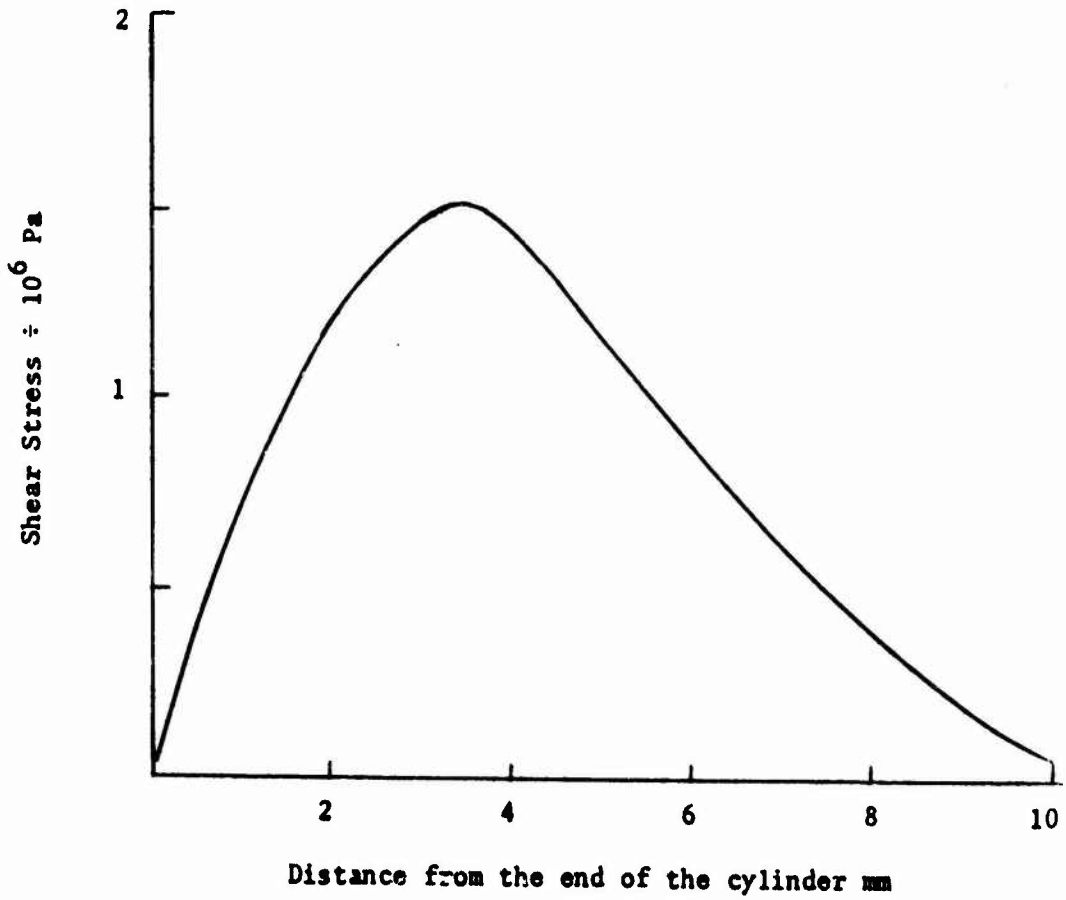


Figure 22. Axial distribution of the shear stress  $\sigma_{rz}$ .

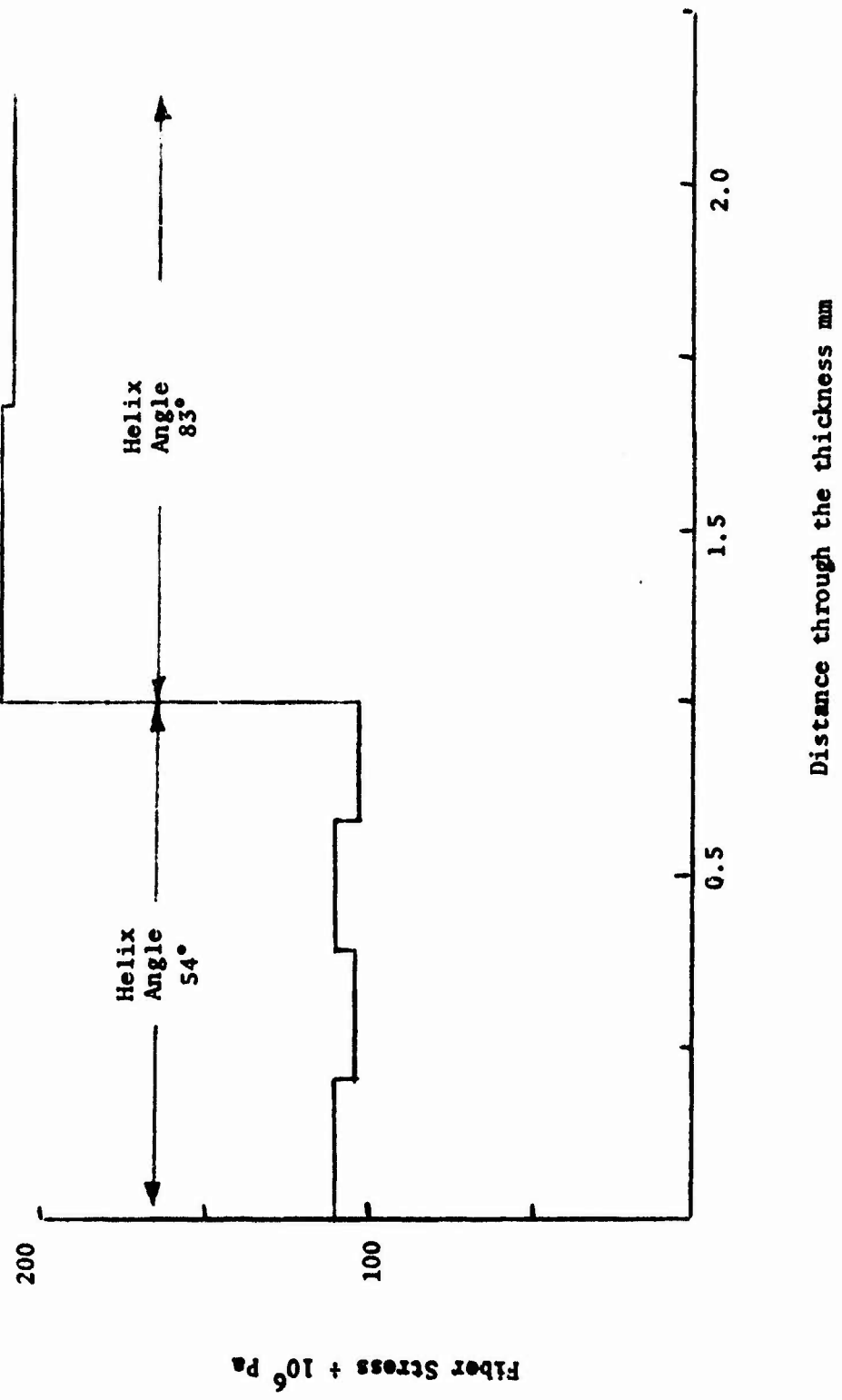


Figure 23. Radial distribution of the fiber stress  $\sigma_n$  calculated by using 4 elements to represent each ply in the thickness direction.

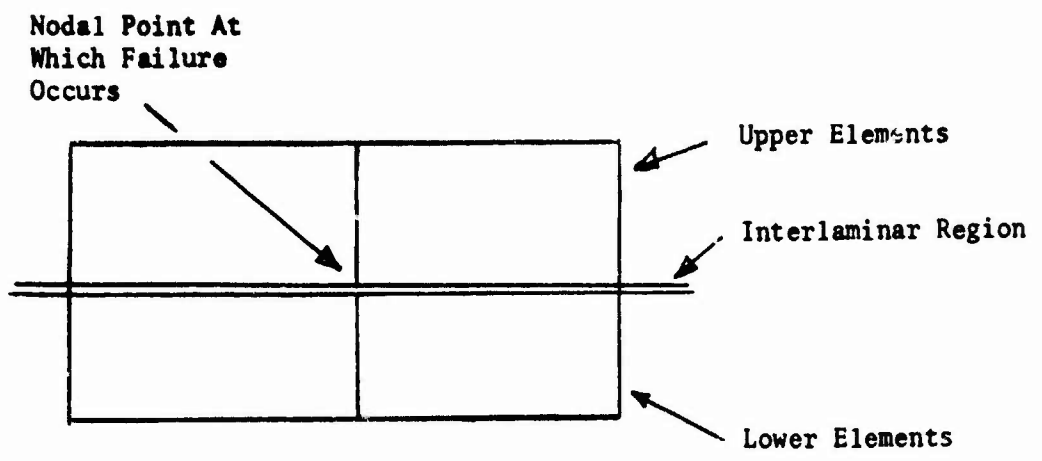


Figure 2a. Nodal Point On Interlaminar Plane

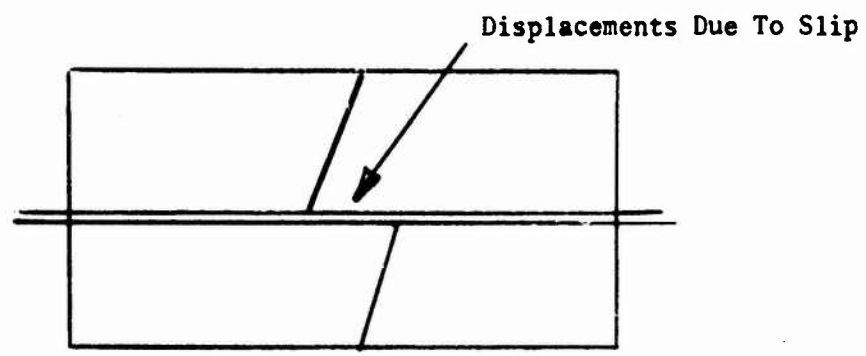


Figure 2b. Relative Slip At The Nodal Point Following Failure

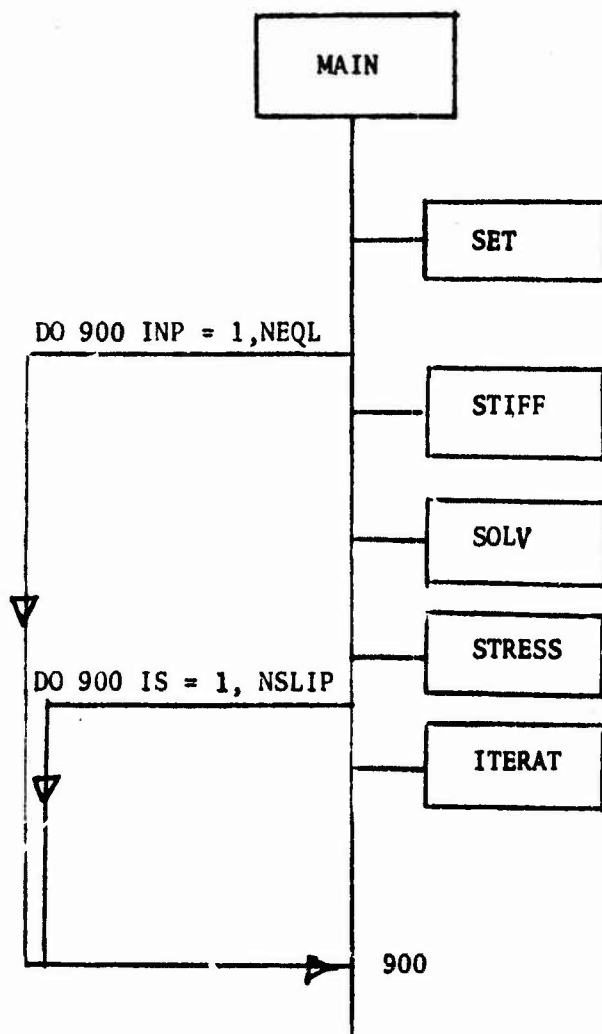


Figure 25. Simplified Computer Flow Chart Showing The Arrangement of The Iterative Schemes



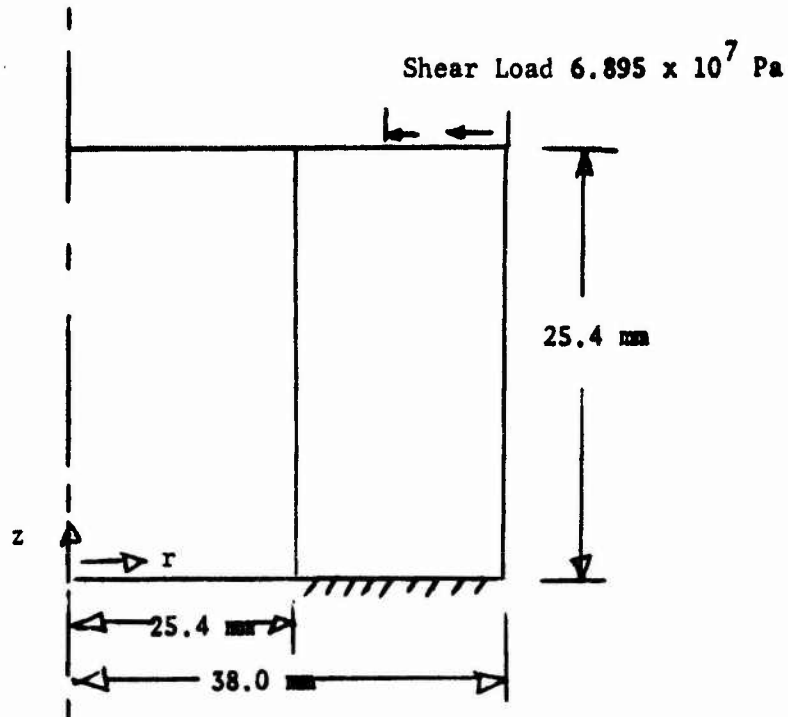


Figure 26a. Cylindrical Configuration Used In The Numerical Example

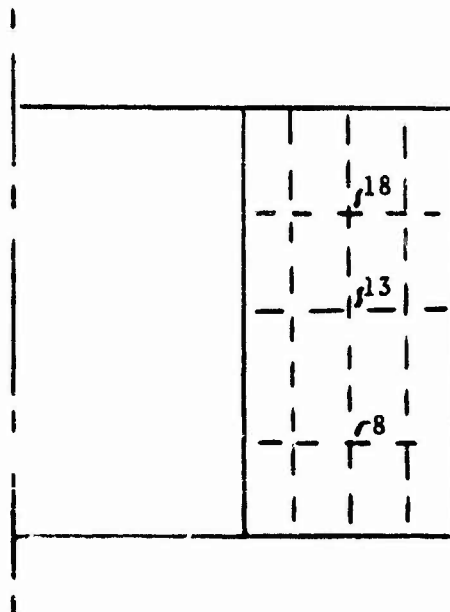


Figure 26b. Finite-Element Grid Used In The Numerical Calculations.

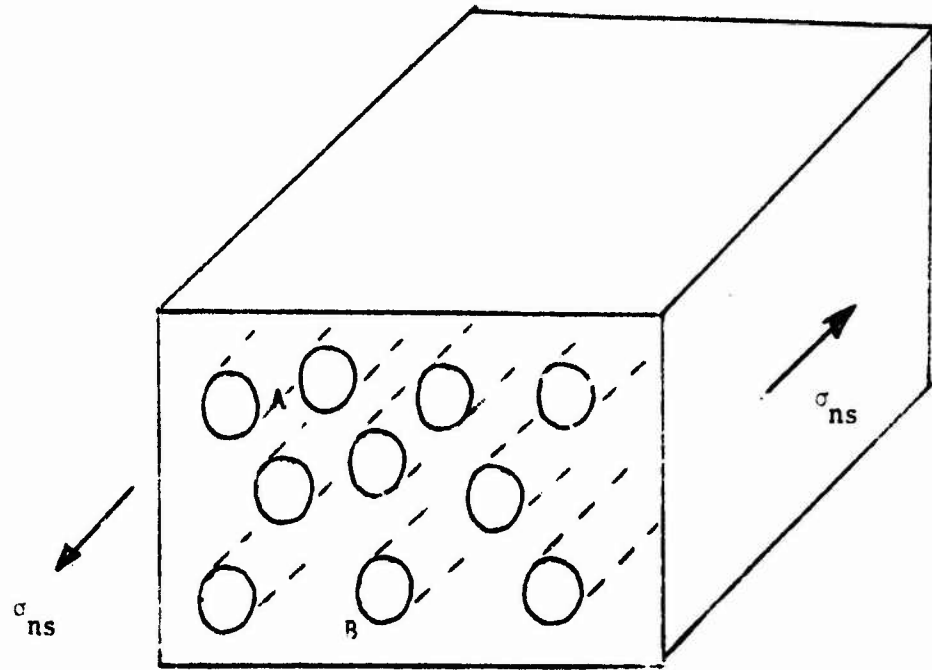


Figure 27. Macroscopic model of composite material subject to shear stress.

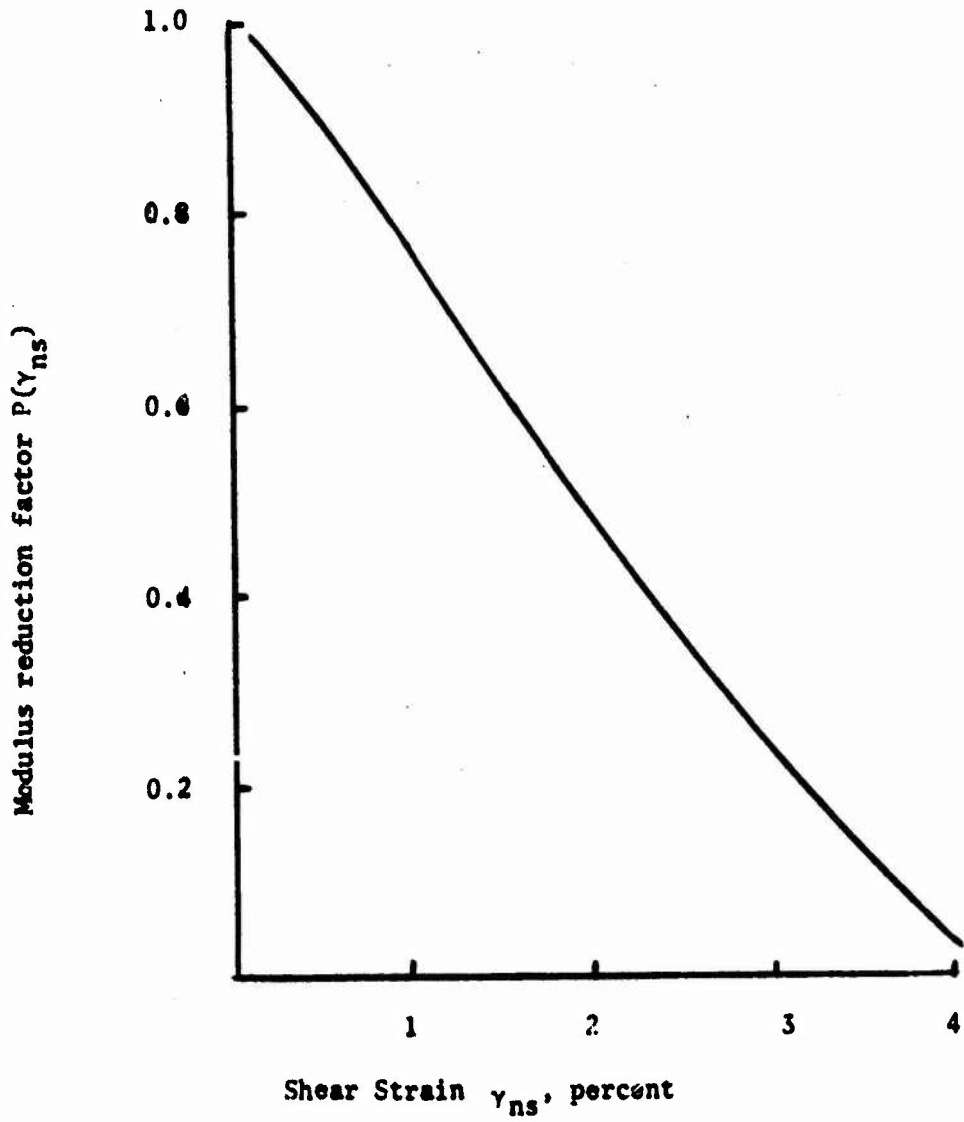


Figure 28. Dependence of shear modulus factor on the shear strain.

APPENDIX A

INPUT CARDS FOR INTERLAMINAR FAILURE  
FINITE-ELEMENT PROGRAM

TITLE CARD

Format (20A4)  
Columns 1-80 TITLE (Title for particular case)

CONTROL CARD

Format (6I5, F5.0, 5I5)  
Columns 1-5 NNLA (Number of nonlinear approximations; NNLA=1 for this version of the program)  
6-10 NUMTC (Number of temperature cards; if -2, a constant temperature is specified)  
11-15 NUMMAT (Number of different materials; 6 maximum)  
16-20 NUMPC (Number of boundary pressure cards; 200 maximum)  
21-25 NUMSC (Number of boundary shear cards; 200 maximum)  
26-30 NUMST (Number of boundary shear cards in tangential direction; 200 maximum)  
31-35 TREF (Reference temperature)  
36-40 INERT (This parameter decides if inertia loads will be present, INERT=0 means zero values of axial acceleration, and angular acceleration and velocity for each load increment)  
41-45 NLINC (Number of load increments with time, NLINC>1)  
46-50 INCI (If INCI=0, then inertia loads for each time increment will be the same as for first increment)  
51-55 INCF (If INCF=0, then surface loads for each time increment will be the same as for first increment)  
56-60 IPLOT (Plot parameter, IPLOT = 1 if plot required)

MESH GENERATION CONTROL CARD

Format (5I5)  
Columns 1-5 MAXI (Maximum value of I in mesh; 25 maximum)  
6-10 MAXJ (Maximum value of J in mesh; 100 maximum)  
11-15 NSEG (Number of line segment cards)  
16-20 NBC (Number of boundary condition cards)  
21-25 NMTL (Number of material block cards)

LINE SEGMENT CARDS

The order of line segment cards is immaterial except when plots are requested; in this case, the line segment cards must define the perimeter of the solid continuously. The order of line segment cards defining internal straight lines is always irrelevant.

Format (3(2I3, 2F8.3), I5)  
Columns 1-3 I coordinate of 1st point  
4-6 J coordinate of 1st point  
7-14 R coordinate of 1st point  
15-22 Z coordinate of 1st point  
23-25 I coordinate of 2nd point

Columns (continued)

- 26-28 J coordinate of 2nd point
- 29-36 R coordinate of 2nd point
- 37-44 Z coordinate of 2nd point
- 45-47 I coordinate of 3rd point
- 48-50 J coordinate of 3rd point
- 51-58 R coordinate of 3rd point
- 59-66 Z coordinate of 3rd point
- 67-71 Line segment type parameter

If the number in column 71 is

- 0 Point (input only 1st point)
- 1 straight line (input only 1st and 2nd points)
- 2 straight line as an internal diagonal (input only 1st and 2nd points)
- 3 circular arc specified by 1st and 3rd points at the ends of the arc and 2nd point at the mid-point of the arc.
- 4 circular arc specified by 1st and 2nd points at the ends of the arc with the coordinates of the center of the arc given as the 3rd point (delete I and J for 3rd point).
- 5 straight line as a boundary diagonal for which I of 1st point is minimum for its row and/or I of 2nd point is minimum for its row (input only 1st and 2nd points).
- 6 straight line as a boundary diagonal for which I of 1st point and/or 2nd point is maximum for its row (input only 1st and 2nd points).

NOTE: In specifying a circular arc, the points are ordered such that a counterclockwise direction about the center is obtained upon moving along the boundary.

BOUNDARY CONDITION CARDS

Each card assigns a particular boundary condition to a block of elements bounded by I1, I2, J1, J2. For a line I1 = I2 or J1 = J2. For a point I1 = I2 and J1 = J2.

Format (415, I10, SF10.0)

- Columns 1-5 Minimum I
- 6-10 Maximum I
- 11-15 Minimum J
- 16-20 Maximum J
- 21-30 Boundary condition code
- 31-40 Radial boundary condition, XR
- 41-50 Axial boundary condition, XZ
- 51-60 Tangential boundary condition XT

If the number in Columns 21-30 is

- |   |  |
|---|--|
| 0 | XR is the specified R-load and<br>XZ is the specified Z-load and<br>XT is the specified T-load                         |
| 1 | XR is the specified R-displacement and<br>XZ is the specified Z-load and<br>XT is the specified T-load                 |
| 2 | XR is the specified R-load and<br>XZ is the specified Z-displacement and<br>XT is the specified T-load                 |
| 3 | XR is the specified R-displacement and<br>XZ is the specified Z-displacement and<br>XT is the specified T-load         |
| 4 | XR is the specified R-load and<br>XZ is the specified Z-load and<br>XT is the specified T-displacement                 |
| 5 | XR is the specified R-displacement and<br>XZ is the specified Z-load and<br>XT is the specified T-displacement         |
| 6 | XR is the specified R-load and<br>XZ is the specified Z-displacement and<br>XT is the specified T-displacement         |
| 7 | XR is the specified R-displacement and<br>XZ is the specified Z-displacement and<br>XT is the specified T-displacement |

NOTE: All loads are considered to be total forces acting on one radian segment.

MATERIAL BLOCK ASSIGNMENT CARD

Each card assigns a material definition number to a block of elements defined by the I, J coordinates.

Format (5I5, 2F10.0, 2I5)

- |             |  |
|-------------|--|
| Columns 1-5 | Material definition number (1 through 6)   |
| 6-10        | Minimum I  |
| 11-15       | Maximum I  |
| 16-20       | Minimum J  |
| 21-25       | Maximum J  |
| 26-35       | Material principal property inclination angle BETA<br>in R-Z plane   |
| 36-45       | Material principal property inclination angle ALPHA<br>in N-T plane  |
| 46-50       | IANG (If IANG = 0, then ALPHA is same for total material<br>block. If IANG = 1, the ALPHA varies in sign in the I<br>direction from element to element every NANG elements.<br>This will allow for equal but opposite helical angles.) |
| 51-55       | NANG (Number of elements in the I direction with the<br>same ALPHA)  |

PLOT TITLE CARD\*

Format (20A4)

Columns 1-80 Title (Title printed under each plot)

PLOT GENERATION INFORMATION CARD\*

Format (2F10.0)

Columns 1-10 RMAX (Maximum r coordinate of mesh)  
11-20 ZMAX (Maximum z coordinate of mesh)

\*NOTE: Use only if I PLOT = 1 (plot required)

TEMPERATURE FIELD INFORMATION CARDS

If NUMTC in columns 6-10 of the CONTROL CARD is greater than 1, the temperature field is given on cards. One card must be supplied for each point for which a temperature is specified.

Format (3F10.0)

Columns 1-10 R coordinate  
11-20 Z coordinate  
21-30 Temperature

If NUMTC in columns 6-10 of the CONTROL CARD is -2, a constant temperature field is specified; the value is given on a single card.

Format (F10.0)

Columns 1-10 Temperature

MATERIAL PROPERTY INFORMATION CARDS

The following group of cards must be specified for each material (maximum of 6).

a. MATERIAL IDENTIFICATION CARD

Format (2I5, 2F10.0)

Columns 1-5 Material identification number  
6-10 Number of temperatures for which properties are given  
(12 maximum)  
11-20 Mass density of material (if required)  
21-30 Thermal expansion parameter (If 1, free thermal expansions on the material property cards; otherwise, coefficients of thermal expansion are on the material property cards.)

b. MATERIAL PROPERTY CARDS

Format (7F10.0)

Columns 1-10 Temperature  
11-20 Modulus of elasticity,  $E_N$   
21-30 Modulus of elasticity,  $E_S$   
31-40 Modulus of elasticity,  $E_T$

Columns (continued)

41-50 Poisson's ratio,  $\nu_{NS}$   
 51-60 Poisson's ratio,  $\nu_{NT}$   
 61-70 Poisson's ratio,  $\nu_{ST}$

Second Card

Format (6F10.0)

Columns 1-10 Shear Modulus  $G_{NS}$   
 11-20 Shear Modulus  $G_{ST}$   
 21-30 Shear Modulus  $G_{TN}$   
 31-40  $\alpha_{nT}$  or  $\alpha_n$   
 41-50  $\alpha_{ST}$  or  $\alpha_S$   
 51-60  $\alpha_{TT}$  or  $\alpha_T$

CRACK ITERATION CARD

Format (2I10, F10.3)

Columns 1-10 NSLIP number of iteration steps at each node to satisfy local equilibrium and calculate slip components.  
 11-20 NEQL number of times that the equilibrium of the total structure is to be recalculated.  
 21-30 TFAIL the magnitude of the shear failure stress between plies

CRACK DIRECTION CARD

Format (2I10)

Columns 1-10 NCBI number of blocks of nodal points where slip can occur in I direction  
 11-20 NCBJ number of blocks of nodal points where slip can occur in J direction

FAILURE BLOCK DEFINITION CARDS

Format (4I10)

This card is to be repeated a number of times equal to the sum of NCBI and NCBJ. These cards define blocks of nodes in the I, J coordinates where failure can occur either in the I or J directions.

Columns 1-10 NIMIN minimum I in block  
 11-20 NIMAX maximum I in block  
 21-30 NJMIN minimum J in block  
 31-40 NJMAX maximum J in block



## INERTIA LOAD CARD

Format (3F10.0)

Starting with this input card and including the boundary force cards, this data is to be inputted as a block for each load step, that is NLINC times. There are the following exceptions to this:

- a) If INERT = 0, then this card is to be omitted completely (no inertia load).
- b) If INCI = 0, then this card is not repeated but appears in first block only (the inertia loads are constant for each load step).
- c) If INCF = 0, then the following boundary pressure and shear cards are to be given only for the first block and not repeated again (the pressure and shear loads are constant for each load increment).

Columns 1-10 ACELZ (axial acceleration)  
11-20 ANGVEL (angular velocity)  
21-30 ANGACC (angular acceleration)

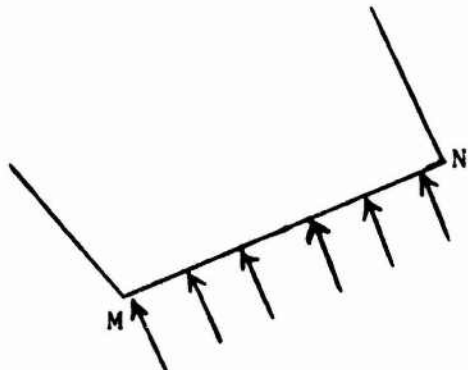
## BOUNDARY PRESSURE CARDS

One card is required for each boundary element which is subjected to a normal pressure, that is the number of these cards is NUMPC for each load increment.

Format (3I5, F10.0)

Columns 1-5 Nodal point M  
6-10 Nodal point N  
11-20 Normal pressure

As shown in the figure below, the boundary element must be on the left when progressing from M to N. Surface normal tension is input as a negative pressure.



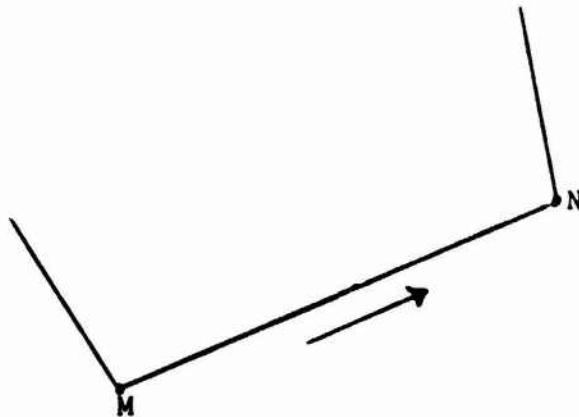
BOUNDARY SHEAR CARDS

One card is required for each boundary element which is subjected to surface shear, that is, the number of these cards is NUMSC for each load increment.

Format (2I5, F10.0)

Columns 1-5 Nodal point M  
6-10 Nodal point N  
11-20 Surface shear,

As shown in the figure below, the boundary element must be on the left when progressing from M to N. The positive sense of the shear is from M to N.

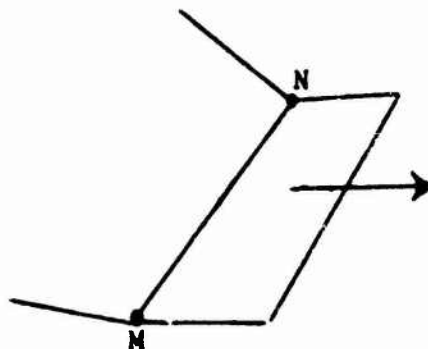


BOUNDARY TRANSVERSE SHEAR CARDS

One card is required for each boundary element which is subject to transverse shear, that is the number of these cards is NUMSC for each load increment.

Format(2I5, F10.0)

Columns 1-5 Nodal point M  
6-10 Nodal point N  
11-20 Surface transverse shear



APPENDIX B

PROGRAM LISTING FOR INTERLAMINAR FAILURE ANALYSIS

LEVEL 21

MAIN

DATE = 75066

14/36/25

```

C   FINITE ELEMENT STRESS ANALYSIS OF AXISYMMETRIC, LAYERED
C   SOLIDS WITH ORTHOTROPIC, TEMPERATURE-DEPENDENT MATERIAL
C   PROPERTIES USING STRAIGHT SIDED ELEMENTS
C* * * * *
    IMPLICIT REAL*8(A-H,O-Z)
    INTEGER CODE
    COMMON/BASIC/ACELZ,ANGVEL,ANGACC,TREF,VOL,NUMNP,NUMEL,NUMPC,NUMSC,
    1NUMST
    COMMON/MATP/RQ(6),E(12,16,6),EE(16),ADFTS(6)
    COMMON/ARG/FPR(5),ZZZ(5),RP(4),ZZ(4),S(15,15),P(15),TT(6),
    1H(6,15),CRZ(6,6),XI(10),ANGLE(4),SIG(18),EPS(18),N
    COMMON/NPDATA/ R(200),CODE(200),XR(200),Z(200),XZ(200),
    1NPNUM(10,20),T(200),XT(200)
    COMMON/ELDATA/ BETA(200),EPR(200),PR(20),SH(20),IX(200,5),IP(20),
    1IP(20),IS(20),JS(20),ALPHA(200),IT(200),JT(200),ST(20)
    COMMON/SOLVE/ X(888),Y(888),TEM(888),NUMTC,MBAND
    COMMON/TD/ TMIN(20),TMAX(20),JMIN(10),JMAX(10),MAXI,MAXJ,
    1AMTL,NBC
    COMMON/CCNVRG/IDONE
    COMMON/PLANE/NPP
    COMMON/RESULT/BS(6,15),D(6,6),C(6,6),AR,BB(6,9),CNS(6,6)
    COMMON/CIT/NEQL,NSLIP,ICRACK,ISLIP,INP,NSKIP
    COMMON/DATA1/RTN(200),RST(200),RNN(200)
    COMMON/DATA2/IFAIL(200),TB(200,12),ICP(200),IAD(200,4)
    DIMENSION TITLE(20)
    DIMENSION TD(100,12)
C* * * * *
C   READ AND WRITE CONTROL INFORMATION
C* * * * *
    50 READ(5,1000,END=920)TITLE,NNLA,NUMTC,NUMMAT,NUMPC,NUMSC,NUMST,TREF
    1,INERT,NLINC,INCF,INCF,IPLDT,ICRACK
    WRITE(6,2000)TITLE,NNLA,NUMTC,NUMMAT,NUMPC,NUMSC,NUMST,TREF,INERT,
    1NLINC
    WRITE(6,4000) ICRACK
    4000 FORMAT(3X,I5)
    NSKIP=0
    NPP=0
C* * * * *
C   GENERATE FINITE ELEMENT MESH
C* * * * *
    100 CALL MESH
    IF (IPLDT.EQ.1) CALL MPLDT
C* * * * *
C   READ AND WRITE TEMPERATURE DATA
C* * * * *
    103 IF(NUMTC.EQ.0) GO TO 440
    IF(NUMTC.GT.0) READ(5,1001) (X(I),Y(I),TEM(I),I=1,NUMTC)
    IF(NUMTC.EQ.-2) CALL TEM2(NUMNP)
    
```

6 LEVEL 21

MAIN

DATE = 75066

14/36/21

```

IF (NUMTC.EQ.-2) GO TO 440
MPRINT=0
DO 210 I=1,NUMTC
IF (MPRINT.NE.0) GO TO 200
WRITE(6,2001)
MPRINT=59
200 MPRINT=MPRINT-1
210 WRITE(6,2002) X(I),Y(I),TEM(I)
MPRINT=0
DO 230 N=1,NUMMP
IF (MPRINT.NE.0) GO TO 220
WRITE(6,2003)
MPRINT=59
220 MPRINT=MPRINT-1
CALL TEMP(F(N),Z(N),T(N))
230 WRITE(6,2004) N,R(N),Z(N),T(N)
440 MPRINT=0
DO 460 N=1,NUMEL
IF (MPRINT.NE.0) GO TO 450
WRITE(6,2008)
MPRINT=59
450 MPRINT=MPRINT-1
II=IX(N,1)
JJ=IX(N,2)
KK=IX(N,3)
LL=IX(N,4)
C
C TEM IS TEMPORARY STORAGE FOR ELEMENT TEMPERATURES
C
TEM(N)=(T(II)+T(JJ)+T(KK)+T(LL))/4.0
460 WRITE(6,2009) N,(IX(N,I),I=1,5),BETA(N),ALPHA(N),TEM(N)
DO 470 K=1,NUMEL
470 T(K)=TEM(K)
C * * * * *
C READ AND WRITE MATERIAL PROPERTIES
C * * * * *
500 CONTINUE
IF (NUMMAT.EQ.0) GO TO 600
DO 510 M=1,NUMMAT
READ(5,1004) MTYPE,(NT,RO(MTYPE),ADFTS(MTYPE))
WRITE(6,2010) MTYPE,NT,RO(MTYPE)
READ(5,1005)((E(I,J,MTYPE),J=1,14),I=1,NT)
IF (ADFTS(MTYPE).NE.1.) WRITE(6,2011)((E(I,J,MTYPE),J=1,13),I=1,NT)
IF (ADFTS(MTYPE).EQ.1.) WRITE(6,2012)((E(I,J,MTYPE),J=1,13),I=1,NT)
DO 510 I=NT,12
DO 510 J=1,16
510 E(I,J,MTYPE)=F(NT,J,MTYPE)
    
```

G LEVEL 21

MAIN

DATE = 75066

14/36/25

```

C   SET INTERLAMINAR SLIP DATA
C
    IF(ICRACK.EQ.0) GO TO 509
    CALL SET
509  CONTINUE
    DO 501 N=1,NUMEL
    DO 501 I=1,12
501  TB(N,I)=0.0
C*****
C*****
C * * * * *
C   DETERMINE BANDWIDTH, INITIALIZE ELASTIC-PLASTIC RATIO,
C   AND CONVERT BETA FROM DEGREES TO PADIAN
C * * * * *
    J=0
    DO 710 N=1,NUMEL
    DO 710 I=1,4
    DO 710 L=1,4
    KK=IABS('X(N,I)-X(N,L))
    IF(KK.GE.J) J=KK
710  CONTINUE
    MBAND=3*J+3
    DO 720 N=1,NUMEL
    EPR(N)=1.
    ALPHA(N)=ALPHA(N)/57.29578
720  BETA(N)=BETA(N)/57.29578
    DO 900 NL=1,NLINC
    WRITE(6,2030) NL
    ACELZ=0.0
    ANGVEL=0.0
    ANGACC=0.0
    IF(INEPT .EQ. 0) GO TO 511
    IF(NL .NE. 1 .AND. INCI .EQ. 0) GO TO 511
    READ(5,1030) ACELZ, ANGVEL, ANGACC
511  CONTINUE
    WRITE(6,2031) ACELZ, ANGVEL, ANGACC
C * * * * *
C   READ AND WRITE PRESSURE AND SHEAR BOUNDARY CONDITIONS
C * * * * *
    IF(NL .NE. 1 .AND. INCF .EQ. 0) GO TO 700
600  IF(NUMPC.EQ.0) GO TO 630
    MPRINT=0
    DO 620 L=1,NUMPC
    IF(MPRINT.NE.0) GO TO 610
    WRITE(6,2013)
    MPRINT=5R
610  MPRINT=MPRINT-1
    READ(5,1006) IP(L),JP(L),PR(L)
    
```

```
620 WRITE(6,2014) IP(L),JP(L),PR(L)
630 IF(NUMSC.EQ.0) GO TO 701
MPRINT=0
DO 650 L=1,NUMSC
IF(MPRINT.NE.0) GO TO 640
WRITE(6,2015)
MPRINT=58
640 MPRINT=MPRINT-1
READ(5,1006) IS(L),JS(L),SH(L)
650 WRITE(6,2014) IS(L),JS(L),SH(L)
701 IF(NUMST.EQ.0) GO TO 700
MPRINT=0
DO 680 L=1,NUMST
IF(MPRINT.NE.0) GO TO 670
WRITE(6,2025)
MPRINT=58
670 MPRINT=MPRINT-1
READ(5,1006) IT(L),JT(L),ST(L)
680 WRITE(6,2014) IT(L),JT(L),ST(L)
700 CONTINUE
IF(ICRACK.EQ.0) GO TO 741
DO 900 INP=1,NEOL
741 CONTINUE
DO 721 N=1,NUMEL
721 IX(N,5)=IABS(IX(N,5))
C
C FORM STIFFNESS MATRIX
C
C CALL STIFF
C
C SOLVE FOR DISPLACEMENTS
C
C CALL SOLV
C
C COMPUTE STRESSES
C
C CALL STRESS
C
C CLIP ITERATION
C
IF(ICRACK.EQ.0) GO TO 731
DO 729 L=1,NSUP
IF(L.GT.1) GO TO 723
DO 723 I=1,NUMEL
DO 723 J=1,12
TD(I,J)=TR(I,J)
723 CONTINUE
CALL ITERAT
```

LEVEL 21

MAIN

DATE = 75066

14/36/25

```

IF(L.NE.NSLIP) GO TO 729
DO 724 I=1,NUMEL
DO 724 J=1,12
724 TB(I,J)=TD(I,J)+(TB(I,J)-TD(I,J))*2.
729 CONTINUE
731 CONTINUE
900 CONTINUE
910 GO TO 50
1000 FORMAT(20A4/6I5,F5.0,6I5)
1001 FORMAT(3F10.0)
1004 FORMAT (2I5,2F10.0)
1005 FORMAT(7F10.0)
1006 FORMAT (2I5,F10.0)
1030 FORMAT(3F10.0)
2000 FORMAT (2H1 ,20A4/
1 33H0 NUMBER OF APPROXIMATIONS-----I4/
2 33H0 NUMBER OF TEMPERATURE CARDS---I4/
3 33H0 NUMBER OF MATERIALS-----I4/
4 33H0 NUMBER OF PRESSURE CARDS-----I4/
5 33H0 NUMBER OF SHEAR CARDS-----I4/
6 33H0 NUMBER OF TORSION CARDS-----I4/
7 33H0 REFERENCE TEMPERATURE-----E12.4/
8 33H0 NUMBER OF INERTIA CARDS-----I4/
9 33H0 NUMBER OF LOAD INCREMENTS-----I4/)
2001 FORMAY (1H1,13X,1HR,14X,1HZ,14X,1HT)
2002 FORMAT (3F15.3)
2003 FORMAT (35H1 N R Z T)
2004 FORMAT (I5,2F10.4,F10.0)
2008 FORMAT (74H1 EL ! J K L MATERIAL ANGLE BETA ANGLE A
1LPHA TEMPERATURE)
2009 FORMAT (I5,4I4,I8,F11.1,2F13.3)
2010 FORMAT (1H!, 'MATERIAL IDENTIFICATION NUMBER =',I2/
11H , 'NO. OF MATERIAL TEMPERATURE CARDS =',I2/
21H , 'MASS DENSITY =',E15.7)
2011 FORMAT (1H , 'TEMPERATURE =',E15.7/
11H , 'MODULUS OF ELASTICITY-EN =',E15.7/
21H , 'MODULUS OF ELASTICITY-ES =',E15.7/
31H , 'MODULUS OF ELASTICITY-ET =',E15.7/
41H , 'POISSON RATIO-NUNS =',E15.7/
51H , 'POISSON RATIO-NUNT =',E15.7/
61H , 'POISSON RATIO-NLST =',E15.7/
71H , 'SHEAR MODULUS-GNS =',E15.7/
81H , 'SHEAR MODULUS-GST =',E15.7/
91H , 'SHEAR MODULUS-GTN =',E15.7/
11H , 'COEFFICIENT OF THERMAL EXPANSION-AN =',E15.7/
21H , 'COEFFICIENT OF THERMAL EXPANSION-AS =',E15.7/
31H , 'COEFFICIENT OF THERMAL EXPANSION-AT =',E15.7/)
2012 FORMAY (1H , 'TEMPERATURE =',E15.7/

```



LEVEL 21 MAIN DATE = 75066 14/36/25

11H , 'MODULUS OF ELASTICITY-EM =', E15.7/  
 21H , 'MODULUS OF ELASTICITY-ES =', E15.7/  
 31H , 'MODULUS OF ELASTICITY-ET =', E15.7/  
 41H , 'POISSON RATIO-NUNS =', E15.7/  
 51H , 'POISSON RATIO-NUNT =', E15.7/  
 61H , 'POISSON RATIO-NUST =', E15.7/  
 71H , 'SHEAR MODULUS-GNS =', E15.7/  
 81H , 'SHEAR MODULUS-GST =', E15.7/  
 91H , 'SHEAR MODULUS-GTN =', E15.7/  
 11H , 'FREE THERMAL STRAIN-FN =', E15.7/  
 21H , 'FREE THERMAL STRAIN-FS =', E15.7/  
 31H , 'FREE THERMAL STRAIN-FT =', E15.7/)

2013 FORMAT (30H1 PRESSURE BOUNDARY CONDITIONS/20H I J PRESSURE)  
 2014 FORMAT (215,F10.1)  
 2015 FORMAT (27H1 SHEAR BOUNDARY CONDITIONS/17H I J SHEAR)  
 2016 FORMAT (26H THE SYSTEM CONVERGED IN 12,11H ITERATIONS)  
 2017 FORMAT (33H THE SYSTEM DID NOT CONVERGE IN 12,11H ITERATIONS)  
 2024 FORMAT (43H0 THE AXISYMMETRIC OPTION HAS BEEN SELECTED)  
 2025 FORMAT(30H1 TORSION BOUNDARY CONDITIONS/17H I J SHEAR)  
 2030 FORMAT(11H1,'LOAD STEP=',I4)  
 2031 FORMAT(11H0,'AXIAL ACCELERATION =',E12.4/  
 11H0,'ANGULAR VELOCITY =',E12.4/  
 21H0,'ANGULAR ACCELERATION=',E12.4)  
 920 STOP  
 END

CATION	SYMBOL	COMMON BLOCK / BASIC	LOCATION	SYMBOL	MAP SIZE	LOCATION	3C	SYMBOL	LOCAT
0	ANGVEL		8	ANGACC		10		TREF	11
28	NUMEL		2C	NUMPC		30		NUMSC	31

CATION	SYMBOL	COMMON BLOCK / MATP	LOCATION	SYMBOL	MAP SIZE	LOCATION	24E0	SYMBOL	LOCAT
0	E		30	EE		2430		AOFTS	2481

CATION	SYMBOL	COMMON BLOCK / ARG	LOCATION	SYMBOL	MAP SIZE	LOCATION	DC4	SYMBOL	LOCAT
0	ZZZ		28	RR		50		ZZ	71
798	TT		810	H		840		CRZ	811
097	STC		CA0	EPS		030		N	0C1

CATION	SYMBOL	COMMON BLOCK / NPODATA	LOCATION	SYMBOL	MAP SIZE	LOCATION	28C0	SYMBOL	LOCAT
0	CODE		640	XR		960		Z	FA1

G LEVEL 21

MAIN

DATE = 75066

14/36/21

```

C* * * * *
SUBROUTINE ANGLE (R,Z,RC,ZC,ANG)
  IMPLICIT REAL*8(A-H,O-Z)
C* * * * *
C   FIND ANGLE OF INCLINATION BETWEEN O AND 2*PI
C* * * * *
  PI=3.1415927
  D1=(Z-ZC)
  D2=(R-RC)
  IF(DABS(R-RC).GT.1.E-8) GO TO 100
  ANG=PI/2.
  IF(D1.GT.1.E-8) RETURN
  ANG=-ANG
  RETURN
C* * * * *
C   ALLOW CIRCLE TO CROSS AXIS
C* * * * *
100 ANG=DATAN2(D1,D2)
  RETURN
  END
    
```

SUBPROGRAMS CALLED

LOCATION	SYMBOL	LOCATION	SYMBOL	LOCATION	SYMBOL	LOCATION
A0						

SCALAR MAP

LOCATION	SYMBOL	LOCATION	SYMBOL	LOCATION	SYMBOL	LOCATION
B0	D1	B8	Z	C0	ZC	
DR	RC	E0	ANG	E8		

STATEMENT NUMBER MAP

LOCATION	STATEMENT	LOCATION	STATEMENT	LOCATION	STATEMENT	LOCATION
ICC	3	ICC	4	1D4	5	1I
200	8	20C	9	222	10	2:
242						

IN EFFECT\* NOID,BCD,SCURCE,NOLIST,NODECK,LOAD,MAP  
 IN EFFECT\* NAME = ANGLE , LINECNT = 50  
 ICS\* SOURCE STATEMENTS = 13, PROGRAM SIZE = 586  
 ICS\* NO DIAGNOSTICS GENERATED

6 LEVEL 21

CIRCLE

DATE = 75066

14/36/25

```

SUBROUTINE CIRCLE(ANG1,DELPHI,RSTR,ZSTR,RC,ZC,I,J)
IMPLICIT REAL*8(A-H,O-Z)
INTEGER CODE
COMMON/TD/ IMIN(20),IMAX(20),JMIN(10),JMAX(10),MAXI,MAXJ,
IMNTL,NBC
COMMON/NPDATA/ R(200),CODE(200),XR(200),Z(200),XZ(200),
INPNUM(10,20),T(200),XT(200)
DIMENSION AR(10,20),AZ(10,20)
EQUIVALENCE (R(1),AR),(Z(1),AZ)
    
```

C\* \* \* \* \*  
 C FIND INTERSECTION OF LINE AND CIRCLE = NEW R AND Z  
 C\* \* \* \* \*

```

ANG1=ANG1+DELPHI
PR=DSQRT((RSTR-RC)**2+(ZSTR-ZC)**2)
AR(I,J)=RC+PR*DCOS(ANG1)
AZ(I,J)=ZC+PR*DSIN(ANG1)
RETURN
END
    
```

LOCATION		COMMON BLOCK /TD		/ MAP SIZE 100		LOCATION	
SYMBOL	LOCATION	SYMBOL	LOCATION	SYMBOL	LOCATION	SYMBOL	LOCAT
0	IMAX	50	JMIN	A0	JMAX		C
F4	NMTL	F8	NBC	FC			

LOCATION		COMMON BLOCK /NPDATA		/ MAP SIZE 2800		LOCATION	
SYMBOL	LOCATION	SYMBOL	LOCATION	SYMBOL	LOCATION	SYMBOL	LOCAT
0	AR	0	CODE	640	XR		9E
FAD	XZ	15E0	NPNUM	1C20	T		1F4

LOCATION		SUBPROGRAMS CALLED				LOCATION	LOCAT
SYMBOL	LOCATION	SYMBOL	LOCATION	SYMBOL	LOCATION	SYMBOL	LOCAT
9E	DCOS	A0	DSIN	A4			

LOCATION		SCALAR MAP				LOCATION	LOCAT
SYMBOL	LOCATION	SYMBOL	LOCATION	SYMBOL	LOCATION	SYMBOL	LOCAT
RB	DELPHI	C0	RR	C8	RSTR		
F0	ZC	E8	I	F0	J		

LOCATION		STATEMENT NUMBER MAP				LOCATION	LOCAT
STATEMENT	LOCATION	STATEMENT	LOCATION	STATEMENT	LOCATION	STATEMENT	LOCAT
206	8	206	9	212	10	21	
292							

G LEVEL 21

INTER

DATE = 75066

14/36/21

```

SUBROUTINE INTER
IMPLICIT REAL*8(A-H, O-Z)
COMMON/ARG/RRR(5),ZZZ(5),RR(4),ZZ(4),S(15,15),P(15),TT(6),
IH(6,15),CRZ(6,6),XI(10),ANGLE(4),SIG(18),EPS(18),N
COMMON/PLANE/NPP
DIMENSION XM(7),R(7),Z(7),XX(9)
DATA XX/3*.1259391805448,3*.1323941527884,.225,
1 .696140478028,.410426192314/
P(7)=(RR(1)+RR(2)+RR(3))/3.
Z(7)=(ZZ(1)+ZZ(2)+ZZ(3))/3.
DO 100 I=1,3
J=I+3.
P(I)=XX(8)*RR(I)+(1.0-XX(8))*R(7)
R(J)=XX(9)*PP(I)+(1.0-XX(9))*R(7)
Z(I)=XX(8)*ZZ(I)+(1.0-XX(8))*Z(7)
100 Z(J)=XX(9)*ZZ(I)+(1.0-XX(9))*Z(7)
DO 200 I=1,7
200 XM(I)=XX(I)*R(I)
DO 300 I=1,10
300 XI(I)=0.0
AREA=.5*(RR(1)*(ZZ(2)-ZZ(3))+RR(2)*(ZZ(3)-ZZ(1))+RR(3)*(ZZ(1)
1 -ZZ(2)))
IF(NPP.NE.0) GO TO 600
DO 400 I=1,7
XI(1)=XI(1)+XM(I)
XI(2)=XI(2)+XM(I)/R(I)
XI(3)=XI(3)+XM(I)/(R(I)**2)
XI(4)=XI(4)+XM(I)*Z(I)/R(I)
XI(5)=XI(5)+XM(I)*Z(I)/(P(I)**2)
XI(6)=XI(6)+XM(I)*(Z(I)**2)/(R(I)**2)
XI(7)=XI(7)+XM(I)*P(I)
XI(8)=XI(8)+XM(I)*Z(I)
XI(9)=XI(9)+XM(I)*(R(I)**2)
400 XI(10)=XI(10)+XM(I)*R(I)*Z(I)
DO 500 I=1,10
500 XI(I)=XI(I)*AREA
RETURN
600 XI(1)=AREA
XI(7)=R(7)*AREA
XI(8)=Z(7)*AREA
RETURN
END
    
```

LOCATION	SYMBOL	COMMON BLOCK / ARG LOCATION	/ MAP SIZE SYMBOL LOCATION	DC4	SYMBOL	LOCATION
0	ZZZ	28	RR	50	ZZ	
798	TT	810	H	840	CRZ	H

6 LEVEL 21

ITERAT

DATE = 75066

14/36/25

SUBROUTINE ITERAT

C  
C  
C

NODAL SLIP IS FOUND BY ITERATION

```

IMPLICIT REAL*8(A-H,O-Z)
INTEGER CCDE
COMMON/ARG/PPR(5),ZZZ(5),RR(4),ZZ(4),S(15,15),P(15),TT(6),
IH(6,15),CFZ(6,6),XI(10),ANGLE(4),SIG(18),EPS(18),N
COMMON/SOLVE/B(72),A(72,36),NUMTC,MBAND
COMMON/BASIC/ACELZ,ANGVEL,ANGACC,TREF,VOL,NUMNP,NUMEL,NUMPC,NUMSC,
INUMST
COMMON/NPDATA/ R(200),CODE(200),XR(200),Z(200),XZ(200),
INPNUM(10,20),F(200),XT(200)
COMMON/ELDATA/ BETA(200),EPR(200),PR(20),SH(20),IX(200,5),IP(20),
IIP(20),IS(20),JS(20),ALPHA(200),IT(200),JT(200),ST(20)
COMMON/RESULT/BS(6,15),D(6,6),C(6,6),AR,BB(6,9),CNS(6,6)
COMMON/CIT/NEOL,NSLIP,ICRACK,ISLIP,INP,NSKIP
COMMON/DATA1/RTN(200),RST(200),RNN(200)
COMMON/DATA2/IFAIL(200),TB(200,12),ICR(200),IAD(200,4)
COMMON/DATA3/TFAIL,CF
DIMENSION T(3,2),SQ(4,15,15),PQ(4,15),AU(2,2),AL(2,2),BU(2),BL(2),
ITNL(3),YM(3,2),ZM(3,2),TNU(3),DM(4,12),FM(2,12),SU(2),SL(2)
DIMENSION S2(12,3),S3(3,12),S4(3,3),S5(12,3),S6(12,12)
    
```

C  
C

START LOOP ON NODAL POINTS

```

DO 900 NP=1,NUMNP
IF(ICR(NP).EQ.0) GO TO 900
AV=0.0
ANGC=0.0
TRES=0.0
DO 7 I=1,4
DO 6 K=1,15
PQ(I,K)=C.0
DO 6 L=1,15
5 SQ(I,K,L)=0.0
N=IAD(NP,I)
IF(N.EQ.0) GO TO 7
AV=AV+1.
TRES=TRES+DSQRT(PRTN(N)**2+RST(N)**2)
7 CONTINUE
IF(IFAIL(NP).EQ.1) GO TO 8
TRES=DABS(TRES)/AV
TFAIL=DABS(TFAIL)
IF(TRES.LT.*TFAIL) GO TO 900
IFAIL(NP)=1
9 CONTINUE
DO 10 I=1,4
N=IAD(NP,I)
    
```

G LEVEL 21

ITERAT

DATE = 75066

14/36/2

```

IF(N.EQ.0) GC TC 10
ANGS=ANGS+BETA(N)
10 CONTINUE
ANGS=ANGS/AV
DO 11 I=1,3
DO 11 J=1,2
11 T(I,J)=0.0
T(1,1)=DSIN(ANGS)
T(2,1)=DCOS(ANGS)
T(3,2)=1.0
DO 14 I=1,4
N=IAD(NP,I)
IF(N.EQ.0) GC TC 14
CALL QUAD
IX(N,5)=-IX(N,5)
DO 100 K=1,4
II=3*K
JJ=3*IX(N,K)
P(II-2)=8(JJ-2)
P(II-1)=8(JJ-1)
100 P(II) =8(JJ)
DO 231 II=1,3
DO 231 JJ=1,3
231 S4(II, JJ)=S(II+12, JJ+12)
CALL SYMINV(S4,3)
DO 232 II=1,12
DO 232 JJ=1,3
232 S2(II, JJ)=S(II, JJ+12)
DO 233 II=1,3
DO 233 JJ=1,12
233 S3(II, JJ)=S(II+12, JJ)
DO 240 L=1,12
DO 240 J=1,3
S5(L, J)=0.000
DO 240 K=1,3
240 S5(L, J) = S5(L, J) + S2(L, K) * S4(K, J)
DO 241 L=1,12
DO 241 J=1,12
S6(L, J)=0.000
DO 241 K=1,3
241 S6(L, J) = S6(L, J) + S5(L, K) * S3(K, J)
DO 235 II=1,12
DO 235 JJ=1,12
235 S(II, JJ)=S(II, JJ)-S6(II, JJ)
C
C
DO 13 II=1,12
PO(I, II)=P(II)+TB(N, II)
    
```

G LEVEL 21

ITERAT

DATE = 75066

14/36/2

```

13  DO 13 JJ=1,12
    SO(I,II,JJ)=S(II,JJ)
    NS=ICR(NP)
14  CONTINUE
    IF(NS.EQ.2) GO TO 24
    DO 23 K=1,3
    FM(1,K)=0.0
    FM(2,K)=0.0
    DO 21 I=1,2
    NN=3*(I-1)+K
    DO 20 M=1,12
20  FM(1,K)=FM(1,K)+SO(I,NN,M)*PQ(I,M)
    DO 21 J=1,2
    YM(K,J)=0.0
    DO 21 L=1,3
    NQ=3*(I-1)+L
21  YM(K,J)=YM(K,J)+SO(I,NN,NQ)*T(L,J)
    DO 23 I=3,4
    NN=3*(I-1)+K
    DO 22 M=1,12
22  FM(2,K)=FM(2,K)+SO(I,NN,M)*PQ(I,M)
    DO 23 J=1,2
    ZM(K,J)=0.0
    DO 23 L=1,3
    NQ=3*(I-1)+L
23  ZM(K,J)=ZM(K,J)+SO(I,NN,NQ)*T(L,J)
    GO TO 29
24  DO 28 K=1,3
    FM(1,K)=0.0
    FM(2,K)=0.0
    DO 26 I=1,4,3
    NN=3*(I-1)+K
    DO 25 M=1,12
25  FM(1,K)=FM(1,K)+SO(I,NN,M)*PQ(I,M)
    DO 26 J=1,2
    YM(K,J)=0.0
    DO 26 L=1,3
    NQ=3*(I-1)+L
26  YM(K,J)=YM(K,J)+SO(I,NN,NQ)*T(L,J)
    DO 28 I=2,3
    NN=3*(I-1)+K
    DO 27 M=1,12
27  FM(2,K)=FM(2,K)+SO(I,NN,M)*PQ(I,M)
    DO 28 J=1,2
    ZM(K,J)=0.0
    DO 28 L=1,3
    NQ=3*(I-1)+L
28  ZM(K,J)=ZM(K,J)+SO(I,NN,NQ)*T(L,J)
    
```

G LEVEL 21

ITERAT

DATE = 75066

14/36/2

```

29  CONTINUE
    AU(1,1)=YM(3,2)
    AU(1,2)=-YM(1,2)*T(1,1)-YM(2,2)*T(2,1)
    AU(2,1)=-YM(3,1)
    AU(2,2)= YM(1,1)*T(1,1)+YM(2,1)*T(2,1)
    BU(2)=-FM(1,3)
    BU(1)=-FM(1,1)*T(1,1)-FM(1,2)*T(2,1)
    DET=AU(1,1)*AU(2,2)-AU(2,1)*AU(1,2)
    DO 31 I=1,2
    SU(I)=0.0
    DO 31 J=1,2
31  SU(I)=SU(I)+AU(I,J)*BU(J)/DET
    AL(1,1)=ZM(3,2)
    AL(1,2)=-ZM(1,2)*T(1,1)-ZM(2,2)*T(2,1)
    AL(2,1)=-ZM(3,1)
    AL(2,2)= ZM(1,1)*T(1,1)+ZM(2,1)*T(2,1)
    BL(2)=-FM(2,3)
    BL(1)=-FM(2,1)*T(1,1)-FM(2,2)*T(2,1)
    DET=AL(1,1)*AL(2,2)-AL(2,1)*AL(1,2)
    DO 32 I=1,2
    SL(I)=0.0
    DO 32 J=1,2
32  SL(I)=SL(I)+AL(I,J)*BL(J)/DET
    DO 35 I=1,3
    TNU(I)=0.0
    TNL(I)=0.0
    DO 35 J=1,2
    TNU(I)=TNU(I)+T(I,J)*SU(J)
    TNL(I)=TNL(I)+T(I,J)*SL(J)
35  CONTINUE
    IF(ICR(NP).EQ.2) GO TO 45
    DO 43 I=1,4
    DO 41 J=1,12
41  DM(I,J)=0.0
    DO 43 J=1,3
    NJ=3*(I-1)+J
    IF(I.GT.2) GO TO 42
    DM(I,NJ)=TNU(J)
    GO TO 43
42  DM(I,NJ)=TNL(J)
43  CONTINUE
    GO TO 49
45  DO 48 I=1,4
    DO 46 J=1,12
46  DM(I,J)=0.0
    DO 48 J=1,3
    NJ=3*(I-1)+J
    IF(I.EQ.2.CR.I.EQ.3) GO TO 47
    
```



G LEVEL 21

ITERAT

DATE = 75066

14/36/21

```

DM(I,NJ)=TNI(J)
GO TO 48
47 DM(I,NJ)=TNL(J)
48 CONTINUE
49 CONTINUE
DO 62 I=1,4
N=IAD(NP,I)
IF(N.EQ.0) GO TO 62
DO 61 J=1,12
61 TB(N,J)=TB(N,J)+DM(I,J)/2.0
62 CONTINUE
C
900 CONTINUE
RETURN
END
    
```

LOCATION	SYMBOL	COMMON BLOCK LOCATION	/ ARG	/ MAP SIZE	DC4	SYMBOL	LOCATION
0	ZZZ	28	RR	50		ZZ	
798	TT	810	H	840		CRZ	B
CRJ	SIG	CA0	EPS	D30		N	D

LOCATION	SYMBOL	COMMON BLOCK LOCATION	/ SOLVE	/ MAP SIZE	5348	SYMBOL	LOCATION
0	A	240	NUMTC	5340		MBAND	53

LOCATION	SYMBOL	COMMON BLOCK LOCATION	/ BASIC	/ MAP SIZE	3C	SYMBOL	LOCATION
J	ANGVEL	8	ANGACC	10		TREF	
28	NUMEL	2C	NUMPC	30		NUMSC	

LOCATION	SYMBOL	COMMON BLOCK LOCATION	/ NPDATA	/ MAP SIZE	2BC0	SYMBOL	LOCATION
0	CODE	640	XR	960		Z	F
1020	F	1F40	XT	2580			

LOCATION	SYMBOL	COMMON BLOCK LOCATION	/ ELDATA	/ MAP SIZE	2BC0	SYMBOL	LOCATION
0	EPF	640	PR	80		SH	D
1060	JP	1080	IS	1E00		JS	1E
24E0	JT	2800	ST	2B20			

G LEVEL 21

MESH

DATE = 75066

14/36/2!

SUBROUTINE MESH

IMPLICIT REAL\*8(A-H,O-Z)

INTEGER CODE

DIMENSION AR(10,20),AZ(10,20),NCODE(10,20)

COMMON/TD/ IMIN(20),IMAX(20),JMIN(10),JMAX(10),MAXI,MAXJ,

INMTL,NBC

COMMON/NPDATA/ R(200),CODE(200),XR(200),Z(200),XZ(200),

INPNUM(10,20),T(200),XT(200)

COMMON/ELDATA/ BETA(200),EPR(200),PR(20),SH(20),IX(200,5),IP(20),

IJP(20),IS(20),JS(20),ALPHA(200),IT(200),JT(200),ST(20)

EQUIVALENCE (R(1),AR),(Z(1),AZ),(IX(1,1),NCODE)

C\* \* \* \* \*

C MESH CONTROL INFORMATION

C\* \* \* \* \*

READ (5,1000) MAXI,MAXJ,NSEG,NBC,NMTL

WRITE(6,2000) MAXI,MAXJ,NSEG,NBC,NMTL

C\* \* \* \* \*

C INITIALIZE

C\* \* \* \* \*

ISEG=-1

PI=3.1415927

DO 110 J=1,10

DO 100 I=1,5

NCODE(I,J)=0

AR(I,J)=0.

AZ(I,J)=0.

JMAX(I)=0

100 JMIN(I)=MAXI

IMIN(J)=MAXJ

110 IMAX(J)=0

C\* \* \* \* \*

C LINE SEGMENT CARDS

C\* \* \* \* \*

150 ISEG=ISEG+1

159 IF(ISEG.EQ.NSEG) GO TO 400

READ(5,1001) I1,J1,P1,Z1,I2,J2,R2,Z2,I3,J3,R3,Z3,IPTION

WRITE(6,2001)I1,J1,R1,Z1,I2,J2,R2,Z2,I3,J3,R3,Z3,IPTION

IPTION=IPTION+1

AR(I1,J1)=R1

AZ(I1,J1)=Z1

NCODE(I1,J1)=1

CALL MNIMX(I1,J1)

GO TO (150,200,200,300,300,200,200), IPTION

C\* \* \* \* \*

C GENERATE STRAIGHT LINES ON BOUNDARY

C\* \* \* \* \*

200 DI=ABS(FLOAT(I2-I1))

DJ=ABS(FLOAT(J2-J1))

G LEVEL 21

MESH

DATE = 75066

14/36/21

```

AR(I2,J2)=P2
AZ(I2,J2)=Z2
NCODE(I2,J2)=1
CALL MNIMX(I2,J2)
ISTR=I1
ISTP=I2
JSTR=J1
JSTP=J2
DIFF=OMAX1(DI,DJ)
ITER=DIFF-1.
IINC=0
JINC=0
IF(I2.NE.I1) JINC=(I2-I1)/IABS(I2-I1)
IF(J2.NE.J1) JINC=(J2-J1)/IABS(J2-J1)
KAPPA=1
IF(I2.NE.I1.AND.J2.NE.J1.AND.IPTION.NE.3) KAPPA=2
IF(KAPPA.EQ.2) DIFF=2.*DIFF
RINC=(P2-P1)/DIFF
ZINC=(Z2-Z1)/DIFF
WRITE(6,2002) DI,DJ,DIFF,RINC,ZINC,ITER,IINC,JINC,KAPPA

```

C  
C  
C

CHECK FOR INPLT ERROR

```

IF(KAPPA.NE.2.OR.DI.EQ.DJ) GO TO 210
WRITE(6,2003)
GO TO 150

```

C  
C  
C

INTERPOLATE

```

210 I=I1
    J=J1
    WRITE(6,2004)
    DO 230 M=1,ITER
    IF(ITER.EQ.0.AND.IPTION.EQ.2) GO TO 230
    IF(ITER.EQ.0.AND.IPTION.EQ.6) GO TO 230
    IF(ITER.EQ.0.AND.IPTION.EQ.7) GO TO 230
    IF(KAPPA.EQ.2) GO TO 220
    IOLD=I
    I=I+IINC
    JOLD=J
    J=J+JINC
    AP(I,J)=AP(IOLD,JOLD)+RINC
    AZ(I,J)=AZ(IOLD,JOLD)+ZINC
    WRITE(6,2005) I,J,AR(I,J),AZ(I,J)
    CALL MNIMX(I,J)
    NCODE(I,J)=1
    GO TO 230
220 CONTINUE

```

```

IF(I1.GT.I2.AND.IPTION.EQ.7) GO TO 221
IF(I1.LT.I2.AND.IPTION.EQ.6) GO TO 221
IOLD=I
I=I+IINC
AR(I,J)=AR(IOLD,J)+RINC
AZ(I,J)=AZ(IOLD,J)+ZINC
WRITE(6,2005) I,J,AR(I,J),AZ(I,J)
NCODE(I,J)=1
CALL MNIMX(I,J)
JOLD=J
J=J+JINC
AR(I,J)=AR(I,JOLD)+RINC
AZ(I,J)=AZ(I,JOLD)+ZINC
NCODE(I,J)=1
WRITE(6,2005) I,J,AR(I,J),AZ(I,J)
CALL MNIMX(I,J)
GO TO 230
221 JOLD=J
J=J+JINC
AR(I,J)=AR(I,JOLD)+RINC
AZ(I,J)=AZ(I,JOLD)+ZINC
NCODE(I,J)=1
WRITE(6,2005) I,J,AR(I,J),AZ(I,J)
CALL MNIMX(I,J)
IOLD=I
I=I+IINC
AR(I,J)=AR(IOLD,J)+RINC
AZ(I,J)=AZ(IOLD,J)+ZINC
NCODE(I,J)=1
WRITE(6,2005) I,J,AR(I,J),AZ(I,J)
CALL MNIMX(I,J)
230 CONTINUE
IF(KAPPA.EQ.1) GO TO 150
IF(I1.GT.I2.AND.IPTION.EQ.7) GO TO 231
IF(I1.LT.I2.AND.IPTION.EQ.6) GO TO 231
IOLD=I
I=I+IINC
AR(I,J)=AR(IOLD,J)+RINC
AZ(I,J)=AZ(IOLD,J)+ZINC
GO TO 232
231 CONTINUE
JOLD=J
J=J+JINC
AR(I,J)=AR(I,JOLD)+RINC
AZ(I,J)=AZ(I,JOLD)+ZINC
232 CONTINUE
NCODE(I,J)=1
WRITE(6,2005) I,J,AR(I,J),AZ(I,J)
    
```

CALL MNIMX(I,J)

GO TO 150

C\* \* \* \* \*

C GENERATE CIRCULAR ARCS ON BOUNDARY

C\* \* \* \* \*

300 AR(I2,J2)=R2

AZ(I2,J2)=Z2

NCODE(I2,J2) = 1

CALL MNIMX(I2,J2)

IF(IPTION.EQ.5) GO TO 320

C

C

C

FIND CENTER OF CIRCLE

AP(I3,J3)=P3

AZ(I3,J3)=Z3

NCODE(I3,J3)=1

CALL MNIMX(I3,J3)

SLAC=(Z2-Z1)/(R2-R1)

SLBF=-1./SLAC

SLCE=(Z3-Z2)/(R3-R2)

SLDF=-1./SLCE

C

C

C

CHECK FOR INPUT ERROR

IF(DABS(SLAC-SLCE).GT..001) GO TO 310

WRITE(6,2006) P1,Z1,R2,Z2,P3,Z3,SLAC,SLCE

GO TO 150

310 R4=R1+(R2-R1)/2.

Z4=Z1+(Z2-Z1)/2.

R5=R2+(R3-R2)/2.

Z5=Z2+(Z3-Z2)/2.

BBF=Z4-SLBF\*R4

BDF=Z5-SLDF\*R5

PC=(BBF-BDF)/(SLDF-SLBF)

ZC=SLBF\*PC+BBF

WRITE(6,2007) PC,ZC

KAPPA=1

GO TO 330

320 KAPPA=2

RC=P3

ZC=Z3

330 ISTRT=I1

ISTOP=I2

JSTRT=J1

JSTOP=J2

PSTPT=R1

RSTD=R2

ZSTRT=Z1

G LEVEL 21

MESH

DATE = 75066

14/36/2

```

ZSTP=Z2
340 CALL ANGLE(RSTRT,ZSTRT,RC,ZC,ANG1)
CALL ANGLE(RSTP,ZSTP,RC,ZC,ANG2)
IF(ANG2.LE.ANG1) ANG2=2.0*PI+ANG2

C
C
C
FIND ANGULAR INCREMENT

DI=ABS(FLOAT(ISTP-ISTRT))
DJ=ABS(FLOAT(JSTP-JSTRT))
IINC=0
JINC=0
IF(ISTRT.NE.ISTP) IINC=(ISTP-ISTRT)/IABS(ISTP-ISTRT)
IF(JSTRT.NE.JSTP) JINC=(JSTP-JSTRT)/IABS(JSTP-JSTRT)
LAMDA=1
IF(IINC.NE.0.AND.JINC.NE.0) LAMDA=2
DIFF=DMAX1(DI,DJ)
ITER=DIFF-1.
IF(LAMDA.EQ.2) DIFF=2.*DIFF
DELPHI=(ANG2-ANG1)/DIFF
WRITE(6,2008) ANG1,ANG2,DIFF,DELPHI

C
C
C
CHECK FOR INPUT ERROR

IF(LAMDA.NE.2.OR.DI.EQ.DJ) GO TO 350
WRITE(6,2003)
GO TO 150
350 IO=ISTRT
JO=JSTRT
WRITE(6,2004)

C
C
C
INTERPOLATE

NPT=IABS(I2-I1)+IABS(J2-J1)-1
DO 380 M=1,ITER
359 IF(LAMDA.EQ.2) GO TO 360
I=IO+IINC
J=JO+JINC
CALL MNIMX(I,J)
NCODE(I,J)=1
CALL CIRCLE(ANG1,DELPHI,RSTRT,ZSTRT,RC,ZC,I,J)
WRITE(6,2005) I,J,AR(I,J),AZ(I,J)
GO TO 370
360 I=IO+IINC
J=JO
NCODE(I,J)=1
CALL MNIMX(I,J)
CALL CIRCLE(ANG1,DELPHI,RSTRT,ZSTRT,RC,ZC,I,J)
WRITE(6,2005) I,J,AR(I,J),AZ(I,J)
    
```



G LEVEL 21

MESH

DATE = 75066

14/36/25

CALL POINTS

```

C* * * * *
1000 FORMAT (5I5)
1001 FORMAT (3(2I3,2F8.3),I5)
2000 FORMAT (30H1 MESH GENERATION INFORMATION//
1 4IHO MAXIMUM VALUE OF I IN THE MESH-----I3/
2 4IHO MAXIMUM VALUE OF J IN THE MESH-----I3/
3 4IHO NUMBER OF LINE SEGMENT CARDS-----I3/
4 4IHO NUMBER OF BOUNDARY CONDITION CARDS----I3/
5 4IHO NUMBER OF MATERIAL BLOCK CARDS-----I3///)
2001 FORMAT (/88H INPUT I1 J1 R1 Z1 I2 J2 R2 Z
2 I3 J3 R3 Z3 IPTION/8X,3(2I4,2F8.4),I6)
2002 FORMAT (5H DI=F4.0,5H DJ=F4.0,7H DIFF=F4.0,7H RINC=F8.3,7H ZI
INC=F8.3,7H ITER=I3,7H IINC=I3,7H JINC=I3,8H KAPPA=I1)
2003 FORMAT(1X,38H**BAD INPUT--THIS LINE IS NOT DIAGONAL)
2004 FORMAT (30H I J AR AZ)
2005 FORMAT (2I5,2F11.6)
2006 FORMAT (51H ** BAD INPUT - THESE POINTS DO NOT DEFINE A CIRCLE,/,
13X,6F12.4,10X,2E20.8)
2007 FORMAT(19H CENTER COORDINATE,(F11.6,1X,F11.6,1X))
2008 FORMAT (7H ANG1=F9.6,7H ANG2=F9.6,7H DIFF=F3.0,9H DELPHI=F9.6)
2009 FORMAT (/30H COORDINATES CALCULATED AFTER I3,I1H ITERATIONS)
RETURN
END
    
```

LOCATION	SYMBOL	COMMON BLOCK /TD LOCATION	SYMBOL	/ MAP SIZE LOCATION	100	SYMBOL	LOCA
0	IMAX	50	JMIN	A0		JMAX	
F4	NMTL	F8	NBC	FC			

LOCATION	SYMBOL	COMMON BLOCK /NPDATA LOCATION	SYMBOL	/ MAP SIZE LOCATION	28C0	SYMBOL	LOCA
0	AR	0	CODE	640		XR	9
FA0	XZ	15E0	NPNUM	1C20		T	1F

LOCATION	SYMBOL	COMMON BLOCK /ELDATA LOCATION	SYMBOL	/ MAP SIZE LOCATION	28C0	SYMBOL	LOCA
0	EPP	640	PR	C80		SH	D
DC0	IP	1060	JP	10B0		IS	1E
1EA0	IT	24E0	JT	2800		ST	2B

LOCATION	SYMBOL	SUBPROGRAMS CALLED LOCATION		SYMBOL	LOCATION	SYMBOL	LOCA
10C	MNIMX	1E0	ANGLE	1E4		CIRCLE	1



```

SUBROUTINE MNIMX(I,J)
IMPLICIT REAL*8(A-H,O-Z)
COMMON/TD/ IMIN(20),IMAX(20),JMIN(10),JMAX(10),MAXI,MAXJ,
INMTL,NBC
IF(J.LT.JMIN(I)) JMIN(I)=J
IF(J.GT.JMAX(I)) JMAX(I)=J
IF(I.LT.IMIN(J)) IMIN(J)=I
IF(I.GT.IMAX(J)) IMAX(J)=I
RETURN
END
    
```

		COMMON BLOCK /TD		/ MAP SIZE 100	
LOCATION	SYMBOL	LOCATION	SYMBOL	LOCATION	SYMBOL
0	IMAX	50	JMIN	A0	JMAX
F4	NMTL	F8	NBC	FC	

		SCALAR MAP			
LOCATION	SYMBOL	LOCATION	SYMBOL	LOCATION	SYMBOL
A4	I	A8			

		STATEMENT NUMBER MAP			
ENT LOCATION	STATEMENT LOCATION	STATEMENT LOCATION	STATEMENT LOCATION	STATEMENT	STATEMENT
13A	4	13A	5	15C	6
1C6					

TIONS IN EFFECT\* NOID,BCD,SOURCE,NOLIST,NODECK,LOAD,MAP  
 TIONS IN EFFECT\* NAME = MNIMX , LINECNT = 50  
 ATISTICS\* SOURCE STATEMENTS = 9, PROGRAM SIZE = 462  
 ATISTICS\* NO DIAGNOSTICS GENERATED

```

SUBROUTINE MODIFY(NEQ,N,U)
IMPLICIT REAL*8(A-H,O-Z)
COMMON/SOLVE/B(72),A(72,36),NUMTC,MBAND
DO 10 M=2,MBAND
K=N-M+1
IF(K.LE.0) GO TO 5
R(K)=B(K)-A(K,M)*U
A(K,M)=0.0
5 K=N+M-1
IF(NEQ.LT.K) GO TO 10
B(K)=B(K)-A(N,M)*U
A(N,M)=0.0
10 CONTINUE
A(N,1)=1.0
B(N)=U
RETURN
END
    
```

LOCATION	SYMBOL	COMMON BLOCK / SOLVE / MAP SIZE	LOCATION	SYMBOL	LOCATION	SYMBOL	LOCATION
0	A	240	5340	NUMTC	5340	MBAND	53

LOCATION	SYMBOL	SCALAR MAP	LOCATION	SYMBOL	LOCATION	SYMBOL	LOCATION
88	M	CO	K	C4	N		

LOCATION	STATEMENT	LOCATION	STATEMENT	LOCATION	STATEMENT	LOCATION
18C	4	18C	5	198	6	1
1E0	9	1F0	10	200	11	2
248	14	264	15	278	16	2

; IN EFFECT\* NOID,BCD,SOURCE,NOLIST,NODECK,LOAD,MAP  
 ; IN EFFECT\* NAME = MODIFY , LINECNT = 50  
 ; TCS\* SOURCE STATEMENTS = 17, PROGRAM SIZE = 660  
 ; TCS\* NO DIAGNOSTICS GENERATED

```

SUBROUTINE MPL0T
IMPLICIT REAL*8(A-H, O-Z)
INTEGER CODE
COMMON/TO/ IMIN(20), IMAX(20), JMIN(10), JMAX(10), MAXI, MAXJ,
INMTL, NBC
COMMON/NPCDATA/ R(200), CODE(200), XR(200), Z(200), XZ(200),
INPNUM(10, 20), T(200), XT(200)
REAL*4 X(100), Y(100), TX(2), TY(2), TITLE(20), ZMAX
READ (5, 1000) TITLE, RMAX, ZMAX
CALL CCP2SY (0.7, 0.2, 0.2, TITLE, 0.0, 80)
CALL CCP1PL (0.7, 0.7, -3)
TX(1)=0.0
TY(1)=0.0
TX(2)=RMAX/9.0
TY(2)=RMAX/9.0
ZMAX=ZMAX*TY(2)+2.0
IF (ZMAX.LT.17.0) ZMAX=17.0
D0 100 J=1, MAXJ
NSTART=IMIN(J)
NSTOP=IMAX(J)
N=0
D0 101 I=NSTART, NSTOP
N=N+1
NP=NPNUM(I, J)
Y(N)=R(NP)
101 X(N)=Z(NP)
CALL CCP6LN (X, Y, N, 1, TX, TY)
100 CONTINUE
D0 102 I=1, MAXI
NSTART=JMIN(I)
NSTOP=JMAX(I)
N=0
D0 103 J=NSTART, NSTOP
N=N+1
NP=NPNUM(I, J)
Y(N)=R(NP)
103 X(N)=Z(NP)
CALL CCP6LN (X, Y, N, 1, TX, TY)
102 CONTINUE
CALL CCP1PL (ZMAX, -0.7, -3)
1000 FORMAT (20A4/2F10.0)
RETURN
END
    
```

LOCATION	SYMBOL	COMMON BLOCK / TO	LOCATION	SYMBOL	MAP SIZE	LOCATION	SYMBOL	LOCATION
0	IMAX		50	JMIN	100	A0	JMAX	

G LEVEL 21

NODE

DATE = 75066

14/36/21

```

FUNCTION NODE(I,J)
  IMPLICIT REAL*8(A-H,O-Z)
  COMMON/TD/ IMIN(20),IMAX(20),JMIN(10),JMAX(10),MAXI,MAXJ,
  1NMTL,NBC
  NODE=0
  DO 100 JJ=1,J
  NSTART=IMIN(JJ)
  NSTOP=IMAX(JJ)
  DO 100 II=NSTART,NSTOP
  NODE=NODE+1
  IF(JJ.EQ.J.AND.II.EQ.I) RETURN
100 CONTINUE
  RETURN
  END
    
```

LOCATION	SYMBOL	COMMON BLOCK /TD	LOCATION	/ MAP	SIZE	100	SYMBOL	LOCATION
0	IMAX		50	JMIN		A0	JMAX	
F4	NMTL		F8	NBC		FC		

LOCATION	SYMBOL	EQUIVALENCE DATA	MAP	SYMBOL	LOCATION	SYMBOL	LOCATION
A0							

LOCATION	SYMBOL	SCALAR MAP	LOCATION	SYMBOL	LOCATION	SYMBOL	LOCATION
A4	J		A8	NSTART		AC	
BR						NSTOP	

LOCATION	STATEMENT	LOCATION	STATEMENT	LOCATION	STATEMENT	LOCATION
156	4	156	5	15E	6	11
17A	9	182	10	18E	11	11

IN EFFECT\* NOID,BCD,SOURCE,NOLIST,NODECK,LOAD,MAP  
 IN EFFECT\* NAME = NODE , LINECNT = 50  
 ICS\* SOURCE STATEMENTS = 13, PROGRAM SIZE = 508  
 ICS\* NO DIAGNOSTICS GENERATED

SUBROUTINE POINTS

IMPLICIT REAL\*8(A-H, O-Z)

INTEGER CODE

COMMON/BASIC/ ACCELZ, ANGVEL, ANGACC, TREF, VOL, NUMNP, NUMEL, NUMPC, NUMSC, INUMST

COMMON/MATP/RO(6), E(12,16,6), EE(16), AOFTS(6)

COMMON/NPDATA/ R(200), CODE(200), XR(200), Z(200), XZ(200),

INPNUM(10,20), T(200), XT(200)

COMMON/ELDATA/ BETA(200), EPR(200), PR(20), SH(20), IX(200,5), IP(20),

IJP(20), IS(20), ISI(20), ALPHA(200), IT(200), JT(200), ST(20)

COMMON/SOLVE/ X(888), Y(888), TEM(888), NUMTC, MBAND

COMMON/TD/ IMIN(20), IMAX(20), JMIN(10), JMAX(10), MAXI, MAXJ,

IMMTL, NBC

COMMON/PLANE/NPP

DIMENSIONAR(10,20), AZ(10,20), MATRIL(200,5), BLKANG(200),

IBLKALF(200)

DIMENSION IBNG(130), NBNG(130)

EQUIVALENCE (R(1), AR), (Z(1), AZ)

C\* \* \* \* \* \*

C ESTABLISH NODAL POINT INFORMATION

C\* \* \* \* \* \*

NEL=0

NODSUM=0

DO 100 J=1, MAXJ

NSTART=IMIN(J)

NSTOP=IMAX(J)

DO 100 I=NSTART, NSTOP

100 NODSUM=NODSUM+1

NELSUM=0

JJMAX=MAXJ-1

DO 110 JJ=1, JJMAX

NSTOP=MINO(IMAX(JJ), IMAX(JJ+1))-1

NSTART=MAXO(IMIN(JJ), IMIN(JJ+1))

DO 110 II=NSTART, NSTOP

110 NELSUM=NELSUM+1

NUMNP=NODSUM

NUMEL=NELSUM

DO 120 J=1, MAXJ

NSTART=IMIN(J)

NSTOP=IMAX(J)

DO 120 I=NSTART, NSTOP

NPNUM(I, J)=NCODE(I, J)

NP=NPNUM(I, J)

R(NP)=AR(I, J)

120 Z(NP)=AZ(I, J)

C\* \* \* \* \* \*

C READ AND ASSIGN BOUNDARY CONDITIONS

C\* \* \* \* \* \*

LEVEL 21

POINTS

DATE = 75066

14/36/25

C INITIALIZE

```
C* * * * *  
DO 130 I=1,NUMNP  
CODE(I)=0  
IF(R(I).EQ.0..AND.NPP.EQ.0) CODE(I)=1.  
XR(I)=0.  
XZ(I)=0.  
XT(I)=0.0  
130 T(I)=0.  
IF(NBC.EQ.0) GO TO 210  
DO 200 IBCON=1,NBC  
READ(5,1002) I1,I2,J1,J2,ICN,PCON,ZCON,TCON  
DO 200 I=I1,I2  
DO 200 J=J1,J2  
NP=NPNUM(I,J)  
CODE(NP)=ICN  
XP(NP)=PCON  
XT(NP)=TCON  
200 XZ(NP)=ZCON  
210 MPRINT=0  
DO 230 J=1,MAXJ  
NSTART=IMIN(J)  
NSTOP=IMAX(J)  
DO 230 I=NSTART,NSTOP  
NP=NPNUM(I,J)  
IF(MPRINT.NE.0) GO TO 220  
WRITE(6,2000)  
MPRINT=59  
220 MPRINT=MPRINT-1  
230 WRITE(6,2001) I,J,NP,CODE(NP),R(NP),Z(NP),XP(NP),XZ(NP),XT(NP)
```

C\* \* \* \* \*

C ASSIGN MATERIALS IN BLOCKS

C\* \* \* \* \*

```
DO 300 M=1,NUMEL  
300 IX(M,5)=0  
DO 310 IMTL=1,NMTL  
READ(5,1000) MTL,(MATRIL(IMTL,IM),IM=2,5),BLKANG(IMTL),  
IBLKALF(IMTL),IBNG(IMTL),NBNG(IMTL)  
310 MATRIL(IMTL,1)=MTL  
ICNG=0  
NCNG=0
```

C\* \* \* \* \*

C ESTABLISH ELEMENT INFORMATION

C\* \* \* \* \*

```
JJMAX=MAXJ-1  
N=0  
MTL=1  
KTL=1
```

```

DO 440 JJ=1, JJMAX
NSTOP=MINO(IMAX(JJ), IMAX(JJ+1))-1
NSTART=MAXO(IMIN(JJ), IMIN(JJ+1))
DO 440 II=NSTART, NSTOP
NEL=NEL+1
DO 400 IMTL=1, NMTL
IF (II.LT.MATRIL(IMTL,2)) GO TO 400
IF (II.GE.MATRIL(IMTL,3)) GO TO 400
IF (JJ.LT.MATRIL(IMTL,4)) GO TO 400
IF (JJ.GE.MATRIL(IMTL,5)) GO TO 400
KAT=IMTL
MAT=MATRIL(IMTL,1)
400 CONTINUE
IF (KAT.EQ.KTL) GO TO 410
KTL=KAT
MTL=MAT
GO TO 420
410 IF (II.EQ.NSTART) GO TO 420
IF (JJ.NE.JJMAX.OF.II.NE.NSTOP) GO TO 440
M=NEL+1
IANG=ICNG
NANG=NCNG
GO TO 421
420 I=NPNUM(II, JJ)
J=I+1
K=NPNUM(II+1, JJ+1)
L=K-1
M=NEL
IX(M,1)=I
IX(M,2)=J
IX(M,3)=K
IX(M,4)=L
IX(M,5)=MTL
BETA(M)=BLKANG(KTL)
ALPHA(M)=BLKALF(KTL)
IANG=ICNG
NANG=NCNG
ICNG=IBNG(KTL)
NCNG=NBNG(KTL)
421 NC=2
430 N=N+1
IF (M.LE.N) GO TO 440
IX(N,1)=IX(N-1,1)+1
IX(N,2)=IX(N-1,2)+1
IX(N,3)=IX(N-1,3)+1
IX(N,4)=IX(N-1,4)+1
IX(N,5)=IX(N-1,5)
BETA(N)=BETA(N-1)
    
```





LEVEL 21

QUAD

DATE = 75066

14/36/25

SUBROUTINE QUAD

IMPLICIT REAL\*8(A-H,O-Z)

INTEGER CODE

REAL\*8 NUSN,NUTN,NUTS,NUNS,NUNT,NUST

DIMENSION DUMMY(6,6),DUMMY1(6,6)

COMMON/BASIC/ACELZ,ANGVEL,ANGACC,TREF,VOL,NUMNP,NUMEL,NUMPC,NUMSC,

INUMST

COMMON/MATP/R(6),E(12,16,6),EE(16),ADFTS(6)

COMMON/NPDATA/ R(200),CODE(200),XR(200),Z(200),XZ(200),

INPNUM(10,20),T(200),XT(200)

COMMON/ELDATA/ BETA(200),EPR(200),PR(20),SH(20),IX(200,5),IP(20),

IJP(20),IS(20),JS(20),ALPHA(200),IT(200),JT(200),ST(20)

COMMON/ARG/PRR(5),ZZZ(5),RR(4),ZZ(4),S(15,15),P(15),TT(6),

IH(6,15),CPZ(6,6),XT(10),ANGLE(4),SIG(18),EPS(18),N

COMMON/RESULT/BS(6,15),D(6,6),C(6,6),AR,BB(6,9),CNS(6,6)

COMMON/PLANE/NPP

I1=IX(N,1)

J1=IX(N,2)

K1=IX(N,3)

L1=IX(N,4)

MTYPE=IABS(IX(N,5))

IX(N,5)=-IX(N,5)

C\* \* \* \* \*

C INTERPOLATE MATERIAL PROPERTIES

C\* \* \* \* \*

DO 100 I=1,12

100 EE(I)=E(1,I+1,MTYPE)

DO 110 I=1,6

DO 110 J=1,6

CNS(I,J)=0.0

C(I,J)=0.0

110 D(I,J)=0.0

C\* \* \* \* \*

C FORM STRESS-STRAIN RELATIONSHIP IN N-S-T SYSTEM

C\* \* \* \* \*

NUNS=EE(4)

NUNT=EE(5)

NLST=EE(6)

NLSN=(EE(2)\*NUNS)/EE(1)

NUTN=(EE(3)\*NUNT)/EE(1)

NUTS=(EE(3)\*NLST)/EE(2)

DIV=1.0-NUNS\*NLSN-NUST\*NUTS-NUNT\*NUTN-NUSN\*NUNT\*NUTS

I=NUNS\*NUTN\*NLST

CNS(1,1)=EE(1)\*(1.0-NUST\*NUTS)/DIV

CNS(1,2)=EE(2)\*(NUNS+NUNT\*NUTS)/DIV

CNS(1,3)=EE(3)\*(NUNT\*NUNS\*NUST)/DIV

CNS(2,1)=CNS(1,2)

CNS(2,2)=EE(2)\*(1.0-NUNT\*NUTN)/DIV

G LEVEL 21

QUAD

DATE = 75066

14/36/2

```

CNS(2,3)=EE(3)*(NUST+NUSN*NUNT)/DIV
CNS(3,1)=CNS(1,3)
CNS(3,2)=CNS(2,3)
CNS(3,3)=EE(3)*(1.0-NUNS*NUSN)/DIV
CNS(4,4)=EE(7)
CNS(5,5)=EE(8)
CNS(6,6)=EE(9)
C   SET UP STRAIN TRANSFORM TO N-S-T SYSTEM
    SINA=DSIN(ALPHA(N))
    COSA=DCOS(ALPHA(N))
    S2=SINA**2
    C2=COSA**2
    SC=SINA*COSA
    D(1,1)=C2
    D(1,3)=S2
    D(1,6)=-SC
    D(2,1)=S2
    D(2,3)=C2
    D(2,6)=SC
    D(3,2)=1.0
    D(4,1)=2.0*SC
    D(4,3)=-2.0*SC
    D(4,6)=C2-S2
    D(5,4)=SINA
    D(5,5)=COSA
    D(6,4)=COSA
    D(6,5)=-SINA
C   SET UP STRAIN TRANSFORMATION TO R-Z-T SYSTEM
    SINB=DSIN(BETA(N))
    COSB=DCOS(BETA(N))
    S2=SINB**2
    C2=COSB**2
    SC=SINB*COSB
    C(1,1)=S2
    C(1,2)=C2
    C(1,4)=SC
    C(2,1)=C2
    C(2,2)=S2
    C(2,4)=-SC
    C(3,3)=1.0
    C(4,1)=-2.0*SC
    C(4,2)=2.0*SC
    C(4,4)=S2-C2
    C(5,5)=SINB
    C(5,6)=-COSB
    C(6,5)=COSB
    C(6,6)=SINB
C   CALCULATE CRZ MATRIX
    
```

G LEVEL 21

QUAD

DATE = 75066

14/36/25

```

DO 120 I=1,6
DO 120 J=1,6
DUMMY(I,J)=0.0
DO 120 K=1,6
120 DUMMY(I,J)=DUMMY(I,J)+D(I,K)*C(K,J)
DO 130 I=1,6
DO 130 J=1,6
DUMMY1(I,J)=0.0
DO 130 K=1,6
130 DUMMY1(I,J)=DUMMY1(I,J)+CNS(I,K)*DUMMY(K,J)
DO 140 I=1,6
DO 140 J=1,6
DUMMY(I,J)=0.0
DO 140 K=1,6
140 DUMMY(I,J)=DUMMY(I,J)+D(K,I)*DUMMY1(K,J)
DO 160 I=1,6
DO 150 J=1,6
CRZ(I,J)=0.0
DO 150 K=1,6
150 CRZ(I,J)=CPZ(I,J)+C(K,I)*DUMMY(K,J)
TT(I)=0.0
DO 160 M=1,6
P(M)=0.0
DO 161 II=1,3
IF(A7FTS(MTYPE).EQ.1.) P(M)=CNS(M,II)*EE(II+9)
161 P(M)=P(M)+(T(N)-TREF)*CNS(M,II)*EE(II+9)
DO 160 K=1,6
160 TT(I)=TT(I)+C(K,I)*D(N,K)*P(M)
    
```

C  
C

```

FORM QUADRILATERAL STIFFNESS MATRIX
PRP(5)=(P(II)+P(JI)+R(KI)+R(LI))/4.
ZZZ(5)=(Z(II)+Z(JI)+Z(KI)+Z(LI))/4.
DO 200 M=1,4
MM=IX(N,M)
IF(NPP.NE.0) GO TO 190
IF(P(MM).EQ.0..AND.CODE(MM).EQ.0.)CODE(MM)=1.
190 PRP(M)=R(MM)
200 ZZZ(M)=Z(MM)
DO 220 II=1,15
P(II)=0.0
DO 220 JJ=1,15
220 S(II,JJ)=0.0
DO 90 I=1,6
VNL=0.
DO 90 J=1,15
90 RS(I,J)=0.0
AR=0.0
240 CALL TRISTF(4,1,5)
    
```

G LEVEL 21

QUAD

DATE = 75066

14/36/25

```

CALL TRISTF(1,2,5)
CALL TRISTF(2,3,5)
CALL TRISTF(3,4,5)
DO 91 I=1,6
DO 91 J=1,15
91 BS(I,J)=BS(I,J)/AR
RETURN
END
    
```

LOCATION	SYMBOL	COMMON BLOCK LOCATION	/BASIC	SYMBOL	/ MAP LOCATION	SIZE	3C	SYMBOL	LOCATION
0	ANGVEL	8		ANGACC	10			TREF	
28	NUMEL	2C		NUMPC	30			NUMSC	

LOCATION	SYMBOL	COMMON BLOCK LOCATION	/MAP	SYMBOL	/ MAP LOCATION	SIZE	24E0	SYMBOL	LOCATION
0	E	30		EE	2430			AOFTS	24E

LOCATION	SYMBOL	COMMON BLOCK LOCATION	/NPDATA	SYMBOL	/ MAP LOCATION	SIZE	28C0	SYMBOL	LOCATION
0	CODE	640		XR	960			Z	F.
1C20	T	1F40		XT	2580				

LOCATION	SYMBOL	COMMON BLOCK LOCATION	/ELDATA	SYMBOL	/ MAP LOCATION	SIZE	28C0	SYMBOL	LOCATION
0	EPR	640		PR	C80			SH	D.
1D60	JP	1D80		IS	1E00			JS	1E
24E0	JT	2800		ST	2820				

LOCATION	SYMBOL	COMMON BLOCK LOCATION	/ARG	SYMBOL	/ MAP LOCATION	SIZE	DC4	SYMBOL	LOCATION
0	ZZZ	79		RP	50			ZZ	
79A	TT	810		H	840			CPZ	B
C80	SIG	CA0		EPS	D30			N	D

LOCATION	SYMBOL	COMMON BLOCK LOCATION	/RESULT	SYMBOL	/ MAP LOCATION	SIZE	7E8	SYMBOL	LOCATION
0	D	200		C	3F0			AR	5
6C8									

COMMON BLOCK /PLANE / MAP SIZE 4

LEVEL 21

SET

DATE = 75066

14/36/25

## SUBROUTINE SET

IMPLICIT REAL\*8(A-H,O-Z)

INTEGER CODE

COMMON/BASIC/ACELZ,ANGVEL,ANGACC,TREF,VOL,NUMNP,NUMEL,NUMPC,NUMSC,  
INUMST

COMMON/NPDATA/ R(200),CODE(200),XR(200),Z(200),XZ(200),

INPNUM(10,20),T(200),XT(200)

COMMON/ELDATA/ BETAT(200),EPR(200),PR(20),SH(20),IX(200,5),IP(20),

IJP(20),IS(20),JS(20),ALPHA(200),IT(200),JT(200),ST(20)

COMMON/CIT/NEQL,NSLIP,ICRACK,ISLIP,INP,NSKIP

COMMON/DATA1/RTN(200),RST(200),RNN(200)

COMMON/DATA2/IFAIL(200),TB(200,12),ICR(200),IAD(200,4)

COMMON/DATA3/TFAIL,CF

C  
C  
C  
CREAD NUMBER OF ITERATIONS FOR SLIP, FOR EQUILIBRIUM, COEFFICIENT  
OF FRICTION AND MAXIMUM ALLOWED INTERLAMINAR SMEAR STRESS

READ(5,1001) NSLIP,NEQL,TFAIL

DO 10 I=1,NUMNP

IFAIL(I)=0

ICR(I)=0

10

C  
C  
C

READ PARAMETERS OFFINING DIRECTION OF SLIP

READ(5,1001) NCBI,NCBJ

IF(NCBI.EQ.0) GO TO 13

DO 11 N=1,NCBI

READ(5,1000) NIMIN,NIMAX,NJMIN,NJMAX

DO 11 I=NIMIN,NIMAX

DO 11 J=NJMIN,NJMAX

NPIJ=NPNUM(I,J)

ICR(NPIJ)=1

11

13

CONTINUE

IF(NCBJ.EQ.0) GO TO 14

DO 12 N=1,NCBJ

READ(5,1000) NIMIN,NIMAX,NJMIN,NJMAX

DO 12 I=NIMIN,NIMAX

DO 12 J=NJMIN,NJMAX

NPIJ=NPNUM(I,J)

ICR(NPIJ)=2

12

14

CONTINUE

C  
C  
C

IDENTIFY FOUR ADJACENT ELEMENTS FOR EACH NODE

DO 21 N=1,NUMNP

DO 21 I=1,4

IAD(N,I)=0

21

DO 22 N=1,NUMEL

G LEVEL 21

SET

DATE = 75066

14/36/21

```

DO 22 I=1,4
  IXX=IX(N,I)
  22  IAD(IXX,I)=N
  1000 FORMAT(4I10)
  1001 FORMAT(2I10, F10.3)
  RETURN
  END
    
```

LOCATION	SYMBOL	COMMON BLOCK LOCATION	/BASIC	/ MAP	SIZE LOCATION	3C	SYMBOL	LOCA
0	ANGVEL	8			10		TREF	
28	NUMEL	2C			30		NUMSC	

LOCATION	SYMBOL	COMMON BLOCK LOCATION	/NPDATA	/ MAP	SIZE LOCATION	28C0	SYMBOL	LOCA
0	CODE	640			960		Z	F
1020	T	1F40			2580			

LOCATION	SYMBOL	COMMON BLOCK LOCATION	/ELDATA	/ MAP	SIZE LOCATION	28C0	SYMBOL	LOCA
0	EPP	640			680		SH	D
1060	JP	1080			1E00		JS	IE
24E0	JT	2800			2B20			

LOCATION	SYMBOL	COMMON BLOCK LOCATION	/CIT	/ MAP	SIZE LOCATION	18	SYMBOL	LOCA
0	NSLIP	4			8		ISLIP	
14								

LOCATION	SYMBOL	COMMON BLOCK LOCATION	/DATA1	/ MAP	SIZE LOCATION	12C0	SYMBOL	LOCA
0	PST	640			680			

LOCATION	SYMBOL	COMMON BLOCK LOCATION	/DATA2	/ MAP	SIZE LOCATION	5DC0	SYMBOL	LOCA
0	TB	320			4E20		IAD	51

LOCATION	SYMBOL	COMMON BLOCK LOCATION	/DATA3	/ MAP	SIZE LOCATION	10	SYMBOL	LOCA
0	CF	8						

G LEVEL 21

SOLV

DATE = 75066

14/36/2

```
SUBROUTINE SOLV
IMPLICIT REAL*8(A-H,O-Z)
COMMON/BASIC/ACELZ,ANGVEL,ANGACC,TREF,VOL,NUMNP,NUMEL,NUMPC,NUMSC,
1 NUMST
COMMON/SOLVE/B(72),A(72,36),NUMTC,HBAND
MM=MBAND
NN=36
NL=NN+1
NH=NN+NN
REWIND 1
REWIND 2
NR=0
GO TO 150
C REDUCE EQUATIONS BY BLOCKS
C * * * * *
C
C 1. SHIFT BLOCK OF EQUATIONS
C
100 NB=NB+1
DO 125 N=1,NA
NM=NN+N
B(N)=B(NM)
B(NM)=0.0
DO 125 M=1,MM
A(N,M)=A(NM,M)
125 A(NM,M)=0.0
C
C 2. READ NEXT BLOCK OF EQUATIONS INTO CORE
C
IF(NUMBLK.EQ.NB) GO TO 200
150 READ(2) (B(N),(A(N,M),M=1,MM),N=NL,NH)
IF(NB.EQ.0) GO TO 100
C
C 3. REDUCE BLOCK OF EQUATIONS
C
200 DO 300 N=1,NA
IF(A(N,1).EQ.0.0) GO TO 300
B(N)=B(N)/A(N,1)
DO 275 L=2,MM
IF(A(N,L).EQ.0.0) GO TO 275
C=A(N,L)/A(N,1)
I=N+L-1
J=0
DO 250 K=L,MM
J=J+1
250 A(I,J)=A(I,J)-C*A(N,K)
B(I)=B(I)-A(N,L)*B(N)
A(N,L)=C
```

G LEVEL 21

SOLV

DATE = 75066

14/36/21

275 CONTINUE

300 CONTINUE

C  
C  
C

4. WRITE BLOCK OF REDUCED EQUATIONS ON FORTRAN UNIT 1

IF(NUMBLK.EQ.NB) GO TO 400  
WRITE (1) (B(N), (A(N,M), M=2,MM), N=1,NN)  
GO TO 100

C\* \* \* \* \*  
C BACK-SUBSTITUCN  
C\* \* \* \* \*

400 DO 450 M=1, MN  
N=NN+1-M  
DO 425 K=2, MM  
L=N+K-1  
425 B(N)=B(N)-A(N,K)\*B(L)  
NM=N+NN  
B(NM)=B(N)  
450 A(NM,NB)=B(N)  
NB=NB-1  
IF(NB.EQ.0) GO TO 500  
BACKSPACE 1  
READ (1) (B(N), (A(N,M), M=2,MM), N=1,NN)  
BACKSPACE 1  
GO TO 400

C\* \* \* \* \*  
C ORDER FORMER UNKNOWN IN B ARRAY  
C\* \* \* \* \*

500 K=0  
DO 600 NB=1, NUMBLK  
DO 600 N=1, NN  
NM=N+NN  
K=K+1

600 B(K)=A(NM,NB)

C\* \* \* \* \*

C WRITE SOLUTION  
MPRINT=0  
DO 710 N=1, NUMNP  
IF(MPRINT.NE.0) GO TO 700  
WRITE (6,2000)  
MPRINT=59

700 MPRINT=MPRINT-1  
710 WRITE (6,2001) N, B(3\*N-2), B(3\*N-1), B(3\*N)  
2000 FORMAT (I3H1 NCCAL POINT, 18X, 2HUR, 18X, 2HUZ, 18X, 2HUT)  
2001 FORMAT (I13, 3E20.7)  
RETURN  
END



```

SUBROUTINE STIFF
  IMPLICIT REAL*8(A-H,O-Z)
  INTEGER CODE
  COMMON/BASIC/ACELZ,ANGVEL,ANGACC,TREF,VOL,NUMNP,NUMEL,NUMPC,NUMSC,
  1 NUMST
  COMMON/NPDATA/ R(200),CODE(200),XR(200),Z(200),XZ(200),
  INPNUM(10,20),T(200),XT(200)
  COMMON/ELDATA/ BETA(200),EPR(200),FR(20),SH(20),IX(200,5),IP(20),
  1JP(20),IS(20),JS(20),ALPHA(200),IT(200),JT(200),ST(20)
  COMMON/ARG/EPR(5),ZZZ(5),RR(4),ZZ(4),S(15,15),P(15),TT(6),
  1H(6,15),CPZ(6,6),XI(10),ANGLE(4),SIG(18),EPS(18),N
  COMMON/SOLVE/B(72),A(72,36),NUMTC,MBAND
  COMMON/PLANE/NPP
  COMMON/DATA2/IFAIL(200),TB(200,12),ICR(200),IAD(200,4)
  DIMENSION LM(4),S2(12,3),S3(3,12),S4(3,3),S5(12,3),S6(12,12)
C * * * * *
C   INITIALIZATION
C * * * * *
  REWIND 2
  ND=36
  ND2=2*ND
  STOP=0.
  NUMBLK=0
  DO 100 N=1,ND2
    B(N)=0.0
  DO 100 M=1,ND
  100 A(N,M)=0.0
C * * * * *
C   FORM STIFFNESS MATRIX IN BLOCKS
C * * * * *
  200 NUMBLK=NUMBLK+1
  NH=NB*(NUMBLK+1)
  NM=NH-NB
  NL=NM-NB+1
  KSHIFT=3*NL-3
  DO 340 N=1,NL*NL
  IF(IX(N,5).LE.0) GO TO 340
  DO 210 I=1,4
  IF(IX(N,I).LT.AL) GO TO 210
  IF(IX(N,I).LE.NM) GO TO 220
  210 CONTINUE
  GO TO 340
  220 CALL QUAD
  IF(VOL.GT.0.) GO TO 230
  WRITE(6,2000) N
  STOP=1.
  230 IF(IX(N,3).EQ.IX(N,4)) GO TO 300
  DO 231 !I=1,3
    
```

G LEVEL 21

STIFF

DATE = 75066

14/36/25

```

DO 231 JJ=1,3
231 S4(II,JJ)=S(II+12, JJ+12)
CALL SYMINV(S4,3)
DO 232 II=1,12
DO 232 JJ=1,3
232 S2(II,JJ)=S(II, JJ+12)
DO 233 II=1,3
DO 233 JJ=1,12
233 S3(II,JJ)=S(II+12, JJ)
DO 240 I=1,12
DO 240 J=1,3
S5(I, J)=0.0
DO 240 K=1,3
240 S5(I, J) = S5(I, J) + S2(I, K) * S4(K, J)
DO 241 I=1,12
DO 241 J=1,12
S6(I, J)=0.0
DO 241 K=1,3
241 S6(I, J) = S6(I, J) + S5(I, K) * S3(K, J)
DO 234 II=1,12
DO 234 JJ=1,3
234 P(II)=P(II)-S5(II, JJ)*P(JJ+12)
DO 235 II=1,12
DO 235 JJ=1,12
235 S(II, JJ)=S(II, JJ)-S6(II, JJ)
DO 93 I=1,12
DO 93 J=1,12
93 P(I)=P(I)-S(I, J)*TB(N, J)
C* * * * *
C ADD ELEMENT STIFFNESS MATRIX TO BODY STIFFNESS MATRIX
C* * * * *
300 DO 310 I=1,4
310 LM(I)=3*IX(N, I)-3
DO 330 I=1,4
DO 330 K=1,3
II=LM(I)+K-KSHIFT
KK=3*I-3+K
B(II)=B(II)+F(KK)
DO 330 J=1,4
DO 330 L=1,3
JJ=LM(J)+L-?I+1-KSHIFT
LL=3*J-3+L
IF(JJ.LE.0) GO TO 330
IF(ND.GE.JJ) GO TO 320
WRITE(6,2001) N
STOP=1.
GO TO 340
320 A(II, JJ) =A(II, JJ)+S(KK, LL)

```

G LEVEL 21

STIFF

DATE = 75066

14/36/2

330 CONTINUE

340 CONTINUE

C\* \* \* \* \*

C ADD CONCENTRATED FORCES

C\* \* \* \* \*

DO 400 N=NL,AM

IF(N.GT.NUMNP) GO TO 500

K=3\*N-KSHIFT

B(K)=B(K)+XT(N)

B(K-1)=B(K-1)+XZ(N)

400 B(K-2)=B(K-2)+XP(N)

C\* \* \* \* \*

C ADD PRESSURE BOUNDARY CONDITIONS

C\* \* \* \* \*

500 IF(NUMPC.EQ.0) GO TO 600

DO 540 L=1,NLMPC

I=IP(L)

J=JP(L)

PP=PD(L)/6.

DR=(D(J)-F(I))\*PP

DZ=(Z(I)-Z(J))\*PP

FX=2.\*P(I)+R(J)

ZX=P(I)+2.\*P(J)

II=3\*I-KSHIFT-1

JJ=3\*J-KSHIFT-1

IF(II.LE.0.OR.II.GT.ND) GO TO 520

SINA=0.

COSA=1.

510 B(II-1)=B(II-1)+PX\*(COSA\*DZ+SINA\*DR)

B(II)=B(II)-FX\*(SINA\*DZ-COSA\*DR)

520 IF(IJ.LE.0.OR.IJ.GT.ND) GO TO 540

SINA=0.

COSA=1.

530 B(IJ-1)=B(IJ-1)+ZX\*(COSA\*DZ+SINA\*DR)

B(IJ)=B(IJ)-ZX\*(SINA\*DZ-COSA\*DR)

540 CONTINUE

C\* \* \* \* \*

C ADD SHEAR BOUNDARY CONDITIONS

C\* \* \* \* \*

600 IF(NUMSC.EQ.0) GO TO 701

DO 640 L=1,NLMSC

I=IS(L)

J=JS(L)

SS=SH(L)/6.

DZ=(Z(I)-Z(J))\*SS

DR=(F(J)-F(I))\*SS

FX=2.\*P(I)+R(J)

ZX=P(I)+2.\*P(J)

N IV G LEVEL 21

STIFF

DATE = 75066

14

```
II=3*I-KSHIFT-1
JJ=3*J-KSHIFT-1
IF(II.LE.0.OR.II.GT.ND) GO TO 620
SINA=0.
COSA=1.
610 B(II-1)=B(II-1)+RX*(SINA*DZ+COSA*DR)
B(II)=B(II)-RX*(COSA*DZ-SINA*DR)
620 IF(JJ.LE.0.OR.JJ.GT.ND) GO TO 640
SINA=0.
COSA=1.
630 B(JJ-1)=B(JJ-1)+ZX*(SINA*DZ+COSA*DR)
B(JJ)=B(JJ)-ZX*(COSA*DZ-SINA*DR)
640 CONTINUE
701 IF(NUMST.EQ.0) GO TO 700
DO 680 L=1,NUMST
I=IT(L)
J=JT(L)
RT=ST(L)/6.
PX=2.*R(I)+R(J)
ZX=R(I)+2.*P(J)
XX=DSORT((R(J)-R(I))*2+(Z(J)-Z(I))*2)
II=3*I-KSHIFT
JJ=3*J-KSHIFT
IF(II.LE.0.OR.II.GT.ND) GO TO 670
R(II)=B(II)+RT*PX*XX
670 IF(JJ.LE.0.OR.JJ.GT.ND) GO TO 680
B(JJ)=B(JJ)+RT*ZX*XX
680 CONTINUE
C* * * * *
C ADD DISPLACEMENT BOUNDARY CONDITIONS
C* * * * *
700 DO 750 M=NL,NH
IDM=0
IF(M.GT.NUMNP) GO TO 750
IF(CODE(M).GT.3) GO TO 751
U=XR(M)
N=3*M-2-KSHIFT
752 IF(CODE(M)) 740,750,710
710 IF(CODE(M).EQ.1) GO TO 720
IF(CODE(M).EQ.2) GO TO 740
IF(CODE(M).EQ.3) GO TO 730
GO TO 740
720 CALL MODIFY(MD2,N,U)
CODE(M)=CODE(M)+IDM
GO TO 750
730 CALL MODIFY(MD2,N,U)
740 U=XZ(M)
N=N+1
```

LEVEL 21

STIFF

DATE = 75066

14/36/25

```

CALL MODIFY(ND2,N,U)
CODE(M)=CODE(M)+IDM
GO TO 750
751 IDM=IDM+4
    U=XT(M)
    N=3*M-KSHIFT
    CALL MODIFY(ND2,N,U)
    U=XR(M)
    N=3*M-2-KSHIFT
    IF(CODE(M).EQ.4) GO TO 750
    CODE(M)=CODE(M)-4
    GO TO 752
750 CONTINUE
C* * * * *
C    WRITE BLOCK OF EQUATIONS ON FORTRAN UNIT AND SHIFT UP LOWER BLOCK
C* * * * *
    WRITE (2) (B(N),(A(N,M),M=1,MBAND),N=1,ND)
    DO 800 M=1,ND
        K=N+ND
        R(N)=B(K)
        B(K)=0.0
    DO 800 M=1,ND
        A(N,M)=A(K,M)
    800 A(K,M)=0.0
C* * * * *
C    CHECK FOR LAST BLOCK
C* * * * *
    IF(NM.LT.NUMNP) GO TO 200
    IF(STOP.NE.0.) STOP
2000 FORMAT (27H NEGATIVE AREA ELEMENT NO.,I4)
2001 FORMAT (46H BAND WIDTH EXCEEDS ALLOWABLE FOR ELEMENT NO.,I4)
    RETURN
    END
    
```

CATION	SYMBOL	COMMON BLOCK /BASIC	LOCATION	MAP SIZE	3C	SYMBOL	LOCATION	LOCATI
0	ANGVEL		8		10	TREF		18
2R	NUMFL		2C		30	NUMSC		34

CATION	SYMBOL	COMMON BLOCK /NPDATA	LOCATION	MAP SIZE	2BC0	SYMBOL	LOCATION	LOCATI
0	CODE		640		960	Z		FA
1C20	T		1F40		2580			

COMMON BLOCK /ELDATA / MAP SIZE 2BC0

LEVEL 21

STRESS

DATE = 75066

14/36/25

```

SUBROUTINE STRESS
IMPLICIT REAL*8 (A-H, O-Z)
INTEGER CODE
COMMON/BASIC/ACELZ,ANGVEL,ANGACC,TREF,VOL,NUMNP,NUMEL,NUMPC,NUMSC,
INUMST
COMMON/MATP/RQ(6),E(12,16,6),EE(16),ADFTS(6)
COMMON/NPDATA/ R(200),CODE(200),XR(200),Z(200),XZ(200),
INPNUM(10,20),T(200),XT(200)
COMMON/ELDATA/ BETA(200),EPR(200),PR(20),SH(20),IX(200,5),IP(20),
LIP(20),IS(20),JS(20),ALPHA(200),IT(200),JT(200),ST(20)
COMMON/ARG/RRR(5),ZZZ(5),RR(4),ZZ(4),S(15,15),P(15),TT(6),
IH(6,15),CRZ(6,6),XI(10),ANGLE(4),SIG(18),EPS(18),N
COMMON/CCNVPG/IDONE
COMMON/SCLVE/R(72),A(72,36),NUMTC,MBAND
COMMON/PLANE/NPD
COMMON/RESULT/BS(6,15),D(6,6),C(6,6),AR,BR(6,9),CNS(6,6)
COMMON/CIT/NEOL ,NSLIP,ICRACK,ISLIP,INP,NSKIP
COMMON/DATA1/PTN(200),RST(200),RNN(200)
COMMON/DATA2/TFAIL(200),TB(200,12),ICR(200),IAD(200,4)
DIMENSION LM(4),TP(6),TR(3,3),O(3)
    
```

```

C* * * * *
C INITIALIZE
C* * * * *
    
```

```

XKE=0.
XPE=0.
MPRINT=0
FEROU=.005
IDONE=1
DO 200 N=1,NUMEL
IX(N,5)=IABS(IX(N,5))
CALL QUAD
DO 100 I=1,4
    I=3*I
    JJ=3*IX(N,I)
    P(II-2)=9(JJ-2)
    P(II-1)=8(JJ-1)
100 P(II) =8(JJ)
    DO 11 I=1,12
11 P(I)=P(I)+TB(N,I)
    DO 110 I=1,3
110 O(I)=P(I+12)
    DO 120 I=1,3
    DO 120 J=1,3
120 TR(I,J)=S(I+12,J+12)
CALL SYMINV(TP,3)
DO 130 I=1,3
P(I+12)=0.0
DO 130 J=1,3
    
```

3 LEVEL 21

STRESS

DATE = 75066

14/36/25

```

D0 130 K=1,12
130 P(I+12)=P(I+12)+TR(I,J)*(Q(J)-S(IJ+12,K))*P(K)
MTYPE=IABS(IX(N,5))
C
C MATRIX P NOW CONTAINS 15 DISPLACEMENTS FOR QUADRILATERAL ELEMENT
C
C CALCULATE AVERAGE STRAINS
C
D0 140 I=1,6
EPS(I)=0.0
D0 140 J=1,15
140 EPS(I)=EPS(I)+BS(I,J)*D(J)
C
C CALCULATE AVERAGE STRESSES
C
D0 151 I=1,6
SIG(I)=0.0
D0 151 J=1,6
151 SIG(I)=SIG(I)+CRZ(I,J)*EPS(J)
D0 152 I=1,6
152 SIG(I)=SIG(I)-TT(I)
C
C CALCULATE STRAINS IN N-S-T COORDINATES
C
D0 150 I=1,6
EPS(I+6)=0.0
D0 150 J=1,6
D0 150 K=1,6
150 EPS(I+6)=EPS(I+6)+D(I,J)*C(J,K)*EPS(K)
C
C CALCULATE STRESSES IN N-S-T COORDINATES
C
D0 160 I=1,6
SIG(I+6)=0.0
D0 160 J=1,6
160 SIG(I+6)=SIG(I+6)+CNS(I,J)*EPS(J+6)
D0 161 M=1,6
P(M)=0.0
D0 161 II=1,3
IF(ADFS(MTYPE).EQ.1.) P(M)=CNS(M,II)*EE(II+9)
161 P(M)=P(M)+(T(N)-TREF)*CNS(M,II)*EE(II+9)
D0 162 I=1,6
162 SIG(I+6)=SIG(I+6)-P(I)
C
C CALCULATE AND STORE INTERLAMINAR STRESSES
C
IF(!CRACK.EQ.0) GO TO 180
    
```





LEVEL 21 SYMINV DATE = 75066 14/36/7

```

SUBROUTINE SYMINV(A,NMAX)
IMPLICIT REAL*8(A-H,O-Z)
DIMENSION A(NMAX,NMAX)
DO 300 N=1,NMAX
D=A(N,N)
DO 100 J=1,NMAX
100 A(N,J)=-A(N,J)/D
DO 210 I=1,NMAX
IF(N.EQ.I) GO TO 210
DO 200 J=1,NMAX
IF(N.NE.J) A(I,J)=A(I,J)+A(I,N)*A(N,J)
200 CONTINUE
210 A(I,N)=A(I,N)/D
300 A(N,N)=1.0/D
RETURN
END
    
```

SCALAR MAP

SYMBOL	LOCATION	SYMBOL	LOCATION	SYMBOL	LOCATION
NMAX	HR	N	BC	J	

ARRAY MAP

SYMBOL	LOCATION	SYMBOL	LOCATION	SYMBOL	LOCATION

STATEMENT NUMBER MAP

STATEMENT	LOCATION	STATEMENT	LOCATION	STATEMENT	LOCATION
4	194	5	19C	6	1
9	228	10	236	11	2
14	344	15	37F		

EFFECT\* NOID,BCD,SOURCE,NOLIST,NODECK,LOAD,MAP  
 EFFECT\* NAME = SYMINV , LINES = 50  
 SOURCE STATEMENTS = 16, PROGRAM SIZE = 902  
 NO DIAGNOSTICS GENERATED

IN IV G LEVEL 21

TEMP

DATE = 75066

147

```
SUBROUTINE TEMP(R,Z,T)
IMPLICIT REAL*8(A-H,O-Z)
COMMON/SOLVE/ X(888),Y(888),TEM(888),NUMTC,MBAND
DIMENSION SMALL(20),ISM(20)
C* * * * *
C INITIALIZE
C* * * * *
  J=1
  JMAX=16
  IF(NUMTC.LT.JMAX) JMAX=NUMTC
  DO 10 I=1,JMAX
    SMALL(I)=0.
10 ISM(I)=0
C* * * * *
C FIND THE JMAX CLOSEST POINTS
C* * * * *
  DO 50 I=1,NUMTC
    DSQ=(X(I)-R)**2+(Y(I)-Z)**2
    IF(DSQ.GT..1E-4) GO TO 20
    T=TEM(I)
    RETURN
20 IF(I.EQ.1) SMALL(I)=DSQ
   IF(I.EQ.1) ISM(I)=1
   IF(I.EQ.1) GO TO 50
   IF(SMALL(J).LE.DSQ.AND.J.LT.JMAX) SMALL(J+1)=DSQ
   IF(SMALL(J).LE.DSQ.AND.J.LT.JMAX) ISM(J+1)=I
   IF(SMALL(J).LE.DSQ) GO TO 40
   DO 30 K=1,J
     JB=J-K +1
     IF(JB.EQ.0) GO TO 40
     SMALL(JB+1)=SMALL(JB)
     ISM(JB+1)=ISM(JB)
     SMALL(JB)=DSQ
     ISM(JB)=I
     IF(JB.EQ.1) GO TO 40
     IF(SMALL(JB-1).LE.DSQ) GO TO 40
30 CONTINUE
40 IF(J.LT.JMAX) J=J+1
50 CONTINUE
C* * * * *
C FIND THE THIRD TEMPERATURE POINT BY AREA TEST
C* * * * *
  ICHK=JMAX-2
  J=0
  I1=ISM(1)
  I2=ISM(2)
60 I3=ISM(J+3)
  AREA=.5*(Y(I1)*X(I3)-Y(I3)*X(I1)+Y(I3)*X(I2)-Y(I2)*X(I3)+
```

G LEVEL 21

TEMP

DATE = 75066

14/36/2'

```

1      Y(I2)*X(I1)-Y(I1)*X(I2))
      D1=(X(I2)-X(I1))**2+(Y(I2)-Y(I1))**2
      IF D1 IS APPROXIMATELY 0. IT IS ASSUMED THAT THERE EXISTS A
      DUPLICATION OF INPUT
      IF(D1.GT..1E-3) GO TO 70
      I2=I3
      I=J+1
      GO TO 60
70 IF(AREA**2.GT..1*D1*SMALL(I)) GO TO 80
      I=J+1
      IF(I.LT.3000) GO TO 60
      WRITE(6,2000) I1,I2,I3,J
      T=TEM(I1)
      RETURN
C* * * * *
C      FIND TEMPERATURE INTERCEPT
C* * * * *
80 DETA=Y(I1)*(TEM(I3)-TEM(I2))+Y(I2)*(TEM(I1)-TEM(I3))
      I      +Y(I3)*(TEM(I2)-TEM(I1))
      DETB=X(I1)*(TEM(I2)-TEM(I3))+X(I2)*(TEM(I3)-TEM(I1))
      I      +X(I3)*(TEM(I1)-TEM(I2))
      DETC=TEM(I1)*(X(I2)*Y(I3)-X(I3)*Y(I2))+TEM(I2)*(X(I3)*Y(I1)-X(I1)*
      Y(I3))+TEM(I3)*(X(I1)*Y(I2)-X(I2)*Y(I1))
      T=(DETA*P+DETB*Z+DETC)/(2.*AREA)
2000 FORMAT (2AH ERROR IN TEMPERATURE INPUT,5H I1=I4,5H I2=I4,
15H I3=I4,4H J=I4)
      RETURN
      END
    
```

LOCATION	SYMBOL	COPYING BLOCK / SOLVE	MAP SIZE	5348	SYMBOL	LOCATION
0	Y	IBCO	TEM	3780	NUMTC	53

LOCATION	SYMBOL	SUBPROGRAMS CALLED	SYMBOL	LOCATION	SYMBOL	LOCATION
113						

LOCATION	SYMBOL	SCALAR MAP	SYMBOL	LOCATION	SYMBOL	LOCATION
120	F	128	Z	130	T	1
149	DETA	150	DETB	158	DETC	1
160	I	170	K	174	JB	1
182	I2	184	I3	198	IT	1

G LEVEL 21

TEM2

DATE = 75066

14/36/2

```

SUBROUTINE TEM2(NUMNP)
  IMPLICIT REAL*8(A-H,O-Z)
  INTEGER CODE
  COMMON/NPDATA/ R(200),CODE(200),XR(200),Z(200),XZ(200),
  INPN(10,20),T(200),XT(200)
  READ(5,1000) TCCNST
  DO 100 N=1,NUMNP
    T(N)=TCCNST
  100 FORMAT(F10.0)
  RETURN
  END
    
```

LOCATION	SYMBOL	COMMON BLOCK /NPDATA /	MAP SIZE	28CO	SYMBOL	LOCAT
0	CODE	640	XR	960	Z	F
1020	T	1F40	XT	2580		

LOCATION	SYMBOL	LOCATION	SYMBOL	LOCATION	SYMBOL	LOCAT
9C						

LOCATION	SYMBOL	LOCATION	SYMBOL	LOCATION	SYMBOL	LOCAT
A0	N	A8	NUMNP	AC		

LOCATION	SYMBOL	LOCATION	SYMBOL	LOCATION	SYMBOL	LOCAT
B0						

LOCATION	STATEMENT	LOCATION	STATEMENT	LOCATION	STATEMENT	LOCAT
138	5	138	6	154	7	1

IN EFFECT\* ACID,BCD,SOURCE,N7LIST,N7DECK,LOAD,MAP  
 IN EFFECT\* NAME = TEM2 , LINECNT = 50  
 ICS\* SOURCE STATEMENTS = 10, PROGRAM SIZE = 392  
 ICS\* NO DIAGNOSTICS GENERATED

```
SUBROUTINE TRISTF (II,JJ,KK)
IMPLICIT REAL*8(A-H,O-Z)
INTEGER CODE
COMMON/MATP/RO(6),E(12,16,6),EE(16),AOFTS(6)
COMMON/BASIC/ACELZ,ANGVEL,ANGACC,TREF,VOL,NUMNP,NUMEL,NUMPC,NUMSC,
INUMST
COMMON/ARG/RRR(5),ZZZ(5),RR(4),ZZ(4),S(15,15),P(15),TT(6),
M(6,15),CPZ(6,6),XT(10),ANGLE(4),SIG(18),EPS(18),N
COMMON/NPDATA/ R(200),CODE(200),XR(200),Z(200),XZ(200),
INPNUM(10,20),T(200),XT(200)
COMMON/ELDATA/ BETA(200),EPR(200),PR(20),SH(20),IX(200,5),IP(20),
IJP(20),IS(20),JS(20),ALPHA(200),IT(200),JT(200),ST(20)
COMMON/RESULT/BS(6,15),D(6,6),C(6,6),AR,BB(6,9),CNS(6,6)
DIMENSION B1(6,9),B2(6,9),B3(6,9),F(6,9),G(9,6),V(9,9)
DIMENSION HF(3),BFR(3),BFZ(3),TP(9),B(9,9)
MTYPE=IABS(IX(N,5))
RF(1)=RPF(II)
RR(2)=RPF(JJ)
RR(3)=RPF(KK)
ZZ(1)=ZZZ(II)
ZZ(2)=ZZZ(JJ)
ZZ(3)=ZZZ(KK)
CALL INTER
VOL=VOL+XI(1)
COMM=RF(2)*(ZZ(3)-ZZ(1))+RR(1)*(ZZ(2)-ZZ(3))+RR(3)*(ZZ(1)-ZZ(2))
DO 10 I=1,6
DO 10 J=1,9
B1(I,J)=0.0
B2(I,J)=0.0
10 B3(I,J)=0.0
C FILL B1 MATRIX-CONSTANT TERMS
B1(1,1)=(ZZ(2)-ZZ(3))/COMM
B1(1,4)=(ZZ(3)-ZZ(1))/COMM
B1(1,7)=(ZZ(1)-ZZ(2))/COMM
B1(3,1)=B1(1,1)
B1(3,4)=B1(1,4)
B1(3,7)=B1(1,7)
B1(2,2)=(RF(3)-RR(2))/COMM
B1(2,5)=(RF(1)-RR(3))/COMM
B1(2,8)=(RR(2)-RR(1))/COMM
B1(4,1)=B1(2,2)
B1(4,4)=B1(2,5)
B1(4,7)=B1(2,8)
B1(4,2)=B1(1,1)
B1(4,5)=B1(1,4)
B1(4,8)=B1(1,7)
B1(5,3)=B1(4,1)
B1(5,6)=B1(4,4)
```

G LEVEL 21

TRISTF

DATE = 75066

14/36/21

```

B1(5,9)=B1(4,7)
C  FILL B2 MATRIX-1/R TERMS
B2(3,1)=(1/COMM)*((ZZ(3)-ZZ(2))*RR(2)+(RR(2)-RR(3))*ZZ(2))
B2(3,4)=(1/COMM)*((ZZ(1)-ZZ(3))*RR(3)-(RR(1)-RR(3))*ZZ(3))
B2(3,7)=(1/COMM)*((ZZ(2)-ZZ(1))*RR(1)+(RR(1)-RR(2))*ZZ(1))
B2(6,3)=-B2(3,1)
B2(6,6)=-B2(3,4)
B2(6,9)=-B2(3,7)
C  FILL B3 MATRIX-Z/R TERMS
B3(3,1)=(RR(3)-PR(2))/COMM
B3(3,4)=(RR(1)-RR(3))/COMM
B3(3,7)=(PP(2)-RR(1))/COMM
B3(6,3)=(RR(2)-RR(3))/COMM
B3(6,6)=(RR(3)-RR(1))/COMM
B3(6,9)=(RR(1)-RR(2))/COMM
AR=AP+XI(1)
D7 80 I=1,6
D8 80 J=1,9
80  BB(I,J)=B1(I,J)*XI(1)+B2(I,J)*XI(2)+B3(I,J)*XI(4)
D9 91 K=1,6
D9 91 I=1,3
AS(K,3*JJ-3+I)=BB(K,I+3)+BS(K,3*JJ-3+I)
AS(K,3*II-3+I)=BB(K,I)+BS(K,3*II-3+I)
91  AS(K,3*KK-3+I)=BB(K,I+6)+BS(K,3*KK-3+I)
D7 110 I=1,9
D8 110 J=1,9
B(I,J)=0.0
D9 110 K=1,6
D9 110 M=1,6
B(I,J)=B(I,J)+B1(K,I)*CRZ(K,M)*(B1(M,J)*XI(1)
1+B2(M,J)*XI(2)+B3(M,J)*XI(4))
2+B2(K,I)*CFZ(K,M)*(B1(M,J)*XI(2)
3+B2(M,J)*XI(3)+B3(M,J)*XI(5))
5+B3(K,I)*CPZ(K,M)*(B1(M,J)*XI(4)
6+B2(M,J)*XI(5)+B3(M,J)*XI(6))
110  CCNTINUE
C  ASSEMBLE QUADRILATERAL STIFFNESS MATRIX, S, FROM TRIANGULAR
C  STIFFNESS MATRIX, B.
IIM=3*II-3
JJM=3*JJ-3
KKM=3*KK-3
D9 120 I=1,3
D8 120 J=1,3
S(IIM+I,IIM+J)=B(I,J)+S(IIM+I,IIM+J)
S(IIM+I,JJM+J)=B(I,J+3)+S(IIM+I,JJM+J)
S(IIM+I,KKM+J)=B(I,J+6)+S(IIM+I,KKM+J)
S(JJM+I,IIM+J)=B(I+3,J)+S(JJM+I,IIM+J)
S(JJM+I,JJM+J)=B(I+3,J+3)+S(JJM+I,JJM+J)
    
```

```

S(IJM+I, KKM+J)=B(I+3, J+6)+S(IJM+I, KKM+J)
S(KKM+I, IIM+J)=B(I+6, J+3)+S(KKM+I, IIM+J)
S(KKM+I, JJM+J)=B(I+6, J+3)+S(KKM+I, JJM+J)
S(KKM+I, KKM+J)=B(I+6, J+6)+S(KKM+I, KKM+J)
120 CONTINUE
C ASSEMBLE BODY FORCES MATRIX
BF(1)=(ZZ(3)*RR(2)-RR(3)*ZZ(2))/COMM
BF(2)=(ZZ(1)*PR(3)-RP(1)*ZZ(3))/COMM
BF(3)=(ZZ(2)*PP(1)-RR(2)*ZZ(1))/COMM
BFP(1)=(ZZ(2)-ZZ(3))/COMM
BFR(2)=(ZZ(3)-ZZ(1))/COMM
BFR(3)=(ZZ(1)-ZZ(2))/COMM
BFZ(1)=(RP(3)-RR(2))/COMM
BFZ(2)=(PP(1)-RR(3))/COMM
BFZ(3)=(PP(2)-RR(1))/COMM
C BODY FORCE IN Z-DIRECTION
COMM=-ACELZ*RO(MTYPE)
DO 140 I=1,3
    IIK=3*I-1
140 TP(IIK)=COMM*(BF(I)*XI(1)+BFR(I)*XI(7)+BFZ(I)*XI(8))
C BODY FORCE IN P-DIRECTION
COMM=ANGVEL**2*RC(MTYPE)
DO 150 I=1,3
    L=3*I-2
150 TP(L)=COMM*(BF(I)*XI(7)+BFR(I)*XI(9)+BFZ(I)*XI(10))
C BODY FORCES IN YANG. DIRECTION
COMM=-ANGACC*RC(MTYPE)
DO 160 I=1,3
    IIM=3*I
160 TP(IIM)=COMM*(BF(I)*XI(7)+BFR(I)*XI(9)+BFZ(I)*XI(10))
C ADD THERMAL EFFECTS
DO 161 J=1,9
DO 161 K=1,6
161 TP(J)=TP(J)+(XI(1)*B1(K, J)+XI(2)*B2(K, J)
    +XI(4)*B3(K, J))*TT(K)
C REARRANGE TP INTO P-MATRIX, THE BODY FORCES MATRIX
K=3*I-2
L=3*JJ-2
M=3*KK-2
DO 170 I=1,3
    J=I-1
    P(K+J)=P(K+J)+TP(I)
    P(L+J)=P(L+J)+TP(I+3)
170 P(M+J)=P(M+J)+TP(I+6)
    PETHON
END
    
```

**DISTRIBUTION LIST**

<u>No. of Copies</u>	<u>Organization</u>	<u>No. of Copies</u>	<u>Organization</u>
12	Commander Defense Documentation Center ATTN: DDC-TCA Cameron Station Alexandria, VA 22314	3	Commander US Army Missile Command ATTN: AMSMI-R AMSMI-RFL, Mr. B. Cobb AMSMI-RL, Mr. N. Comus Redstone Arsenal, AL 35809
1	Director of Defense Research and Engineering ATTN: Tech Lib, Rm 3E-1039 Washington, DC 20301	1	Commander US Army Tank Automotive Command ATTN: AMSTA-RHFL Warren, MI 48090
1	Commander US Army Materiel Command ATTN: AMCDMA-ST 5001 Eisenhower Avenue Alexandria, VA 22333	2	Commander US Army Mobility Equipment Research & Development Center ATTN: Tech Docu Cen, Bldg. 315 AMSME-RZT Fort Belvoir, VA 22060
1	Commander US Army Materiel Command ATTN: AMCRD-T 5001 Eisenhower Avenue Alexandria, VA 22333	2	Commander US Army Armament Command ATTN: AMSAR-RDT Mr. J. Salamon Dr. L. Johnson Rock Island, IL 61202
1	Commander US Army Materiel Command ATTN: AMCRD-R 5001 Eisenhower Avenue Alexandria, VA 22333	6	Commander US Army Picatinny Arsenal ATTN: SARPA-FR-E, Dr. N. Clark Mr. G. Randers-Pherson SARPA-AD-S, S. Polanski SARPA-FR-M-MA, M. Eig SARPA-FR-S-R, C. Larsen Tech Lib Dover, NJ 07801
1	Commander US Army Aviation System Command ATTN: AMSAV-E 12th and Spruce Streets St. Louis, MO 63166	2	Commander US Army Frankford Arsenal ATTN: SARFA-C2500 SARFA-L3200 Mr. P. Gordon Philadelphia, PA 19137
1	Director US Army Air Mobility Research and Development Laboratory Ames Research Center Moffett Field, CA 94035		
1	Commander US Army Electronics Command ATTN: AMSEL-RD Fort Monmouth, NJ 07703		



DISTRIBUTION LIST

<u>No. of Copies</u>	<u>Organization</u>	<u>No. of Copies</u>	<u>Organization</u>
3	Commander US Army Watervliet Arsenal ATTN: SARWV-RPD-SE Mr. M. Dale Dr. J. Santini SARWV-PSD Dr. G. D'Andrea Watervliet, NY 12189	1	Commander US Army Research Office P. O. Box 12211 Research Triangle Park North Carolina 27709
1	Commander US Army Harry Diamond Labs ATTN: AMXDO-TI 2800 Powder Mill Road Adelphi, MD 20783	2	Commander US Naval Air Systems Command ATTN: Code AIR-310 Code AIR-350 Washington, DC 20360
4	Commander US Army Materials and Mechanics Research Center ATTN: AMXMR-ATL, W. Woods AMXMR-T, J. Mescall AMXMR-TM, L. Leone Tech Lib Watertown, MA 02172	1	Commander US Naval Ordnance Systems Command ATTN: Code ORD-0532 Washington, DC 20360
1	Director US Army TRADOC Systems Analysis Activity ATTN: ATAA-SA White Sands Missile Range New Mexico 88002	2	Chief of Naval Research ATTN: Code 427 Code 470 Department of the Navy Washington, DC 20325
1	Assistant Secretary of the Army (R&D) ATTN: Asst for Research Washington, DC 20310	3	Commander US Naval Surface Weapons Center ATTN: Dr. H. Sternburg Dr. Walker Code 730, Lib Silver Spring, MD 20910
2	HQDA (DAMA-ZA; DAMA-AR) Washington, DC 20310	2	Commander US Naval Surface Weapons Center ATTN: Code GWD, K. Bannister Tech Lib Dahlgren, VA 22448
1	HQDA (DAMA-CSM, LTC N. O. Conner, Jr.) Washington, DC 20310	1	Commander US Naval Weapons Center ATTN: Code 45, Tech Lib China Lake, CA 93555
		1	Director US Naval Research Laboratory Washington, DC 20350

**DISTRIBUTION LIST**

<u>No. of Copies</u>	<u>Organization</u>	<u>No. of Copies</u>	<u>Organization</u>
1	USAF (AFRDDA) Washington, DC 20330	1	Director National Aeronautics and Space Administration Langley Research Center Langley Station Hampton, VA 23365
1	AFSC (SDW) Andrews AFB Washington, DC 20331	1	Director National Aeronautics and Space Administration Lewis Research Center 21000 Brookpark Road Cleveland, OH 44135
1	US Air Force Academy ATTN: Code FJS-RL(NC) Tech Lib Colorado Springs, CO 80840	1	Director Lawrence Radiation Laboratory ATTN: Dr. M. Wilkins P. O. Box 808 Livermore, CA 94550
1	Commander Hill Air Force Base ATTN: Code AMA Code MMECB Utah 84401	3	University of Illinois Aeronautical and Astronautical Engineering Department 101 Transportation Building ATTN: Prof. A. R. Zak Urbana, IL 61801
1	AFWL (SUL, LT Tennant) Kirtland AFB, NM 87116		<u>Aberdeen Proving Ground</u>
1	AFLC (MMMC) Wright-Patterson AFB, OH 45433		Marine Corps Ln Ofc Dir, USAMSA
1	AFAL (AVW) Wright-Patterson AFB, OH 45433		
1	Director US Bureau of Mines ATTN: Mr. R. Watson 4800 Forbes Street Pittsburgh, PA 15213		
1	Director Environmental Science Services Administration ATTN: Code R, Dr. J. Rinehart US Department of Commerce Boulder, CO 80302		